MICROLITHOGRAPHY
Science and Technology

edited by

James R. Sheats
Hewlett-Packard Laboratories
Palo Alto, California

Bruce W. Smith
Rochester Institute of Technology
Rochester, New York

MARCEL DEKKER, INC. NEW YORK • BASEL • HONG KONG

IP Bridge Exhibit 2017
TSMC v. IP Bridge
IPR2016-01378
Page 0001

Library of Congress Cataloging-in-Publication Data

Sheats, James R.
Microlithography: science and technology / James R. Sheats, Bruce W. Smith.
p. cm.
Includes bibliographical references and index.
ISBN 0-8247-9953-4 (alk. paper)
1. Microlithography. 2. Integrated circuits—Masks. 3. Metal oxide semiconductors, Complementary—Design and construction. 4. Manufacturing processes. I. Smith, Bruce W. II. Title.
TK7836.S46 1998
621.3815'31--dc21 98-16713
CIP

The publisher offers discounts on this book when ordered in bulk quantities. For more information, write to Special Sales/Professional Marketing at the address below.

This book is printed on acid-free paper.

Copyright © 1998 by MARCEL DEKKER, INC. All Rights Reserved

Neither this book nor any part may be reproduced or transmitted in any form or by any means, electronic or mechanical, including photocopying, microfilming, and recording, or by any information storage and retrieval system, without permission in writing from the publisher.

MARCEL DEKKER, INC.
270 Madison Avenue, New York, New York 10016
http://www.dekker.com

Current printing (last digit):
10 9 8 7 6 5 4 3 2 1

PRINTED IN THE UNITED STATES OF AMERICA

9

Resist Processing

Bruce W. Smith

Rochester Institute of Technology
Rochester, New York

1 INTRODUCTION

For the most part, conventional single-layer photoresists have been based on components with two primary functions. Whether considering older bis-arylazide *cis*-polyisoprene resists, diazonapthoquinone (DNQ)/novolac g/i-line resists, or chemically amplified polyhydroxystyrene (PHS) deep-UV (DUV) resists, an approach has been utilized wherein a base resin material is modified for sensitivity to exposure by a photoactive compound or through photoinduced chemical amplification. The resist base resin is photopolymeric in nature and is responsible for etch resistance, adhesion, coat-ability, and bulk resolution performance. These resins generally do not exhibit photosensitivity on the order required for integrated circuit (IC) manufacturing. Single-component polymeric resists have been utilized for microlithography, including methacrylates, styrenes, and other polymers or copolymers, but sensitization is generally low and limited to exposures at very short ultraviolet (UV) wavelengths or with ionizing radiation. Inherent problems associated with low absorbance and poor radiation resistance (required, for example, during ion implantation or plasma etching steps) generally limit the application of these types of resists to low volumes or processes with unique requirements.

Sensitization of photoresist materials has been accomplished by several methods. In the case of conventional g/i-line resists, a chemical modification of a base-insoluble photoactive compound (PAC), the diazonaphthoquinone, to a base-soluble photoproduct, indene carboxylic acid (ICA), allows an increase in

IPR2016-01378 Page 0003

aqueous base solubility. For chemically amplified PHS-based resists, exposure of a photoacid generator (PAG) leads to the production of an acid, which subsequently allows polymer deprotection (positive behavior) or crosslinking (negative behavior). Other similar processes have been developed (as discussed in Chapter 8) and may involve additional components or mechanisms.

For any resist system, the thermodynamic properties of polymeric resins play an important role in processibility. During the coating, exposure, and development processes of a resist, an understanding of the thermodynamic properties is desirable, as the glass transition temperature (T_g) of a polymer influences planarizability, flow, and diffusion. Although reasonably high T_g values may be desirable, glassy materials with values above 200°C are not suitable because of poor mechanical performance. Once three-dimensional resist features are formed, however, a thermoset material may be desired in which the polymer does not flow with temperature and a T_g essentially does not exist. This ensures the retention of high-aspect-ratio features through subsequent high-temperature and high-energy processes. By appropriate engineering of bake steps during single-layer resist processing, the control of polymer thermoplastic and thermoset properties can be made possible. For negative resists, the situation is inherently simplified. Coated negative resists are thermoplastic in nature, with a well-defined T_g range. Upon exposure and subsequent secondary reactions, crosslinking leads to a networked polymer that will not flow with temperature. At some high temperature of decomposition (T_d) the polymer will break down and begin to lose significant volume. Imaging steps are therefore responsible for the production of thermally stable resist features. Operations are often included in the processing of positive resists that can accomplish similar thermal stability enhancements.

This chapter addresses the critical issues involved in the processing of single-layer resists materials. Process steps to be discussed include:

Resist stability, contamination, and filtration
Substrate priming
Resist coat
Soft bake
Exposure
Postexposure bake
Development
Swing effects
Hard bake and postdevelopment treatment

The step-by-step process flow for DNQ/novolac resists has been covered elsewhere, and the reader is directed to these references for additional description [1–3]. Specific details are given here for positive DNQ/novolac resists and both positive and negative DUV chemically amplified resists based on PHS.

IPR2016-01378 Page 0004

2 RESIST STABILITY, CONTAMINATION, AND FILTRATION

2.1 DNQ/Novolac Resist Stability and Filtration

DNQ/novolac resists have proved to be robust materials with respect to sensitivity to thermodynamic and aging effects while stored in uncast form. A resist shelf life of several months can be expected with no significant change in lithographic performance. As resists are considered for application in production, the stability of materials at various points of the process also needs to be considered.

For DNQ/novolac resists, aging can lead to an increase in absorption at longer wavelengths. Resist materials are susceptible to several thermal and acid/base (hydrolytic) reactions when stored [4]. These include thermal degradation of the DNQ to ICA followed by acid-induced azo dye formation and azo coupling of the DNQ and novolac. A characteristic "red darkening" results from this coupling, induced by the presence of acids and bases in the resist. Although long-wavelength absorbance is altered by this red azo dye, the impact on UV absorbance and process performance is most often negligible. Degradation mechanisms can also result in crosslinking, leading to an increase in high-molecular-weight components. Hydrolysis of DNQ may occur to form more soluble products and hydrolysis of solvents is possible, which can lead to the formation of acids [5]. The practical limitation of shelf life for DNQ/novolac resists is generally on the order of 6 months to 1 year. Once coated, resist films can absorb water and exhibit a decrease in sensitivity, which can often be regained through use of a second soft bake step. As will be described, process delays for chemically amplified PHS resists are much more critical than for DNQ/novolac materials.

A larger problem encountered when storing DNQ/novolac resists is sensitizer precipitation. With time, DNQ PAC can fall out of solution, especially at high temperatures. These crystallized precipitates can form most readily with high loading levels of DNQ. In addition, resist particulate levels can be increased by the formation of gel particles, a result of acid-induced novolac crosslinking via thermal decomposition of DNQ. Any of these routes to particulate formation can lead to levels exceeding that measured by the resist manufacturer. Because of this, point-of-use filtration has become common practice for most production applications to ensure photoresist consistency [6]. Resist materials are commonly filtered at a level of approximately 25% of the minimum geometry size. As the geometry size approaches sub-0.35 μm, filtration requirements may approach 0.05 μm. Such ultrafiltering will have an impact on how resists can be manufactured and used. Filtration speed is dramatically reduced and material preparation becomes more costly. Similar concerns can exist for pump throughput during resist dispensing. Fractionation of a resist material can also occur,

resulting in the removal of long polymer chains and a change in process performance. To illustrate this, consider an i-line resist (DNQ/novolac) with a molecular weight on the order of 10–20 × 10^3 g/mol (number average). The resulting average polymer chain size is nearly 5 to 6 nm with a maximum as large as 40 nm. In highly concentrated resist formulations (>30 wt. %), intertwisting of polymers can result in chain sizes greater than 80 nm. If such a resist is filtered to 0.05 μm, the largest polymer chains can be removed. As technology progresses toward smaller feature resolution, it is clear that particulate and filtration issues need to be carefully considered.

2.2 Stability Issues for Chemically Amplified PHS Resists

Filtration concerns for i-line resists are extended to deep UV lithography as PHS resists are considered. As sub-0.25 μm geometry is pursued, the issue of ultrafiltering becomes an increasingly important problem. In addition, environmental stability issues are present for many chemically amplified resists (CARs) that are not issues for DNQ/novolac resists, especially for resists based on acid-catalyzed reactions and PHS resins. Ion exchange methods are conventionally used to reduce ion contamination levels in resists below 50 ppb. Ionic contamination reduction in both positive and negative CAR systems needs to be carefully considered. Deprotection of acid-labile components can result from reaction with cationic exchange resins. The catalytic acid produced upon exposure of these resists is also easily neutralized with base contamination at ppb levels. These contaminants can include such things as ammonia, amines, and NMP, which are often present in IC processing environments [7]. Any delay between exposure and postexposure bake (PEB) can result in a decrease in sensitivity and the formation of a less soluble resist top layer or "T-top."

To reduce the likelihood of base contamination of these resists, several improvements have been made in resist formulations. One method explored to reduce acid loss is the use of low-activation-energy (E_a) polymers with highly reactive protection groups. These resists are sufficiently active that deprotection can occur immediately upon exposure, significantly reducing the sensitivity to PEB delay effects [8,9]. Additives have also been incorporated into DUV PHS resists to improve their robustness to contamination effects [10,11] and resist topcoating approaches have been introduced [12]. By coating a thin water-soluble transparent polymeric film over a resist layer, protection from airborne contamination can be made possible. This "sealing" layer is removed prior to development with a water rinse. Although such a solution leads to minimal additional process complexity, it is still desirable to use resist techniques that do not require additional material layers. An alternative route for the reduction of contamination effects is the use of high-activation-energy resist materials. By reducing the reactivity of a resist, much higher bake processes are allowed. In-

IPR2016-01378 Page 0006

creasing the bake temperatures above a polymer's T_g results in a densification of the photoresist. This leads to a significant decrease in the diffusion rate of airborne base contamination prior to or after exposure [13,14]. These high-E_a resists also require that a photoacid generator be chosen that can withstand high temperatures. Other methods used to reduce base contamination of acid-acatalyzed resists include the use of activated charcoal air filtration during resist coating exposure, and development operations [15]. This is now considered a requirement for processing of PHS CAR resists. Environmental base contamination can be neutralized and further reduced by adding weak acids to these filters.

The stability or shelf life of PHS-based resists is also influenced by the structure of polymer protective groups. This is especially true for low-activation-energy (high-reactivity) resists, for which the liability of protective groups may decrease usable resist shelf life. Conversely, the more stable protective groups utilized with high-activation-energy (low-reactivity) resists lead to a higher degree of stability.

3 RESIST ADHESION AND SUBSTRATE PRIMING

Adequate adhesion of photoresist to a wafer surface is critical for proper process performance. Resist adhesion failure can occur not only during photolithography operations but also in subsequent etch, implant, or other masking steps. Negative resists are less prone to adhesion failure, as crosslinking results in a networked polymer that is bound to the wafer surface. Positive resists (especially phenolic-based materials such as novolac or PHS resists) are more likely to be single-polymer chains and rely on weaker physical and chemical forces for adhesion. Etch process undercutting can often result from inadequacies at the resist interface, resulting in loss of etch line width control. The causes of resist adhesion failure are generally related to dewetting of a photoresist film. This can result from a large discordance between the surface tension of the wafer and that of the resist material, especially when coating over silicon oxide. Silicon dioxide is an especially difficult layer to coat over because it provides a hydrophilic surface (water attracting) to a hydrophobic resist (water repelling). The surface tension of thermal silicon dioxide may be on the order of 15 dynes/cm^2, whereas the surface tension of phenolic resists in casting solvent may be near 30 dynes/cm^2. Surface defects can also cause adhesion failure as surface free energy can result in dewetting.

Methods of adhesion promotion can be used for most silicon oxide layers, whether thermally grown, deposited, native, or glasslike. Chemical passivation of these surfaces is generally carried out using silylating priming agents, which act to modify the wafer surface. Some benefit can be realized with priming of layers other than oxides if techniques promote a closer match-

ing of material surface tension. Alkylsilane compounds are generally used to prime oxide surfaces, leading to a lowering of surface hydrophilicity. The most commonly used silane-type adhesion promoter is hexamethyldisilazane (HMDS). Other similar promoters are available, including trimethylsilyldiethylamine (TMSDEA), which can be more effective but also less stable, resulting in lower shelf and coated lifetimes. Reduction of substrate surface tension is carried out in two stages, as shown in Fig. 1. Shown here is a silicon oxide surface with adsorbed water and OH groups. An initial reaction of water with an alkylsilane (HMDS) produces an inert hexamethyldisiloxane and ammonia, resulting in a dehydrated surface. Further reaction with HMDS produces a trimethylsilyl-substituted hydroxyl or oxide species and unstable trimethylsilylamine. With heat, this unstable compound reacts with other surface hydroxyl groups to produce further ammonia and a trimethylsiloxy species. The process continues until steric hindrance (via the large trimethylsilyl groups) inhibits further reaction.

Surface priming using HMDS, TMSDEA, or similar agents can be carried out in either liquid- or vapor-phase modes. In either case, elevated process temperatures (~100°C) must be reached to complete the priming reaction. Substrates should be cleaned prior to application using UV ozone, HF dip, plasma,

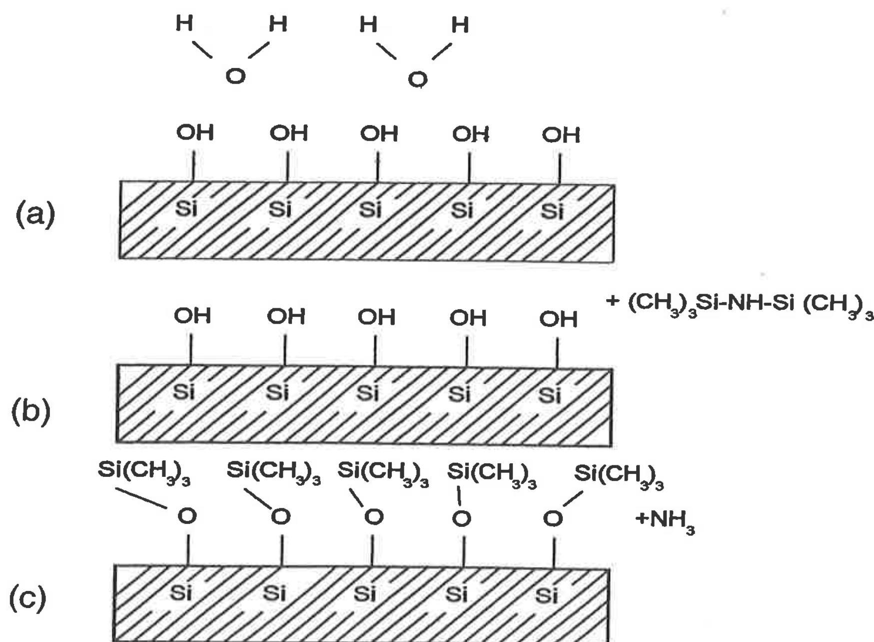

Figure 1 Adhesion promotion of a silicon oxide surface with HMDS surface priming. The substrate is first dehydrated upon reaction with silane promoter. Further reaction with heat leads to a hydrophobic surface.

or other "oxidative" cleaning methods. Adhesion of photoresist to silicon nitride or deposited oxide layers can be enhanced by using an oxygen/ozone plasma treatment. Priming agents are generally best applied using vapor prime methods, either in line or in batch vacuum ovens. Uniformity and reduced chemical usage make this more attractive than liquid methods.

Overpriming of a wafer surface can result in dewetting and lead to further adhesion problems. This can occur with repeated treatment or by using excessive vapor times. Problems are often noticed in isolated substrate areas, depending on device topography or condition. A phenomenon known as resist "popping" can also occur as a result of overpriming; in this case high-fluence exposure (such as that encountered with heavy UV overexposure in ion implantation steps) can cause failure of weakened resist adhesion. Deposition of resist debris onto adjacent substrate areas can result. Measurements of resist surface tension using water contact angle techniques can identify such overpriming problems. Remedies include the use of shorter priming times, resist solvents with lower surface tension, double resist coating steps, or a pretreatment of the wafer surface with the resist casting solvent. Oxygen or ozone plasma treatments can also correct an overprimed wafer surface and allow repriming under more appropriate conditions.

The strength of adhesion bonds between a photoresist and a substrate has also been shown to influence the T_g and thermal expansion coefficient of a thin film. The impact is greatest as resist films approach 1000 Å thicknesses [16].

4 RESIST COATING

4.1 Resist Spin Coating Techniques and Control

Photoresist can be dispensed by several methods, including spin coating, spray coating, and dip coating. The most widely used methods for coating resist onto wafer substrates are spin coating methods. During spin coating, resist is dispensed onto a wafer substrate (either statically or dynamically), accelerated to a final spin speed, and cast to a desired film thickness. Variations on this process have been suggested, including the use of a short-term high-speed initial coating step followed by a slow drying stage [17]. Spin coating processes use the dynamics of centrifugal force to disperse a polymeric resist material over the entire wafer surface. The flow properties (rheology) of the resist influence the coating process and need to be considered to achieve adequate results [18]. In addition, solvent transport through evaporation occurs, which can result in an increase in resist viscosity and shear thinning, affecting the final film properties. As a resist-solvent material is spin cast, the film thickness decreases uniformly, at a rate dependant on the spin speed (ω), kinematic viscos-

ity (υ), solids concentration (c), solvent evaporation rate (e), and initial film thickness, expressed by the following rate equations:

$$\frac{dS}{dt} = \frac{-c2\omega^2 h^3}{3\upsilon} \quad (1)$$

$$\frac{dL}{dt} = (1-c)\frac{2\omega^2 h^3}{3\upsilon} - e \quad (2)$$

where dS/dt and dL/dt are rate of change of solids (S) and solvents (L), respectively [19]. The results are shown in Fig. 2 for a 1-μm film, where both solids and solvent volumes are plotted against spin time. Initially, concentration changes little as resist spread dominates. When the resist thickness drops to one third of its original value, evaporation dominates and solvent content reaches its final value. The high viscosity of the resist eliminates further flow.

The primary material factors that influence spin-coated film properties include the resist polymer molecular weight, solution viscosity, and solvent boiling point (or vapor pressure). Primary process factors include wafer spin speed, acceleration, temperature, and ambient atmosphere. The thickness of a resist film can be modified to some extent through control of the rotation speed of

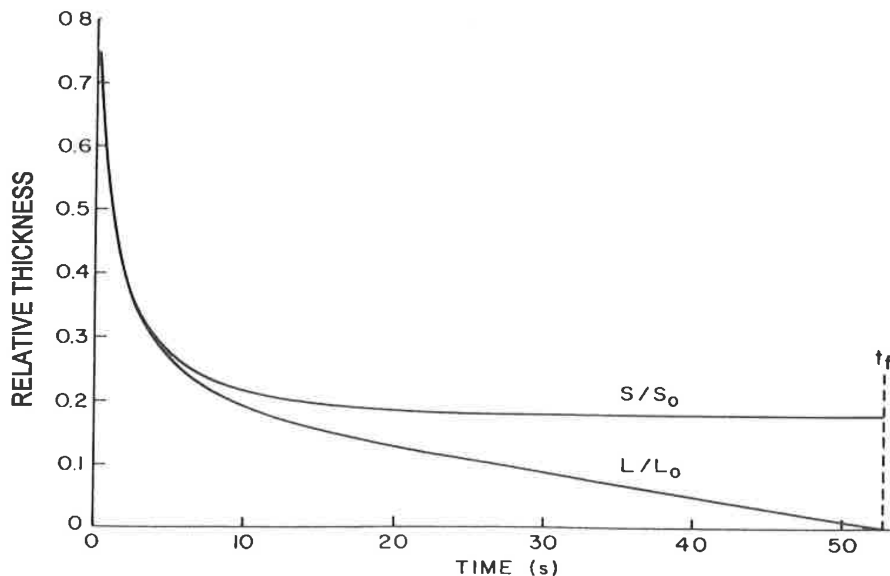

Figure 2 Calculated time dependance during spin coating on the volume of solids (S) and solvent (L) per unit area normalized to initial values. When the resist thickness drops to one third of its original value, evaporation dominates and the solvent content reaches its final value. (From Ref. 19.)

the substrate. Resist thickness is inversely proportional to the square root of spin speed (ω):

$$\text{Thickness} \propto \frac{1}{\sqrt{\omega}} \tag{3}$$

To achieve large thickness changes, modification of the resist solution viscosity is generally required, as coating at excessively low or high speeds results in poor coating uniformity. At excessively high speeds, mechanical vibration and air turbulence result in high levels of across-wafer nonuniformity. At low spin speeds, solvent loss of the resist front as it is cast over the substrate results in a situation of dynamic resist viscosity, also resulting in high levels of nonuniformity. The optimal spin speed range is dependent on wafer size. Wafers up to 150 mm can be coated at rotation speeds on the order of 4000 to 5000 RPM. Larger substrates require lower speeds.

The optimum coating thickness for a resist layer is determined by the position of coherent interference nodes within the resist layer. Standing waves (see Section 9) resulting from reflections at the resist/substrate interface result in a regular distribution of intensity from the top of the resist to the bottom. This distribution results in a "swing" in the required clearing dose (E_0) for a resist, as shown in Fig. 3. Three curves are shown, for polysilicon, silicon nitride (1260 Å), and silicon dioxide (3700 Å) coated substrates. A general upward trend in E_0 is seen as resist thickness increases. This is due to the residual nonbleachable absorp-

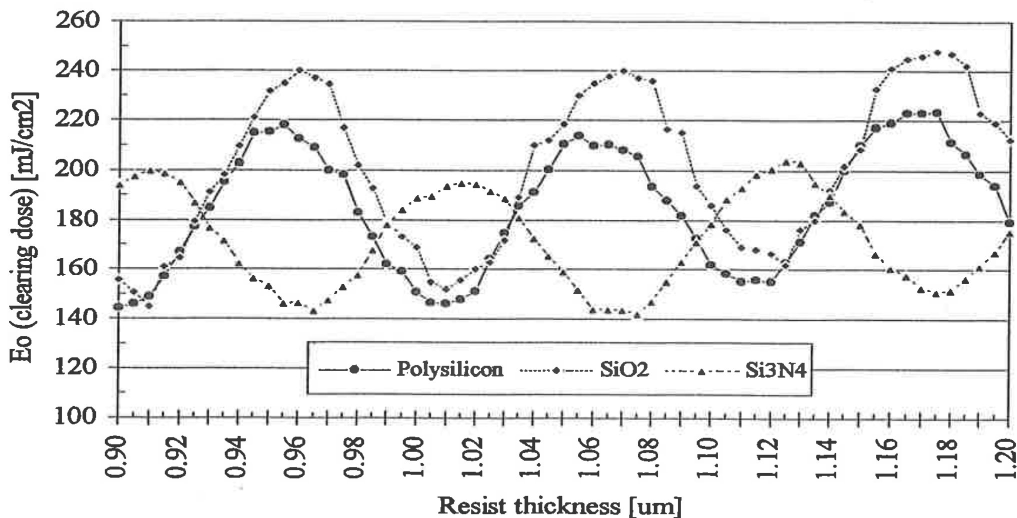

Figure 3 Clearing dose (E_0) swing curves for an i-line resist over polysilicon, silicon dioxide (3700Å), and silicon nitride (1260Å). The increasing trend in required dose is a function of residual absorption. Conditions of minimum interference leads to maximum E_0 values but minimal scumming.

tion of the resist, which can be significant. (For a resist with a residual absorption of 0.10 μm^{-1}, the intensity at the bottom of a 1-μm resist layer is 90% of that experienced at the top.) In addition to this E_0 trend, sensitivity oscillates from minimum to maximum values with thickness. Within one swing cycle, an exposure dose variation of 32% exists for the polysilicon substrate, 27% for silicon nitride, and 36% for silicon dioxide. When resist is coated over a dielectric layer, such as silicon dioxide, silicon nitride, or an antireflective coating (ARC), there will be a shift in the phase of E_0 oscillations. Analysis of swing behavior may therefore be unique for various lithographic levels. Coated thickness optimization can be performed using these swing curves, determined experimentally through open frame exposure of resist coated within a small range of thicknesses. Lithographic modeling can aid in generation of such relationships using knowledge of the resist refractive index, absorption properties (possibly dynamic), exposure wavelength, and resist/substrate reflectivity.

Inspection of the E_0 swing curve in Fig. 3 suggests several possibilities for resist thickness, of which only a few are desirable. For polysilicon, there is a minimum dose requirement at a thickness of ~1.01 μm, where constructive interference occurs, and there is maximum intensity at the resist base. At a resist thickness over polysilicon of ~1.06 μm, destructive interference leads to a maximum E_0 requirement. Other alternatives might include positions on either side of these values (between nodes). Thicknesses corresponding to these midnodal positions allow the least amount of coating process latitude, as small deviations from the targeted film thickness lead to significant changes in dose requirements. Greater latitude exists at maximum interference positions, where there is a minimum requirement for exposure dose, which may be an attractive choice. Small changes in film thickness result only in small E_0 variations but the direction of these changes is toward higher clearing dose values. The result may be scumming of resist features resulting from underexposure, a situation that is unacceptable. The best choice for targeted film thickness may be at a corresponding interference minimum, where small thickness changes result in a small decrease in the dose requirement. Slightly lower throughput may result (generally not a gating factor in today's exposure operations) but this will ensure no resist scumming related to underexposure. Image fidelity at the top surface of a resist film is also influenced by film thickness and positions on the interference curve. By coating at a midnodal thickness, top surface rounding or T-topping can result (see the Section 9 for further discussion).

During spin coating, a large amount of resist "free volume" can be trapped within a resist layer. A simplified free-volume model of molecular transport can be quite useful for correlation and prediction of diffusion properties of resist materials [20,21]. (The reader is directed to Refs. 20 and 21 for a detailed discussion of diffusion in polymer-solvent systems.) Volumetric expansion en-

hances polymer chain mobility and acts similarly to the addition of plasticizers. The resist's glass transition temperature (T_g) is lowered and the dissolution properties of novolac- and PHS-based resist can be increased [22]. Coating-induced free volume has been shown to affect acid diffusion as well and becomes a concern when considering reduction of airborne base contamination and postexposure delay.

4.2 Solvent Contribution to Film Properties

Residual casting solvent can act as a plasticizer and can reduce the T_g of a resist. Resist solvent content has been shown to be dependent on film thickness. A 1000 Å resist film may, for example, exhibit 50% more solvent retention than a 10,000 Å film. Figure 4 shows residual solvent in PHS polymer films coated at thicknesses of 12,000 Å and 1100 Å. Only near the resist T_g (135°C) does the solvent content for the 1100 Å film approach that of the thicker film. Table 1 shows diffusion coefficients for PGMEA solvent in the same PHS film thicknesses, determined by diffusion analysis during 2 hours of baking. These results may be due to a smaller degree of inter- or intramolecular hydrogen bonding in thinner films [23–25], which can allow a stronger polymer interaction with the casting solvent and lower solvent evaporation rates. A higher solvent content leads to an increased dissolution rate and increased diffusivity levels. When considering various resist solvent systems, it might also be expected that lower boiling point (T_b) solvents would lead to lower solvent

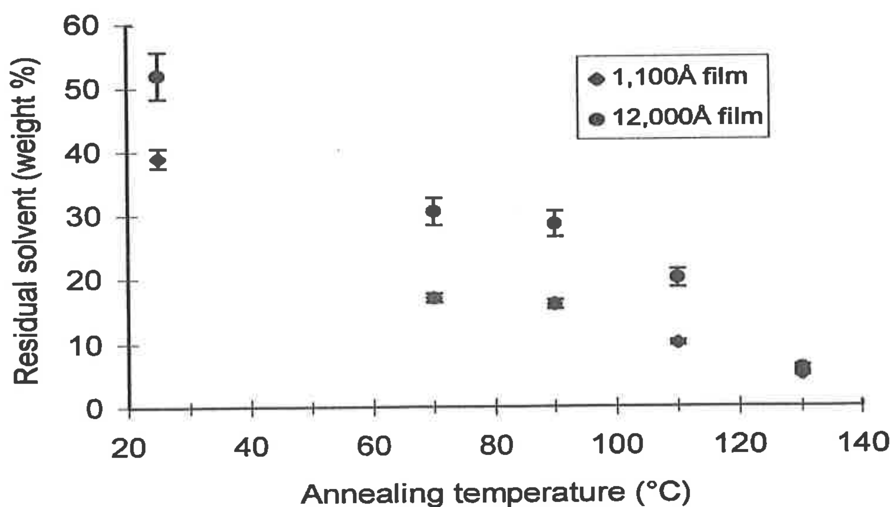

Figure 4 Bake temperature dependence of residual PGMEA solvent in 1,100Å and 12,000Å spin cast films annealed for 1300 minutes. (From Ref. 24.)

Table 1 Diffusion Coefficients of PGMEA Solvent in PHS Films for 2 Hours of Baking

	Diffusion coefficient (cm²/s)	
Temperature	*0.11-μm film*	*1.2-μm film*
70°C	4.2×10^{-14}	1.2×10^{-12}
90°C	9.4×10^{-14}	4.4×10^{-12}
110°C	1.1×10^{-13}	1.4×10^{-11}

retention than higher T_b solvents. The opposite, however, has been demonstrated [26]. PGMEA, for instance, has a boiling point of 146°C and an evaporation rate of 0.34 (relative to *n*-butyl acetate). Ethyl lactate has a higher T_b of 154°C and an evaporation rate of 0.29. Despite its lower boiling point, PGMEA is more likely to be retained in a resist film. The reason for this is a skin formation that results from rapid solvent loss during the coating process [27]. The resist viscosity at the surface increases more rapidly for PGMEA as solvent is exhausted, leading to more residual solvent remaining throughout the resist film. If a resist film is then baked at temperatures below the bulk T_g, densification of surface free volume is allowed only at the top surface of the film and is prevented throughout the bulk. Entrapped solvent therefore leads to an apparent surface induction effect, which can be reduced only if the resist is baked above its T_g. Because solvent content plays an important role in determining the ultimate glass transition temperature of the resist (and therefore its dissolution properties), any postcoating incorporation of solvents can also have an adverse impact on performance. Such additional solvent may be encountered, for instance, when using an edge bead removal process based on acetone, ethyl lactate, pentanone, or other organic solvents.

4.3 Substrate Contribution to Resist Contamination

Continuous improvements have been made in the materials and processes used for DUV PHS chemically amplified resists to reduce top-surface base contamination effects. An additional contamination problem occurs when processing PHS resists over some substrates. Resists coated over Si_3N_4, BPSG, SOG, Al, and TiN have seen shown to initiate a substrate contamination effect that can result in resist scumming or "footing." With TiN substrates, the problem has been attributed to surface N^{-3} and TiO_2, which can act to neutralize photogenerated acid, resulting in a lowering of the dissolution rate at the resist/substrate interface [28]. Sulfuric acid/hydrogen peroxide and oxygen plasma pretreatments have been shown to reduce contamination effects when coating over Si_3N_4 and other problematic substrates [29].

IPR2016-01378 Page 0014

4.4 Edge Bead Removal

After a spin-coating process, a bead of hardened resist exists at the edge of a wafer substrate. Formation of this edge bead is caused in part by excessive resist drying and can result in resist accumulation up to 10 times the thickness of the coated film. Elimination of this edge bead is required to reduce contamination of process and exposure tools. Solvent edge bead removal (EBR) techniques can be utilized to remove this unwanted resist by spraying a resist solvent on the back side of the wafer substrate. Surface tension allows removal of a 2–3-mm resist edge from the front resist surface while removing any back side resist coating. Acetone, ethyl lactate, and pentanone are possible solvent choices for edge bead removal processes.

5 RESIST BAKING—SOFTBAKE

5.1 Goals of Resist Baking

Baking processes are used to accomplish several functions and generally alter the chemical and/or physical nature of a resist material. Goals of resist baking operations may include the following, which are accomplished at various stages during resist processing:

Solvent removal
Stress reduction
Planarization
Reduction of resist voids
Reduction of standing waves
Polymer crosslinking and oxidation
Polymer densification
Volatilization of sensitizer, developer, and water
Induction of (acid) catalytic reactions
Sensitizer/polymer interactions

Polymeric resist resins are thermoplastic in nature, more amorphous than crystalline, and have glass transition temperatures in the 70 to 180°C range. Thermal flow properties are taken advantage of during processing, in which baking steps at or near the T_g allow some degree of fluid-like resist behavior. In a fluid-like state, stress in a coated film can be reduced and diffusion of solvents, sensitizer, and photoproducts is enhanced. At high resist baking temperatures, sensitizer and polymer decomposition can occur. A proper choice of the baking temperature, time, and method must therefore take into account the evaporation and diffusion properties of solvents, decomposition temperature of PAC or PAG, and diffusion properties of the photoinduced acid and base contaminants for chemically amplified resist materials.

5.2 Resist Solvent and T_g Considerations

There is a relationship between a solvent's evaporation rate or boiling point and the residual solvent content in a resist film. Obtaining such a relationship is difficult, however, because residual solvent is highly dependent on the T_g of the resist. If a baking process does not sufficiently reach the resist T_g, it is difficult to remove solvent to levels below a few percent [30]. The resist T_g therefore plays an important role in the evaporation mechanisms of resist solvent removal. Solvent removal has been shown to occur in two stages. The first stage is the diffusion of solvent molecules at temperatures near T_g and their accumulation at the film surface. The second stage is the evaporation of these adsorbed molecules at higher temperatures, dependent on hydrogen bonding properties.

No compaction would be expected if baking temperatures above the resist bulk T_g values were not reached. In fact, soft bake temperatures 10–20°C below a bulk resist T_g are frequently employed with quite successful results. The reason for this is that the T_g of a resist film is not identical to that of bulk resist. It may actually be a great deal lower. This can be explained by the concept of resist free volume, which is minimized if soft bake temperatures above the bulk T_g value are used. If resists are baked more than 5–10°C below the actual resist film T_g, compaction of this intrinsic free volume generally cannot occur [31].

Several resist material factors affect coated PHS film flow properties and may be modified for optimum CAR performance. In general:

Blocking of phenolic groups in PHS generally results in a lowering of T_g, a consequence of the decrease in hydrogen bonding between phenolic groups. A 40–50°C decrease in polymer flow temperature (T_f) has been reported with 25% blocking of PHS [32].

By modifying the molecular weight of the PHS polymer, 20–25°C of the loss in T_g or T_f due to blocking can be regained.

As the number of phenolic groups is increased (relative to t-BOC protective groups), the deprotection temperature is reduced.

As the number of phenolic groups is increased, T_g is also increased.

These relationships can result is a difficult situation if the deprotection temperature is forced lower than the resist T_g. Further manipulation may be possible through the use of copolymerization or by introducing additional hydrogen bonding sites.

There is a trade-off in determining the optimal soft bake temperature. A high soft bake temperature is desired so that the resist film T_g approaches that of the bulk, which leads to the best thermal performance. But at lower soft bake temperatures, an increase in postexposure acid diffusion is made possible, allowing a reduction in standing waves. To accommodate a lower soft bake temperature, a higher postexposure bake (PEB) may be needed to achieve adequate thermal and plasma etch performance properties (see Section 7 for additional description).

IPR2016-01378 Page 0016

5.3 Softbake

Resist films are coated from a polymer solution, making solvent reduction of a coated film a primary action of soft bake (or prebake). Other consequences of soft baking include a reduction of free volume and polymer relaxation, which have been suggested to be important phenomena that affect resist process performance [33]. Prior to coating, photoresist contains between 65 and 85% solvents. Once cast, the solvent content is reduced to 10–20% and the film can still be considered in a "liquid" state. If it was exposed and processed at this point, several adverse consequences would result. At this high solvent level, the film is tacky and highly susceptible to particulate contamination, which can be transferred through handling to subsequent steps. Also, inherent stress resulting from casting a thin film leads to adhesion problems. The most significant impact resulting from the elimination of a soft bake step is lack of dissolution discrimination between exposed and unexposed resist. With such high solvent levels, the expanded resist volume allows a high degree of dissolution regardless of the state of inhibition, protection, acceleration, or crosslinking. Ideally, a solvent content of a few percent would be desirable. Further densification could then be allowed to control the small molecular diffusion properties. To achieve this, the baking operation must approach the boiling point of the casting solvent (on the order of 140°C for conventional solvent systems). At this elevated temperature, decomposition of the resist sensitizer is likely to occur since DNQ decomposition temperatures are on the order of 100–120°C. Some residual solvent may also be desirable for DNQ/novolac to allow water diffusion and conversion of ketene to ICA. Complete solvent removal at prebake is therefore not attempted; instead adequate removal to allow the best exposure and dissolution properties is targeted. Figure 5 shows the development rate versus soft bake temperature for a DNQ/novolac resist. Four zones exist: (I) a no-bake zone where residual solvent and dissolution rates are high; (II) a low-temperature zone (up to 80°C) where the dissolution rate is reduced due to solvent removal; (III) a midtemperature zone (80–110°C) where DNQ is thermally converted to ICA, leading to an increase in development rate; and (IV) a high-temperature zone (>120°C) where film densification occurs, DNQ is further decomposed, and water is removed, leading to an increase in inhibition rather than acceleration. Also, at these temperatures, oxidation and crosslinking of the novolac begin [34].

Whereas a prebake for DNQ/novolac is required to bring the resist to a state suitable for subsequent exposure and development, control to ±1°C is generally adequate to ensure consistent lithographic performance. This is not the case for chemically amplified resists based on PHS, however. Because acid diffusion is an integral part of both positive and negative acid-catalyzed resist, control of polymer composition and density is critical. Consideration for soft bake differs for high-, mid-, and low-E_a CAR resists depending on the reactivity of the resist to acid-induced deprotection. Resists with a moderate activation energy (E_a) had

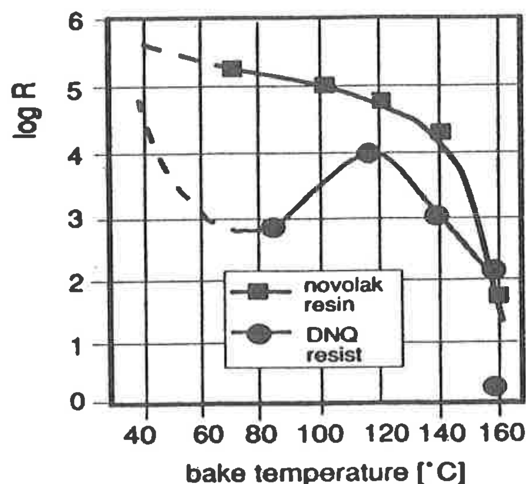

Figure 5 The influence of prebake temperature on dissolution rate (Å/min) for a novolac resin and a DNQ/novolac resist. Prebake time is 30 minutes, developer is 0.25N KOH. (From Ref. 34)

been the conventional route to positive CAR resists. By making use of resists with lower reactivity (high E_a), elevated baking processes above the polymer T_g (~150°C) allow maximum densification and reduction of the diffusion of acid-neutralizing contaminants. This resist design concept also reduces acid diffusion, which can result in an increase in resolution capability [35].

5.4 Resist Baking Methods

The preferred method of resist bake for IC applications utilizes conduction on a vacuum hot plate, usually in line with the entire resist process. Convection baking is another option, performed in an oven and generally used in a batch mode. Loading effects, slow recovery, and poor air circulation uniformity present problems for convection baking with current resist process demands. Microwave and infrared (IR) baking methods have been utilized to a limited extent, but the practicality of these methods is limited because of substrate incompatibility and process control. Both temperature and uniformity control are important for baking processes, the latter becoming most critical as chemically amplified resist requirements are considered. To achieve uniformity, careful consideration of the vacuum plate baking mechanics is required, including temperature uniformity, airflow, and cycle time. To meet the high demands of wafer-to-plate contact across an entire wafer, strict requirements are also placed on contamination control and resist edge bead removal.

Figure 6 shows the mechanisms involved during the first 10 seconds of baking on a vacuum hot plate. Figure 6a shows that the temperature of the wafer

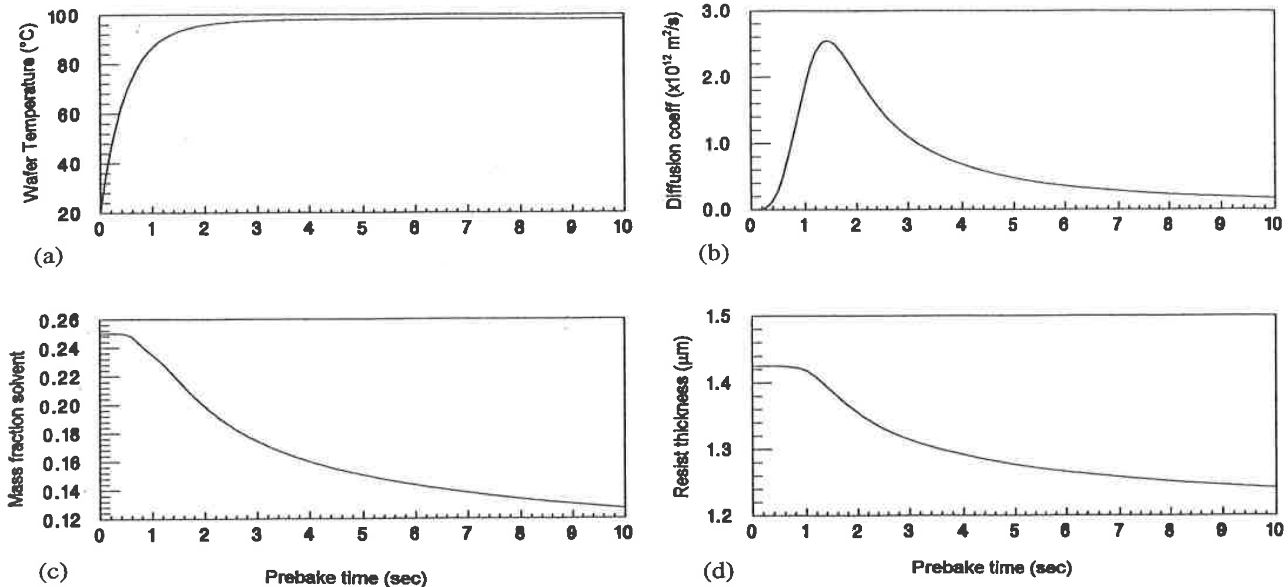

Figure 6 Mechanisms involved during the first ten seconds of hot plate baking of a resist. (a) Rise in wafer temperature; (b) solvent loss; (c) diffusivity; and (d) typical thickness change. [From Mack, C. A. et al., *Proc. SPIE, 2195,* 584 (1994)].

increases with a rapid rise during the first seconds of baking and levels off after 3 seconds. Figure 6b illustrates the solvent loss during this time, which continues to decrease well out to 10 seconds and beyond. Figure 6c shows the impact of baking time on diffusivity, which rises during the initial few seconds and then decreases. Figure 6d shows a typical change in resist thickness during baking, which decreases as the resist density increases.

6 PHOTORESIST EXPOSURE

6.1 Resist Exposure Requirements

Exposure of photoresist involves the absorption of radiation and subsequent photochemical change, generally resulting in a modification of dissolution properties. The absorption characteristics of a photoresist largely influence its resolution and process capabilities. Resists based only on exponential attenuation of radiation (i.e., with no mechanism for photobleaching or chemical amplification) can be limited by a maximum allowable contrast, sidewall angle and ultimate resolution. This is because of the inherent absorption trade-off required when imaging into a resist film. Both maximum transmission (to reach to the bottom of the resist) and maximum absorption (to achieve the highest sensitivity) are desired. There is therefore an optimum resist absorbance value for any resist thickness.

If a resist film has a thickness t and dt is the thickness of the bottommost portion of the resist, the intensity transmitted through the film thickness to dt can be determined from Beer's law:

$$I = I_0 e^{-\varepsilon mt} \tag{4}$$

where ε is the molar extinction coefficient of the sensitizer, and m is the molar concentration. The energy density absorbed at the bottom of the resist is

$$E = I_0 e^{-\varepsilon mt}(1 - e^{-\varepsilon mdt})/dt \tag{5}$$

Since dt is small, $e^{-\varepsilon mdt}$ can be approximated as $I - \varepsilon mdt$ and

$$E = I_0 \varepsilon m e^{-\varepsilon mt} \tag{6}$$

which is maximized when $\varepsilon mt = 1$. Converting to absorbance:

$$\text{Absorbance} = \log_{10} e \cdot \varepsilon mt = 0.434 \tag{7}$$

This is the optimum absorbance for a resist film regardless of thickness. In other words, higher absorption is desired for thinner resists and lower absorption is desired for thicker films. Resists for which chemical amplification or photobleaching is used introduce mechanisms that allow deviation from these constraints. The absorbance of a PAG for chemically amplified resist can be quite low because of the high quantum yield resulting from acatalytic reactions. Photobleaching resists (such as DNQ/novolacs) exhibit dynamic absorption properties, which can allow increased transmission toward the base of a resist film. For these resists, other absorption considerations are required.

The dynamic absorption that exists for DNQ occurs as exposure leads to a more transparent ICA photoproduct. This bleaching phenomenon can be described in terms of Dill absorption parameters A, B, and C [36]. The A parameter describes the exposure-dependent absorption of the resist, the B parameter the exposure-independent absorption, and C the rate of absorption change or bleaching rate. For a DNQ/novolac resist, the C parameter is conveniently related directly to resist sensitivity, since photobleaching corresponds to the conversion of the photoactive compound (PAC) to the photoproduct. (See Chapter 2 for a more detailed discussion of parameter characterization and modeling.) The choice of a specific DNQ compound for mid-UV lithography needs to include evaluation of the unique A, B, and C parameters at the wavelength of exposure. It is generally desirable to have low exposure-independent absorption (B parameter) to achieve maximum exposure efficiency to the bottom of a resist layer. Several approaches exist to minimize residual B parameter absorption of DNQ/novolac resists [37]. These have included the use of highly transparent backbones for multifunctional PACs and binding of the sensitizer to the novolac polymer. A large C parameter is also desirable for maximum sensitivity. Figure 7 shows absorbance spectra for two DNQ/novolac resists. Based only on the evaluation of the absorption prop-

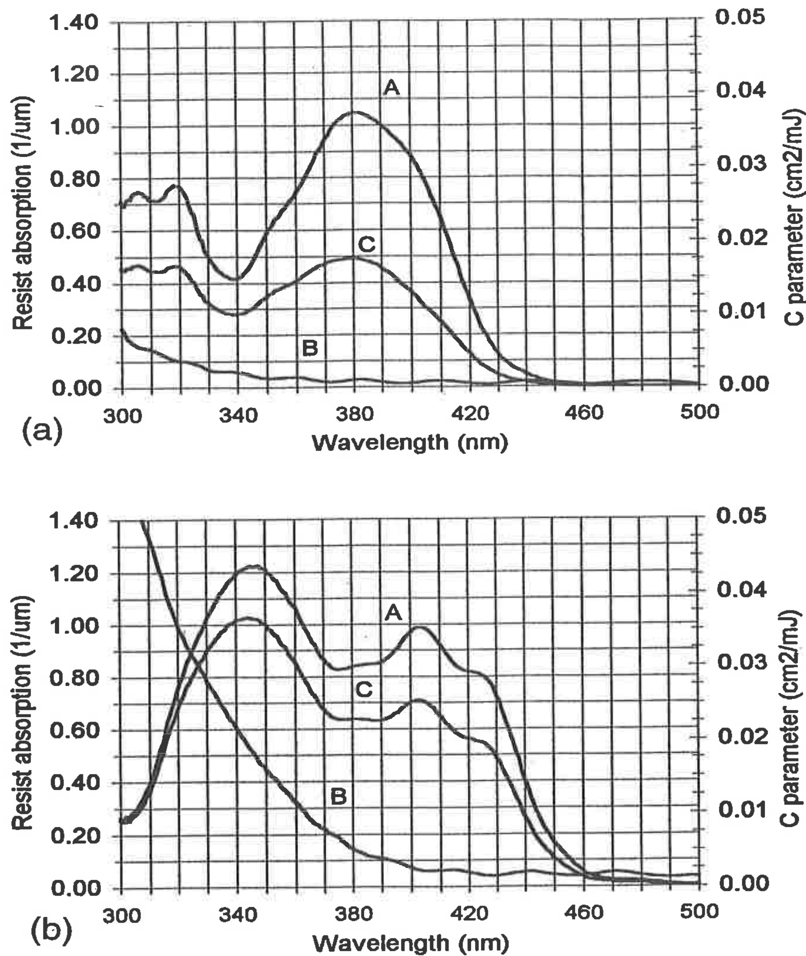

Figure 7 Absorbance curves for two DNQ/novolac resists showing Dill A, B, and C parameters. Resist (a) exhibits lower residual absorption (B parameter) at 365 nm while resist (b) has higher bleachable absorbance and speed (A and C parameters) at 436 nm. (From Prolith/2 V.5.0, 1997.)

erties of these two resists, it can be expected that the resist with a smaller *B* parameter and larger *A* and *C* parameters may perform better (at a specific exposure wavelength) in terms of sensitivity, sidewall angle, and contrast.

Chemical amplification is another avenue that exists to improve the absorption characteristics of a resist. With quantum efficiencies several orders of magnitude higher than what can be achieved for direct photomodified resists, only a small amount of photon absorption is needed. This can be quantified in terms of *A* and *B* parameters, which may be on the order of 0.30 μm^{-1} compared with the 0.90 μm^{-1} levels encountered with i-line materials. The downside of

such high transparency for resist materials is the increased opportunity for substrate reflection to degrade performance. These effects can be manifested as a line width variation over reflective steps (notching) and a sidewall standing wave. Figure 8 shows standing waves resulting from the coherent interference of incident and reflected radiation within a resist layer. Reduction of these standing waves is crucial in order to retain critical dimension (CD) control. This can be dealt with in either resist exposure or process stages and is ordinarily addressed in both. To reduce standing wave effects during exposure, the reflected contribution to exposure must be controlled. This can be accomplished by incorporating a dye in the resist formulation. Dyes such as coumarin or curcumin compounds have been used as additives to DNQ/novolac resists and are very effective at reducing the reflected exposure contribution in a resist layer at g-line and i-line wavelengths. By adding a dye, the exposure-independent absorption (*B* parameter) is increased. The result will be a decrease in reflection effects and standing waves but also a decrease in the amount of energy transferred toward the bottom of the resist. This will result in a decrease in sidewall angle, resist contrast, and sensitivity. Dyed resist for i-line use is therefore usually limited to highly reflective, noncritical layers.

Dyes that play a role in the chemistry of a resist system have also been introduced. By transferring the energy absorbed by a dye to the photosensitive component of a resist (for instance, through energy transfer or photoinduced electron transfer mechanisms), an active dye can allow reduction of reflection effects while maintaining sensitivity and resolution. This has been accom-

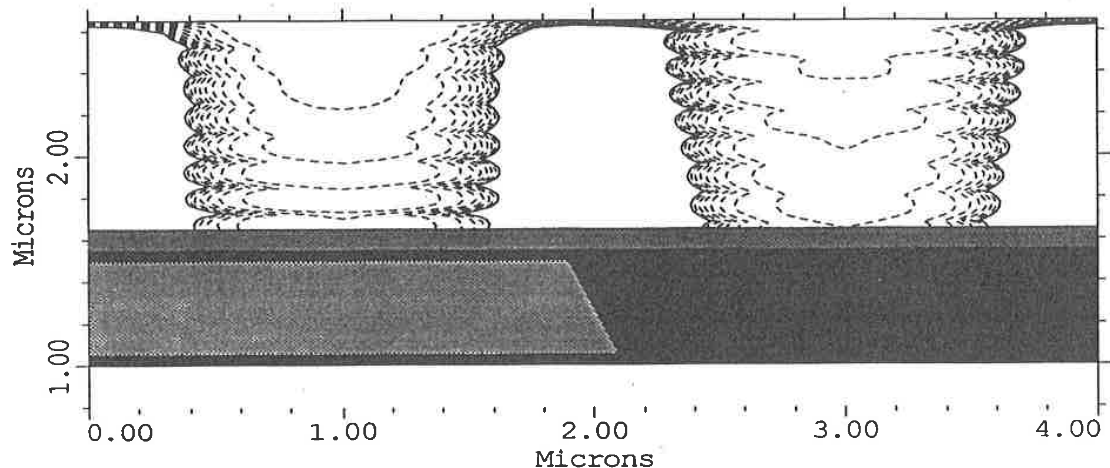

Figure 8 Resist standing waves resulting from coherent interference of incident and reflected radiation within a resist layer. Standing wave phase and amplitude is dependant on the underlying substrate.

plished in chemically amplified PHS resists [38]. The resultant increase in the resist B parameter in this case leads to an increase in photoinduced chemical activity, yielding minimal loss in resist performance. Loading of such photoactive dyes can be determined from the preceding analysis for static absorption resists. Resist absorbance on the order of 0.434 could be expected to be best suited for optimal throughput. An alternative to dye incorporation is the use of an anti-reflective layer below the resist. The requirements of current IC processes will soon demand that substrate reflectivity be reduced to levels below 1% for critical layers. The use of such antireflective coatings (ARCs) has become a popular practice for i-line and DUV lithography and is discussed in more detail in Chapter 10.

6.2 Resist Exposure and Process Performance

The sensitivity (E_0) described earlier is a bulk resist characteristic that is useful for resist process comparisons or non-feature-specific process optimization. Resist E_0 swing curves allow for instance the determination of optimum coating thickness values. Monitoring of clearing dose requirements is also useful for characterization of exposure or development uniformity. Through the use of an exposure response curve, as shown in Fig. 9, two additional bulk resist parameters can be obtained that allow further process characterization. Normalized

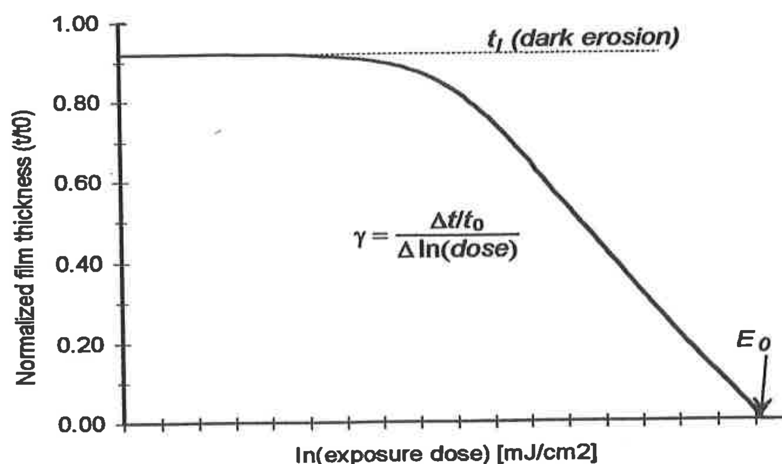

Figure 9 Normalized thickness as a function of $\log_e$-exposure for a positive resist of a given thickness, exposed and developed under specific process conditions. An area of linearity exists in the logarithmic relationship, which can be characterized using a single contrast term (γ). Resist clearing dose (E_0) is the point on the exposure dose axis where normalized thickness becomes zero and the normalized thickness loss (t_l) is an indication of the amount of resist erosion that occurs in unexposed regions.

thickness (normalized to initial predevelopment thickness) is plotted as a function of $\log_e$ exposure for a positive resist of a given thickness, exposed and developed under specific process conditions. An area of linearity exists in the logarithmic relationship, which can be characterized using a single contrast term:

$$\gamma = \frac{\Delta t / t_0}{\Delta \ln(\text{dose})} \tag{8}$$

where t is thickness and t_0 is the initial coating thickness. Resist sensitivity or clearing dose (E_0) is the point on the exposure dose axis at which the normalized thickness becomes zero. A third parameter that is useful for describing resist capability is a normalized thickness loss parameter (t_1), which is an indication of the amount of resist erosion that occurs in unexposed regions (also called dark erosion). An exposure response curve can be generated uniquely for any resist/development process or can be obtained from a more general development rate curve, described in greater detail in Section 8. Figure 10 shows a development rate curve, where resist dissolution rate is plotted as a function of $\log_e$ exposure dose for a positive resist. As exposure is increased, the dissolution rate increases. The linearity of this relationship can be realized on a log-log plot, but a lognormal plot is used here to demonstrate the relationship between a development rate and exposure response curve. Plotted along with dissolution rate in Fig. 10 is an exposure response curve for this resist coated at 9000 Å and developed for 60 seconds.

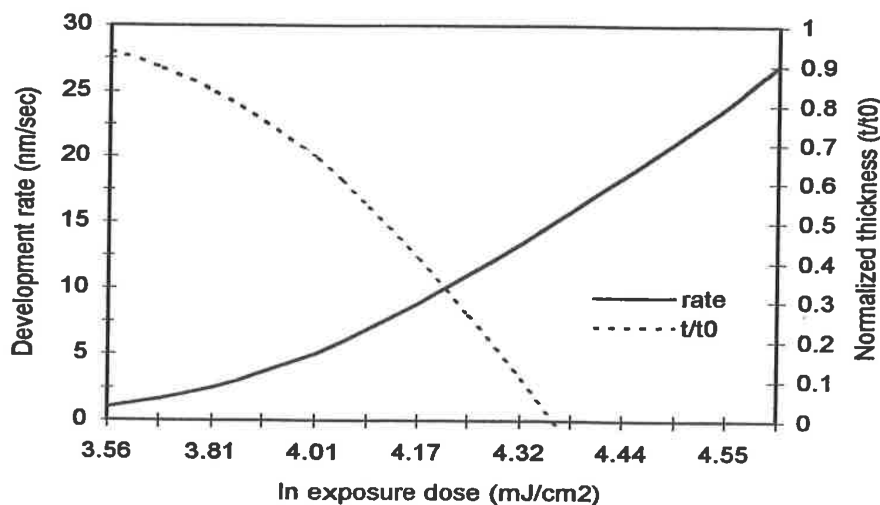

Figure 10 Resist dissolution rate (nm/sec) plotted as a function of $\log_e$ exposure dose for a positive resist. Plotted also is an exposure response curve for this resist coated at 9000 Å and developed for 60 seconds.

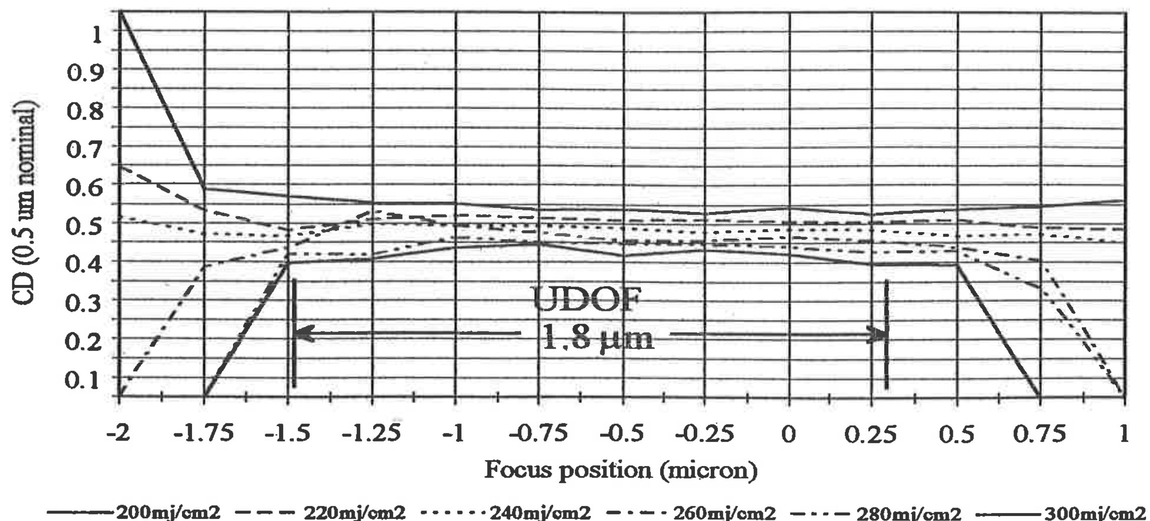

Figure 11 A focus exposure matrix for 0.5 μm dense line features in a positive i-line resist over polysilicon using a numerical aperture of 0.45 and partial coherence of 0.60. Resulting usable depth of focus (UDOF) is 1.8 μm for a CD specification of ± 10% and an exposure latitude requirement of 20%. The corresponding k_2 value for this single layer resist process is near 0.5.

6.3 Exposure and Process Optimization

In order to determine the optimum exposure dose (or range of doses) for a resist process, bulk resist characterization needs to be augmented with feature-specific characterization. To accomplish this, process specifications must be defined uniquely for each feature type and size, mask level, substrate, resist, and process. This is often a difficult task, because definition of an optimum process requires operation at a near-optimum level. The task is therefore an iterative one that can often be made easier through the use of lithographic simulation tools.

Consider the focus-exposure matrix in Fig. 11. Here 0.5-μm dense lines are imaged into an i-line resist with a projection system at a partial coherence of 0.5. Resist CD is plotted against focal position for a series of exposure dose values. The nominal focus setting is labeled 0.0 and is typically at a point near 30% from the top surface, depending on the resist refractive index and to a lesser extent NA and σ (for high NA values). At this position, there is an optimum exposure dose for printing a biased mask CD to its targeted size (see Chapter 3 for a description of mask biasing). As focal position is changed, the feature no longer prints at the target value; it is either too small or too large. The adverse influence of overexposure or underexposure is also increased. This

can be understood by considering an aerial image as it is varied through focus, as shown in Fig. 12. At best focus, a relatively large range of exposure variation can be tolerated. As defocus increases, a small amount of overexposure can result in a large amount of energy in shadow areas. Underexposure can result in insufficient energy in clear areas. An exposure must be chosen, therefore, to allow the greatest range of usable focus that results in a CD that remains within the specified target range. More appropriately, a specification is placed on the required exposure latitude to account for within-field and field-to-field nonuniformities. Together with tolerance limits on CD, a resulting usable depth of focus (UDOF) can be determined. For instance, for a ±10% exposure latitude requirement and a ±10% specification on CD, the optimum exposure from Fig. 11 is 240 mJ/cm² and the UDOF is near 1.8 μm. The resulting UDOF needs to be evaluated with respect to device topography. It should also be noted that any change is resist process will influence the depth of focus. Any process enhancement methods, whether optical or chemical, have the potential to improve focal depth. These can include the use of reflection suppression (e.g., with an ARC), modified PEB, enhancements of contrast, and improvements in developer selectivity. For evaluation purposes, it is convenient to express a normalized UDOF through use of the Raleigh DOF k_2 factor:

$$k_2 = \frac{(\text{UDOF})(\text{NA}^2)}{2\lambda} \tag{9}$$

The corresponding k_2 factor for the focus-exposure matrix of Fig. 11 is near 0.5. Generally, single-layer resist processes can produce k_2 in the range of 0.4 to 0.6.

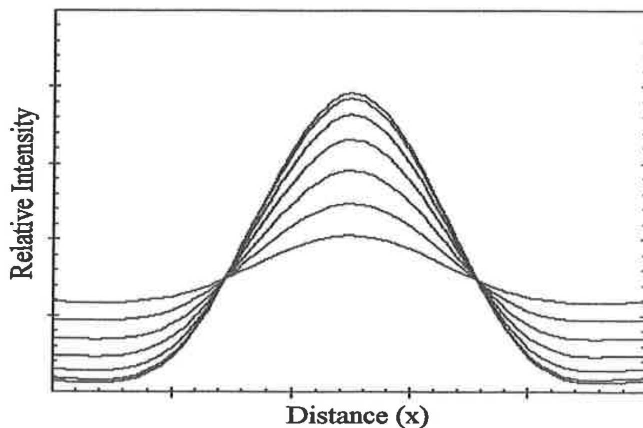

Figure 12 Through focus aerial images for ± 1λ/NA² of defocus. Images with no defocus can tolerate a large exposure variation. As defocus is increased, the choice of optimum exposure becomes more critical.

If a resulting k_2 does not correspond to UDOF values large enough for device topography, techniques of planarization may be required. Polymeric planarization is one alternative but is generally not considered to be robust enough to allow adequate process latitude for high-resolution IC applications. Chemical mechanical polishing (CMP) techniques, in which substrate surfaces are polished to reduce topography, are becoming commonplace in many IC process operations. From lithographic standpoint, CMP can be considered as operation that allows improvements in focal depth, CD tolerance, and exposure dose control.

A focus-exposure matrix can also be generated for resist sidewall angle, although this is a much more difficult task than for CD. Figure 13a shows sidewall angle focus-exposure matrix and Fig. 13b shows the corresponding array of resist feature profiles. At an optimum exposure dose value, the base CD of the features remains tightly controlled. At negative values of focus (corresponding to the bottom of the resist), there is a widening at the base of features. At positive focus values (toward the lens), feature thinning occurs. In order to evaluate the impact of these changes through focus and exposure, subsequent etch process selectivity and isotropy need to be considered. If overexposure or underexposure is used to tune CD over topography (corresponding to a shift in focal position), it is likely that the resulting feature sidewall angle will not be adequate. A growing trend in sidewall angle specification is >85°.

From these types of feature-specific process evaluation techniques, it can be understood why it is difficult to increase exposure throughput for a resist without adversely affecting overall performance. For features large enough that aerial image modulation is high (i.e., there is little energy in shadow regions and sufficient energy in clear areas), there will exist a good deal of exposure latitude and UDOF so that some degree of exposure tuning is possible. As features approach $R = 0.5\lambda/\mathrm{NA}$ in size, the situation becomes challenging for conventional binary masking and single-layer resists.

Line width linearity has already been discussed as it applies to optical imaging systems. Photoresist materials also behave with a nonlinear response to exposure, which can be seen in the exposure response and development rate curves in Figs. 9 and 10. These nonlinearities can be used to the advantage of the lithographic process. Because the modulation needed for small features is much lower than for large features, it would be expected that a resist that reacted linearly to exposure would do a poor job of faithfully reproducing mask features below $1\lambda/\mathrm{NA}$ in size. By tailoring the exposure and dissolution response properties of a resist to operate in a specific desirable nonlinear fashion (nonlinearity itself does not imply added capability), the linearity of the entire lithographic process can be improved. Figure 14 shows a plot of resist CD versus mask CD for an i-line resist process. Only as features approach 0.45 μm in size does the linear relationship between the mask and the resist

IPR2016-01378 Page 0027

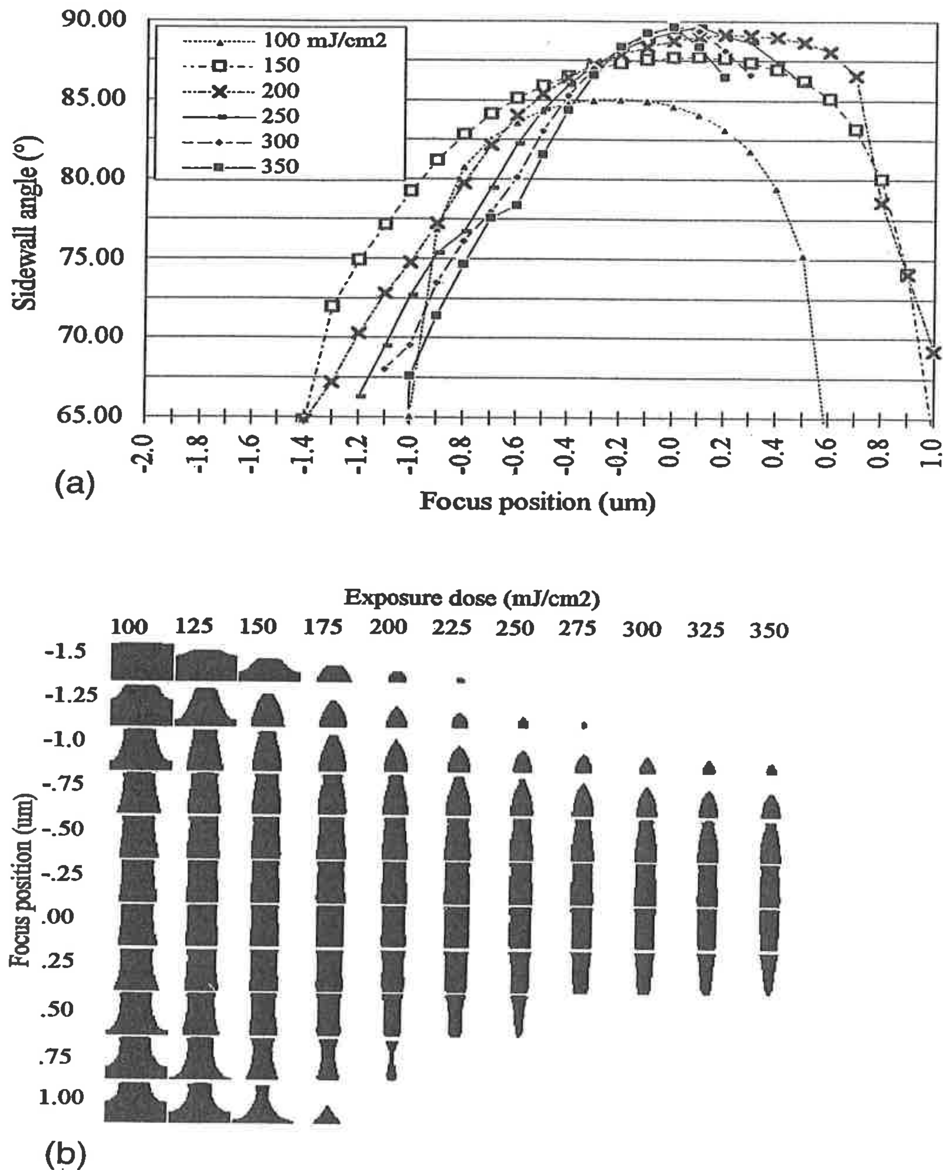

Figure 13 (a) A sidewall angle focus exposure matrix. UDOF can be determined from a sidewall angle specification and exposure latitude requirements. (b) Corresponding array of resist feature profiles.

feature begin to break down. Features in this region require unique mask biasing in order to print to their targeted size. The situation becomes more complex as various feature types are considered and resist linearity down to the minimum size of device geometry is desirable.

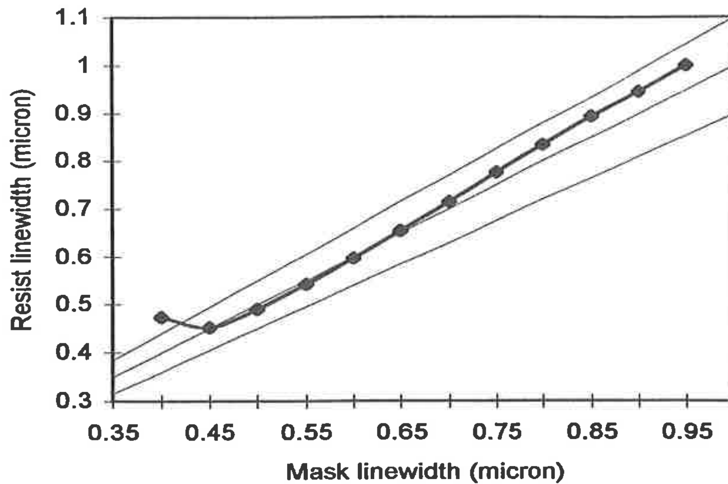

Figure 14 Plot of mask CD vs. resist CD for an i-line resist process. As features approach 0.45 μm, the linear relationship between mask and resist feature begins to break down. Features in this region require unique mask biasing in order to print to their targeted size.

7 POSTEXPOSURE BAKE

A postexposure bake (PEB) of DNQ/novolac resist brings about chemical and physical actions similar to those for prebake. By subjecting resist films to a predevelopment bake step at a temperature higher than that used during prebake, some DNQ decomposition prior to exposure can be reduced. By baking exposed resists at temperatures on the order of 5–15°C higher than prebake temperatures, solvent content can be reduced from 4–7% (prior to exposure) to 2–5%. Whereas prebake is generally performed to bring the resist into region II in Fig. 5, the elevated temperatures used for PEB places the resist toward region III. The most beneficial consequence of a PEB step is, however, not an extended action of earlier bake steps but instead a significant impact on standing wave reduction via thermal flow [39]. During exposure over a reflective substrate, coherent interference produces a distribution of intensity within the resist film. The nodal spacing is a function of the resist refractive index (n_i) and wavelength:

$$\text{Distance between nodes} = \frac{2n_i}{\lambda} \tag{10}$$

The amplitude of the resist standing wave will be affected by absorbance of the resist (α) (which may be dynamic if resist bleaching occurs), resist thickness (t), and reflectance at the resist-air (R_1) and resist-substrate (R_2) interfaces [40] resulting in a swing effect where

$$\text{Standing wave "swing"} = 4\sqrt{R_1 R_2}\,\exp(-\alpha t) \tag{11}$$

Interface reflectance values (R_1 and R_2) are determined from the complex refractive index values of the media involved:

$$\text{Reflectance} = \left(\frac{n_a^* - n_b^*}{n_a^* + n_b^*}\right)^2 \tag{12}$$

In addition to resist and substrate contributions to interference effects, exposure source characteristics need to be considered. The coherence length (l_c) for a radiation source is determined on the basis of the source wavelength (λ) and bandwidth ($\Delta\lambda$) as

$$l_c = \frac{\lambda^2}{\Delta\lambda} \tag{13}$$

As the resist thickness approaches the source coherent length, interference effects (standing waves) become negligible. A typical coherence length for i-line stepper tools may be on the order of 10 μm. For a 248-nm lamp-based step-and-scan system, l_c may be on the same order, but as excimer laser lithography is pursued, a 10^3–10^4 factor increase occurs. Although it is not expected that resist would be coated to thicknesses approaching 10 μm or more, the analysis offers insight into the increasingly critical concern with standing wave control. Considered together with the higher transparency (low α) of chemically amplified resist, it becomes obvious that resist imaging over reflective substrates using an excimer laser source would be difficult without employing means of control or compensation.

To demonstrate the impact that a PEB step can have on resist standing waves, consider Fig. 15. Unexposed regions of photoresist contain photoactive compound, exposed regions contain photoproduct, and the boundary between them is determined by the constructive and destructive interference nodes of the exposure standing wave. If the resist temperature is raised near or above its T_g, the PAC can effectively diffuse through the polymer matrix and produce an averaging effect across the exposed/unexposed boundary. This PAC diffusion is a function of the resist T_g, the PAC size and functionality, bake time and temperature, remaining solvent concentration, resist free volume, and (for DNQ/novolac, for instance) any binding between the PAC and the resin. Figure 16 shows the resist standing wave pattern as a function of the PAC diffusion length.

For chemically amplified resists based on thermally induced acid reactions, PEB is used to accomplish critical chemical stages and must be considered nearly as critical as exposure in terms of control, uniformity, and latitude requirements. The concept of a bake "dose" control is a convenient comparative metric to exposure dose control for acid-catalyzed deprotection (positive resists) or crosslinking (negative resists). An Arrhenius relationship exists between PEB

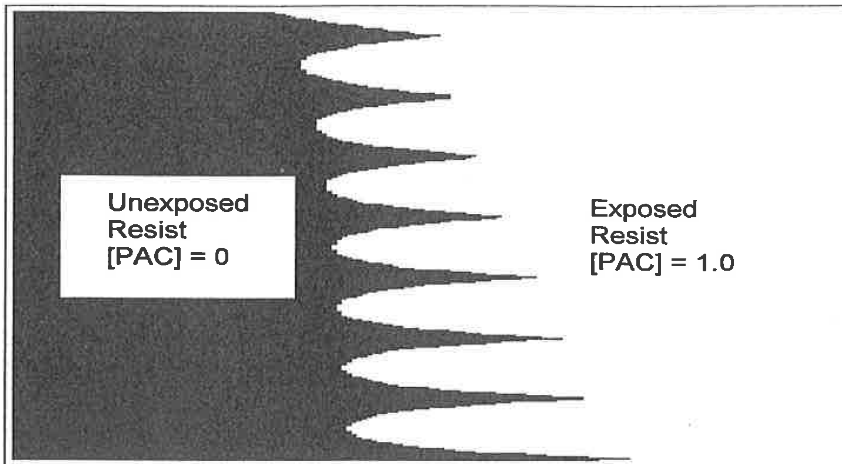

Figure 15 Distribution of photoactive compound (PAC) as a result of standing wave resist exposure. Unexposed regions of photoresist contain PAC, exposed regions contain photo-product. As the resist temperature is raised near or above its T_g, the PAC can effectively diffuse through the polymer matrix to reduce effective standing wave in the developed resist sidewall.

and exposure, such as that shown in Fig. 17 [41]. Here, log exposure dose is plotted against 1/PEB, from which an effective E_a can be determined. Whereas exposure uniformity on the order of ~1% is a current requirement for resist exposure tools, it can be expected that PEB control should be at least as critical. The rate of these reactions is a function of the acid concentration, the activation energy of the protected polymer, the diffusivity of the acid, and the PEB conditions.

Acid diffusion in PHS chemically amplified resists is generally on the order of 50 to a few hundred angstroms, limited by resolution requirements. If neutralization of acid occurs, the exposed resist dissolution rate decreases. If environmental contamination occurs after exposure and prior to PEB, a thin, less soluble inhibition layer forms on the top surface of the resist, which results in the formation of a characteristic T-top upon development, as shown in Fig. 18. Any delay between exposure and PEB (known as postexposure delay, PED) allows this phenomenon to occur. Early material PED time requirements were on the order of a few minutes. Newer resists may allow delays up to several hours. It is important to realize, however, that acid neutralization can begin immediately upon exposure and performance must be evaluated for the specific resist process conditions and process tolerances. Low-E_a resists do not require elevated PEB temperatures for reaction, which can minimize the control requirements for this process step. These resists cannot tolerate high baking temperatures, which may introduce additional stability problems. Choice of the

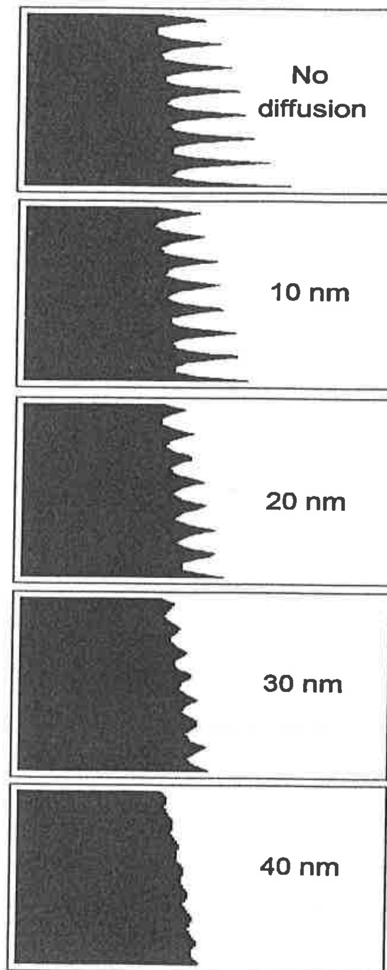

Figure 16 Simulated standing wave pattern in developed resist as a function of increasing PAC diffusion length.

PAG is less critical, allowing choices with smaller cross sections than those needed for high-activation-energy materials. Diffusion properties are also based on size and should be evaluated uniquely for resists of either category.

When determining PEB requirements for deprotection, postexposure solvent content and polymer density also need to be taken into consideration. Temperature control on the order of 0.1°C may be required, with uniformity needs on the same order over wafer diameters approaching 300 mm. Material improvements may relax this requirement somewhat, but control to a few tenths of a degree can be expected as an upper limit.

An additional improvement brought about through the use of a PEB step is a potential increase in resist development rate properties, specifically the dis-

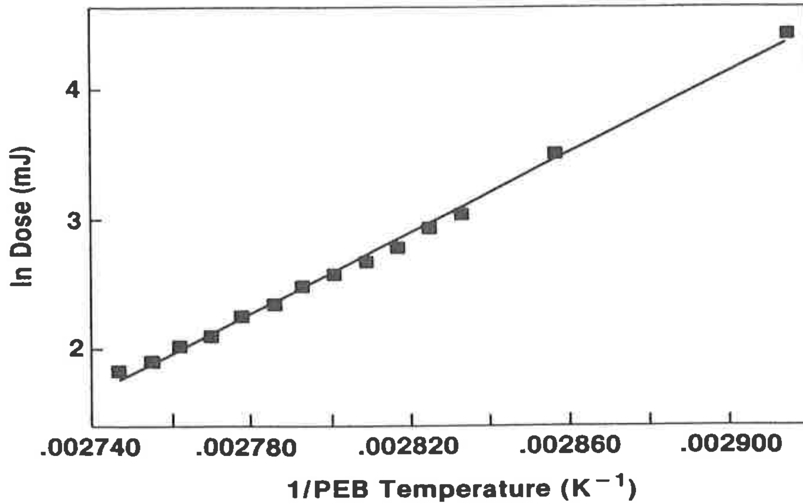

Figure 17 Arrhenius plot of resist sensitivity vs. PEB temperature for a DUV CAR resist. Dose required to print 0.5 μm lines with a 90 second bake is plotted against 1/PEB temperature. An effective activation energy can be calculated from such a plot (130 kJ/mole in this case). (From Ref. 41.)

solution rate log slope (DLS) as discussed in the development section [42]. This occurs as a result of the decrease in resist dissolution rate especially at the resist surface, which is more pronounced in some resists than in others. By reducing the surface dissolution rate, unexposed film erosion can be reduced, resulting in an increase in sidewall slope and an improvement in process latitude. This surface modification is a result of solvent loss and a possible surface "skin" effect, enhanced by resist modification at elevated temperatures.

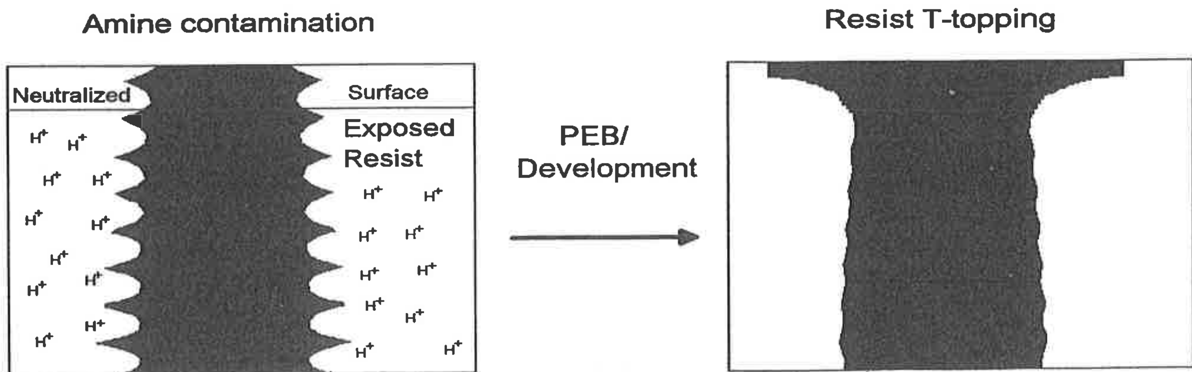

Figure 18 Environmental amine contamination of a chemically amplified (PHS) resist resulting in "T-top" formation after development.

For optimal process performance, PEB processes for chemically amplified PHS resists cannot be considered separately from soft bake steps. There are trade-offs between high and low levels of each. During soft bake of a chemically amplified PHS-based resist, standing waves can be reduced through use of lower temperatures, which allow an increase in acid diffusion across the exposed/unexposed resist boundary. To reduce T-top formation, a high PEB is also desirable. Through use of high PEB temperatures, deprotection can occur even with some degree of reduced acid concentration at the resist top surface. This low soft bake, high PEB combination can result in additional undesirable phenomena. When the resist film is allowed to retain a relatively low T_g, pattern deformation can result from rapid PHS deprotection and subsequent gas evolution at high PEB temperatures. A stepwise PEB has been suggested as a possible solution [43]. An initial low-temperature stage removes protective groups from the bulk of the resist with minimum deformation. A high-temperature stage follows to enhance top surface deprotection and reduce T-top formation.

As discussed earlier, intrinsic or added free volume will affect the glass transition and dissolution properties and deprotection mechanisms of phenolic-based photoresists. The CAR deprotection reaction itself has also been shown to contribute additional free volume [44]. Exposure or PEB-induced variation in resist density can affect dissolution uniformity and CD control. This added influence of exposure and PEB can lead to complex relationships and increased control requirements. The deprotection and densification mechanisms can best be separated in resist systems with low activation energies.

8 RESIST DEVELOPMENT

Resist systems based on solvent development, such as crosslinking bis-arylazide *cis*-polyisoprene negative resists, require some degree of swelling to allow removal of soluble polymer chains or fragments [45]. To keep resist pattern deformation to a minimum, a series of solvents is generally needed for development, with careful consideration of kinetic and thermodynamic properties [46]. The development of resists based on novolac, PHS, or other phenolic resins involves similar dissolution stages but does not require such adverse swelling for dissolution [47–49].

8.1 Dissolution Kinetics of Phenolic Resin Resists

In novolac resins, a narrow penetration zone is formed as water and hydroxyl groups are incorporated in the novolac matrix. This zone is rate limited and does not encompass the entire resist layer, allowing dissolution of resist with minimal swelling. Following the formation of this intermediate layer, phenol is deprotonated and the resulting phenolic ion reacts with water. The negative

charge of the phenolate ion is balanced by the developer cations. Upon sufficient conversion of phenol groups, the polymer is soluble in aqueous alkaline developer. A three-zone model has also been suggested, as shown in Fig. 19 [50]. These zones exist during novolac development:

1. A gel layer containing water, TMAH (base), and partially ionized novolac. The thickness of this layer depends on agitation, novolac microstructure, and the developer cation.
2. A penetration zone with a low degree of ionization. The thickness of this zone also depends on the novolac structure as well as the developer cation size and hydrophobicity.
3. Unreacted bulk novolac resist.

The resulting dissolution rate of a resist material is determined by the formation of the gel and penetration layers and the subsequent dissolution of the gel layer into developer.

In DNQ/novolac resists, exposure of the PAC leads to photoproduction of ICA, which acts as a dissolution accelerator. First-order kinetic models for development are based on this mechanism (see, for instance, Chapter 2). DNQ in sufficiently high concentrations (5–25 wt. %) also acts as a dissolution inhibitor to the phenolic novolac resin, decreasing its hydrophilic nature (enhanced development models described in Chapter 2 also account for this phenomenon). This inhibition effect can also be accomplished with other compatible compounds and is not limited to DNQ. It might be reasoned that a similar mechanism would exist for PHS resins, but this is not the case. Although

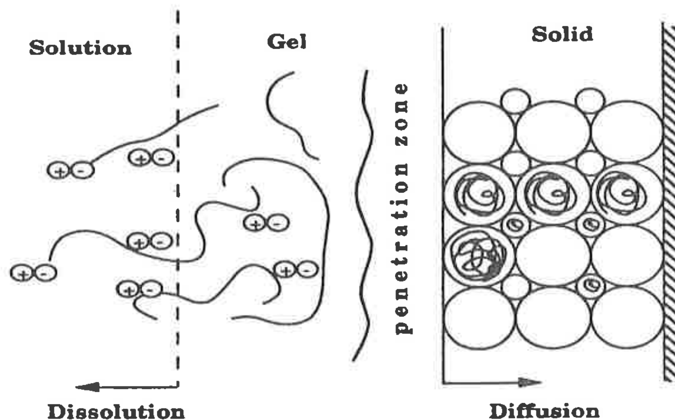

Figure 19 Diagram of a three zone novolac dissolution model with a gel layer containing water, base, and hydrated, partially ionized novolac chains; a penetration zone; and unreacted novolac. (From Ref. 50.)

the dissolution of novolac can be decreased when combined with DNQ by as much as two orders of magnitude, the high dissolution rate of PHS is not significantly reduced. This can be explained by considering the hydrophilic nature of both materials. Novolac is for the most part a hydrophobic resin with hydrophilic sites created when developer reacts with hydroxyl groups. These phenolate ion positions allow a diffusion path for development. The sites of hydroxyl groups are only potential hydrophilic sites, which can be tied up or isolated by the polymer's large aromatic rings. PHS is a vinyl polymer with no aromatic rings in the backbone. Hydroxyl groups exist in a "corkscrew" configuration along the polymer chain, allowing very effective diffusion paths and extremely high dissolution rates.

The dissolution kinetics of chemically amplified resists based on PHS are also quite different from those for DNQ/novolac. Whereas the dissolution of novolac resins is determined by two competitive reactions (inhibition by the DNQ and acceleration resulting from the developer-induced deprotonation of the novolac), there is one primary rate-determining stage for two-component PHS chemically amplified resists. A similar developer-induced deprotonation of phenolic hydroxyl groups has been shown to dominate for negative resists, whereas developer penetration into hydrophobic t-BOC-protected PHS is rate determining for positive resists [51].

8.2 Development and Dissolution Rate Characterization

Development of conventional resist materials is based on imagewise dissolution discrimination. To understand and optimize photoresist development, it is necessary to characterize exposure-dependent dissolution properties. As discussed earlier, the extraction of development rate and exposure relationships allows tremendous insight into the imaging capabilities of a resist process. Shown in Fig. 20 is a family of normalized thickness versus development time curves for a resist material exposed at various dose levels. Such curves can be obtained using laser interferometry techniques and separate substrate exposure [52,53] or a single substrate and multiple exposures [54]. A development rate versus exposure curve such as that in Fig. 21 can be produced from a family of these dissolution curves. To characterize fully the dissolution properties of a resist throughout its entire thickness, a rate curve may not suffice, because development rate is a function of resist thickness. Surface inhibition reduces the development rate significantly at the top surface of the resist. Figure 22 shows a development rate versus resist thickness curve demonstrating that development rate increases from the top surface of the resist toward the bottom.

When development rate and exposure are plotted in a log-log fashion, as shown in Fig. 23, a linear region exists that can be described in terms of a development rate log slope (DLS):

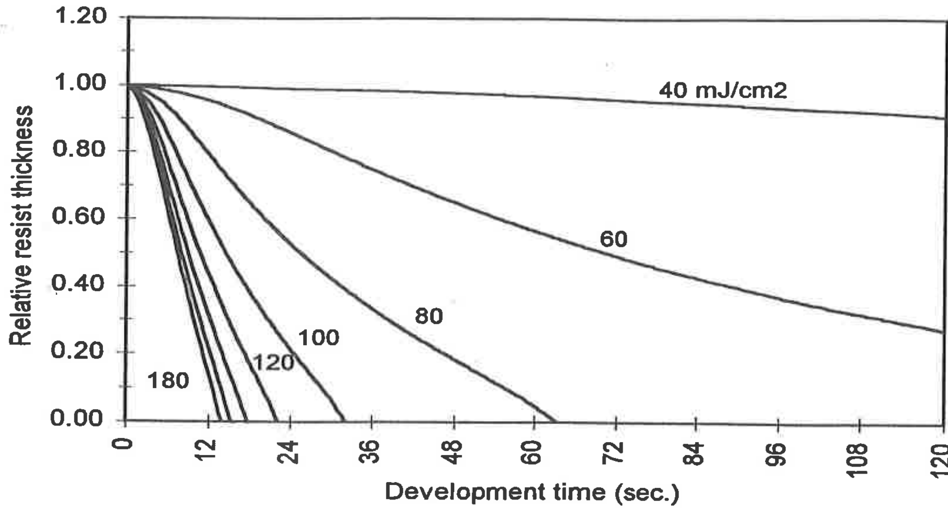

Figure 20 Normalized film thickness versus development time curves for resist exposed at 40 to 180 mJ/cm². Selection of single development time values can lead to development rate vs. relative exposure curves.

$$\mathrm{DLS} = \frac{\partial \ln(\text{dev. rate})}{\partial \ln(\text{dose})} \tag{14}$$

Dissolution rate contrast can be expressed as

$$\text{Contrast} = \frac{R_{\max}}{R_{\min}} \tag{15}$$

where $R_{\max}$ and $R_{\min}$ are the maximum and the minimum development rate, respectively. Together, DLS and dissolution rate contrast are effective measures

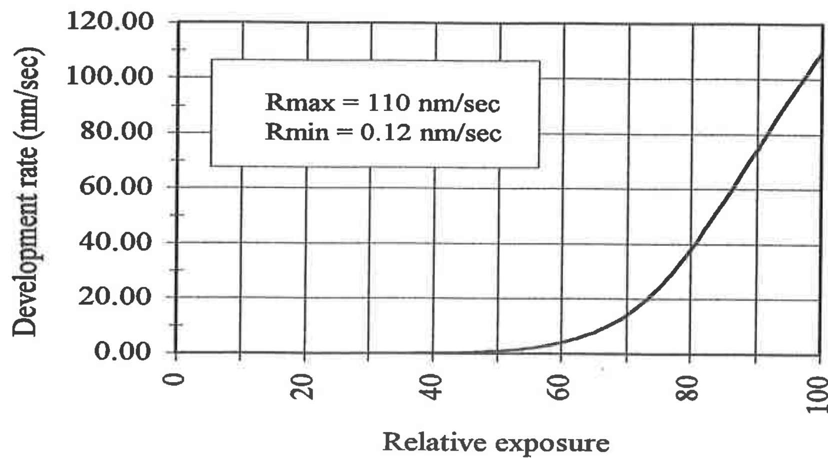

Figure 21 A development rate vs. relative exposure curve from Figure 20.

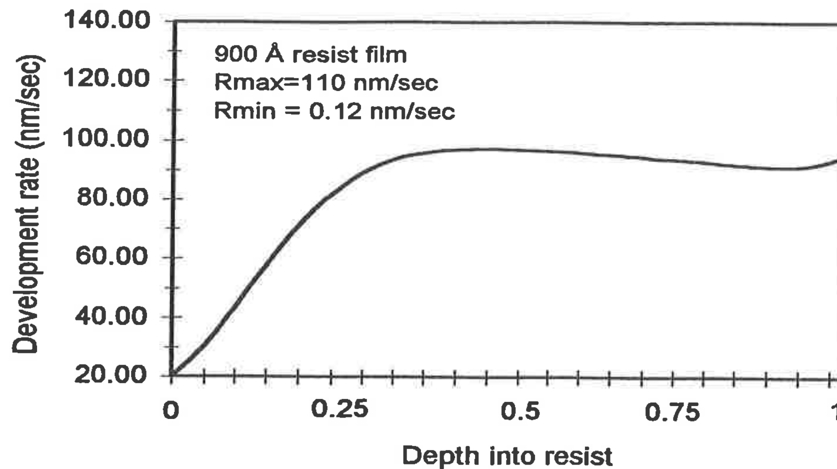

Figure 22 A development rate vs. resist thickness curve, showing distribution of dissolution properties through a resist film.

of the dissolution properties of a resist material. High levels of both metrics are desirable. Control of the resist and development properties can be used can be used to some extent to influence performance. A moderate contrast value near 10,000 is generally sufficient. As developer normality is changed, R_{max} and R_{min} are both affected (as long as base concentration does not fall below a critical level, pH ~12.5), but their ratio and the shape of the curve remain fairly constant [55]. The R_{max} is primarily a function of the polymer itself. Major resist, sensitizer, and solvent factors that influence development rate include:

Polymeric structure
PAC/PAG/inhibitor structure
PAC/PAG/inhibitor concentrations (DNQ loading >20%)
Protection ratio (PHS protection ratio >25%)
Solvent concentration
Polymeric molecular weight (>1.3×10^4 g/mol)
Polydispersity (<3)
Developer composition (metal ion vs. TMAH)
Developer cation size and concentration
Resist surfactant
Resist dissolution inhibition/acceleration state
Developer surfactant

Hydroxyl group positions on PHS polymer also affect the dissolution rate, a function of hydrogen bonding and steric hindrance with the polymer backbone

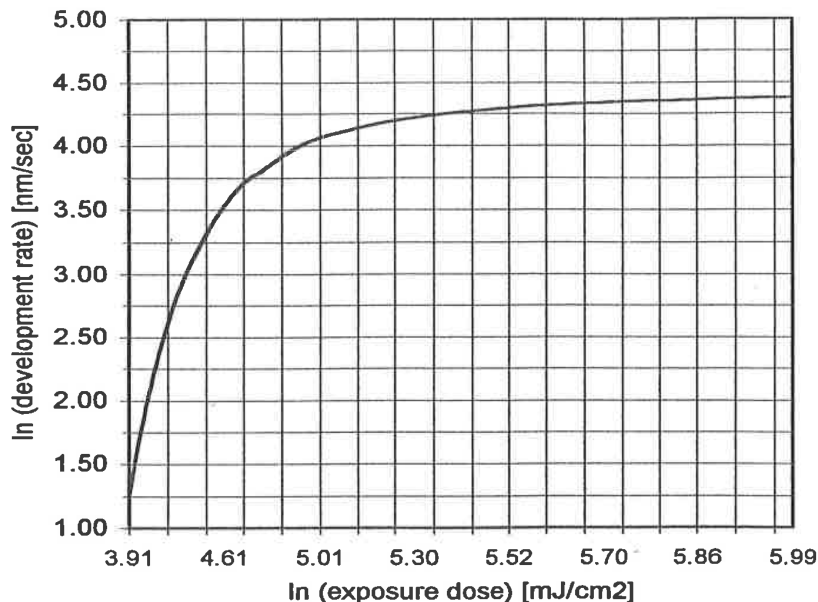

Figure 23 Log development rate vs. log exposure dose. Dissolution rate performance can be evaluated in terms of the slope of the linear region of the curve and the R_{max}/R_{min} ratio.

[56]. Copolymers of 2- and 4-hydroxystyrene have been shown to allow control of PHS dissolution properties.

8.3 Developer Composition

Phenolic resin–based resists can be developed using buffered alkaline solutions such as sodium metal silicates. These metal silicate developers yield a maximum development rate and low dark erosion, compared with most other developer choices. Possible metal ion contamination of devices has nearly eliminated the use of this class developer, however, in favor of metal ion–free tetramethylammonium hydroxide (TMAH). Furthermore, standardization of TMAH developer formulations is becoming widespread, as it is more economical and allows better quality control if there are no requirements for coexistence of several developer types. The larger cross section of TMAH compared with NaOH leads to lower development rates, which may result in lower working sensitivities. TMAH developer concentrations in the range of 0.2 to 0.3 N allow sufficient sensitivity with high contrast and minimum erosion. A 0.26 N solution is becoming a standard for U.S. and overseas resist processing.

In addition to TMAH, surfactants are added to a developer to reduce development time and scumming. Surfactants are used as additives to photoresists,

chemical etchants, and developers to improve surface activity or wetting. TMAH developers often employ surfactants at the ppm level to reduce surface tension. Surfactants are especially useful for improving the dissolution of small-surface-area features such as contacts or small space features. By increasing the effective wetting of the developer, scumming problems can be minimized and overexposure- or overdevelopment-induced process biases can be reduced. Also, through the use of developer surfactants, initial development inhibition at the resist surface can be reduced. Additives used for resist developers are mainly of the nonionic variety with hydrophilic and hydrophobic structural characteristics, such as ethylene oxide/propylene oxide block polymer segments with molecular weights near 1000. Concentrations may be up to 800 ppm or 0.05 wt. %. Surface tension decreases as the concentration of surfactants increases until a critical micelle concentration (CMC) is reached. This CMC level represents an equilibrium state at which aggregation begins. Very small changes in the structure of surfactant molecules have been shown to result in large changes in resist development performance. The number and location of hydroxyl groups in the molecular structure of the surfactant determine the activity of surface dissolution during development [57]. The behavior of developer surfactants also depends on resist material properties. Resists that have a larger degree of surface hydrophobicity benefit most from surfactant additives and have been shown to be less dependent on surfactant type. The benefits gained for a particular resist therefore depend on unique resist and surfactant properties and interactions. Figure 24 shows how surface agents acting at a resist/developer interface enhance the surface activity by decreasing surface free energy [58].

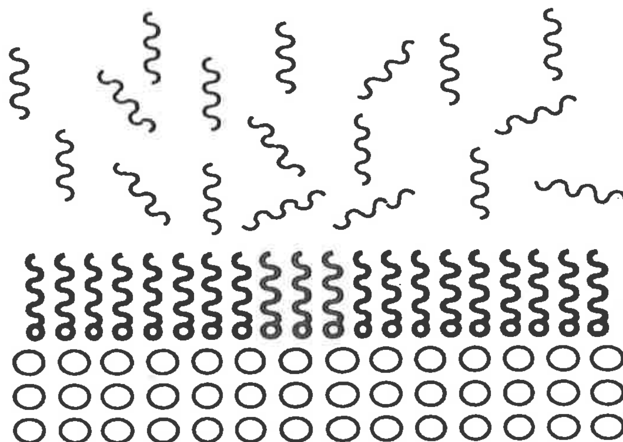

Figure 24 Orientation of surface molecules (center) at a hydrophobic (top) / hydrophilic (bottom) interface. The surfactant molecules are oriented so as to lower the interfacial free energy. (From Ref. 58.)

In addition to the chemical composition of the developer, the concentrations of hydroxyl ions, developer cations, and anions have been shown to strongly influence the dissolution rate of pure novolac films [59]. As the cation concentration is increased, a linear increase in dissolution rate occurs at a constant pH, apparently independent of anion concentration [60]. The structure of the developer cation and anion will determine the maximum allowable concentration before a decrease in dissolution rate begins. Along with the dissolution dependence on the size of the developer cation, its hydrophilicity and the T_g of the partially ionized novolac also influence the development rate [61].

Development temperature is important and requires tight control. This is true not only for the bulk development reservoir and plumbing but also for the development bowl and development atmosphere. The rate of dissolution for TMAH developers follows an Arrhenius relationship:

$$k = A_0 e^{-Ea/RT} \tag{16}$$

with an apparent negative activation energy (E_a) [62]. The reason for this is a highly exothermic sequence of deprotonation steps. A decrease in development temperature results in increased activity, which can seem counterintuitive. This is not the case for development with NaOH or developers with similar chemistry, since no exothermic reactions exist.

8.4 Development Methods

Resist dissolution properties are highly dependent on the development method employed. Development methods commonly used for conventionally coated wafer substrates include static immersion, continuous spray with slow rotation (~500 RPM), and stationary or slow rotation puddle development.

Spray development involves one or more spray nozzles to dispense developer toward the wafer substrate. Processes using ultrasonic atomization of developer allow relatively low velocity dispersion and minimal adiabatic cooling effects during the dispensing. For conventional spray development, the resist dissolution rate has been shown to be relatively insensitive to spray nozzle pressure but linearly dependent on spin speed [63]. With ultrasonic spray development, dissolution variation and resist erosion can result from poor control of the nozzle spray pattern. Dissolution rate and uniformity are also dependent on the uniformity of the spray pattern directed toward the wafer. To minimize nonuniformities, wafer chuck rotation must be carefully controlled at fairly low speeds (100–500 RPM) to ensure adequate developer replenishment. It is for these reasons, along with the excessive developer volume dispensed during processing, that puddle processes are now most common for high-volume production.

Puddle development techniques can improve the tool-to-tool matching of development processes. In addition, the control of puddle development processes

over time is significantly better. For optimal performance, flow is kept low to reduce variations in development rate at the edge of the wafer. The dispensed volume of developer should also be kept low to minimize chemical costs and back side wetting but not so low as to cause localized nonuniformities or scumming. The dispensed volume should be carefully controlled to ensure full and uniform coverage of the entire resist surface. During a puddle development process, slow rotation or single rotation may be used to disperse trapped air and provide agitation. If a surfactant-free developer is used, an increase in dispensing pressure may be required to enhance resist wetting.

There are several trade-offs to consider when making a choice between spray, puddle, and immersion methods. Although immersion development can lead to minimum erosion by physical removal of resist, it is not well suited to the in-line processing that now dominates in production. During puddle development, chemical activity decreases with time as the small developer volume becomes exhausted, a situation that is not encountered during immersion processing. There is a more subtle difference between these two techniques as the depletion of developer additives is considered. At ppm levels, surfactants can be exhausted during static immersion development, significantly changing the chemical nature of the developer with time. Since puddle development introduces fresh chemistry for every wafer, consistent wafer-to-wafer development can be ensured. A multiple-puddle method of development [64] is now commonplace in wafer processing and usually involves two development stages. The process consists of dispensing developer onto a wafer and allowing it to remain for a short time (10–20 seconds). It is then spun off and a second puddle is formed and allowed to complete the process (20–30 seconds). Although such multiple-puddle processes serve to replenish developer to the resist, the effect that makes this technique most attractive is an inhibition that occurs between development cycles. The dissolution of unexposed or partially exposed resist will be preferentially slowed at the location of the resist front after the end of the first development step. This phenomenon can be enhanced if rinse and spin-dry steps are added between development cycles [65]. The inhibition may be a result of base-induced oxidation or azo coupling of the novolac. It has also been suggested that a surface modification occurs with interrupted development and an increase in surface energy can enhance resist dissolution discrimination [66]. Multiple development step processing has been also reported and variations on these techniques are now widespread [67]. Intermediate development baking processes have also been investigated [68]. Figure 25 shows resist film thickness plotted as a function of exposure dose for double-puddle and warm-air intermediate development baking processes. Resist contrast is effectively increased with the use of the warm-air bake.

It is important to rinse remaining chemicals from the wafer surface after development because inadequate removal can result in high defect levels. Not

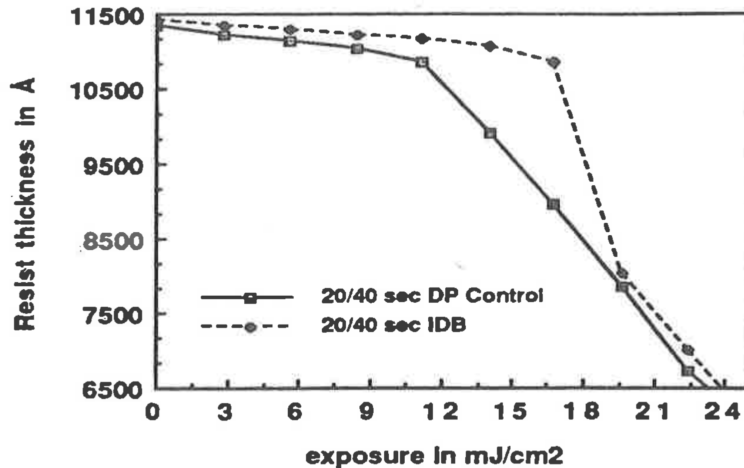

Figure 25 Resist film thickness vs. exposure dose for interrupted double puddle (DP) development and for 50°C warm water intermediate development bake (IDB) showing improvement in resist contrast with IDB. (From Ref. 68.)

only a top-side rinse but also a back side rinse is needed to remove developer and contaminants that could be transferred to subsequent process steps.

8.5 Development Rate Comparison of I-Line and DUV Resists

Although similarities exist between the dissolution properties of DNQ/novolac and PHS-based chemically amplified resists, comparison of these materials demonstrates salient differences in their performance and capabilities. Development rate curves are the tools best suited for this type of comparison. Shown in Fig. 26 are development rate curves for an i-line DNQ/novolac resist, a negative DUV chemically amplified resist, and a positive DUV chemically amplified resist [69]. The negative DUV resist is a three-component acid hardening resist based on a phenolic resin (PHS), a melamine crosslinker, and a photoacid generator [70]. The positive DUV resist is a t-BOC-protected PHS and a photoacid generator [71]. The rate curve for the i-line resist (Fig. 26a) shows a nonlinear dissolution rate that can be divided into three regions. The ability of this resist to achieve high contrast (γ) is evident from the steep development rate log slope (DLS). A large development rate contrast (R_{max}/R_{min}) also exists, leading to high sensitivity and low erosion properties. Figure 27a shows an Arrhenius plot for this resist, where three distinct regions also exist: (I) a high-dose, low-temperature region where E_a is small and positive, (II) an intermediate region where E_a is negative and decreasing, and (III) a low-dose, high-temperature region where E_a is positive and comparatively large. These re-

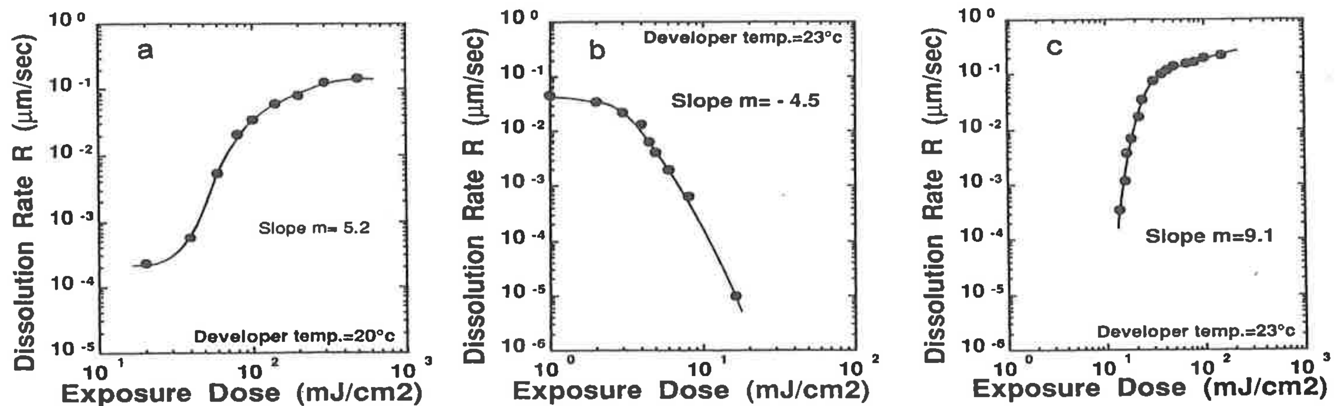

Figure 26 Log development rate curves for (a) an i-line DNQ/novolac resist; (b) a negative DUV chemically amplified resist; and (c) a positive DUV chemically amplified resist. Slope is the development rate log slope (DSL). (From Ref. 69.)

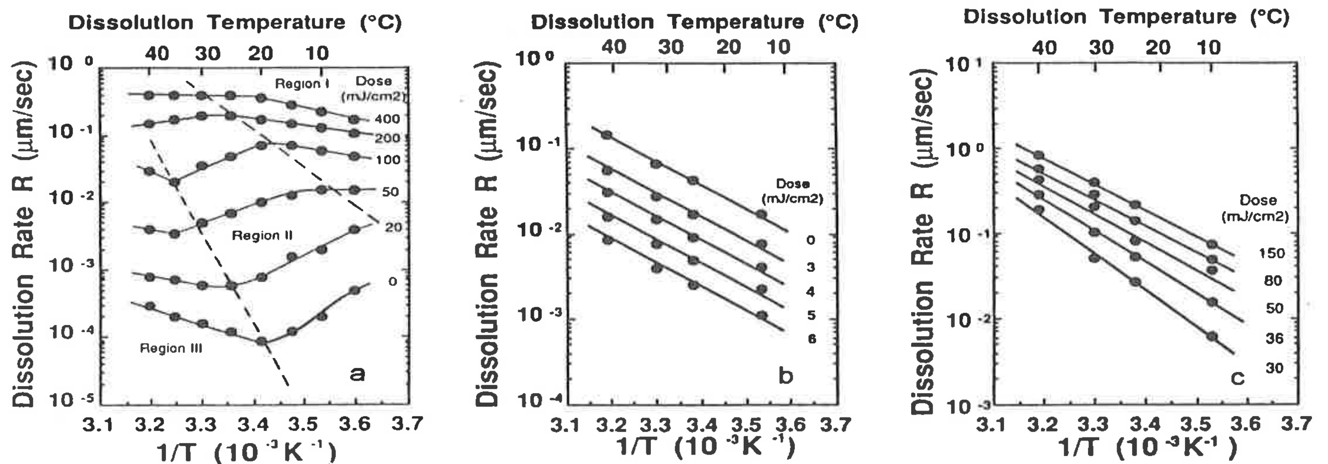

Figure 27 Arrhenius plots for the three resists in Figure 26; (a) shows an Arrhenius plot for the i-line resist where three distinct regions exist: (I) a high dose/low temperature region where E_a is small and positive, (II) an intermediate region where E_a is negative and decreasing, and (III) a low dose/high temperature region where E_a is positive and comparatively large; (b) shows a constant E_a for the negative CAR and suggests that only one reaction mechanism governs development rate; and (c) suggests also a single dissolution mechanism for the positive CAR but a saturation of E_a appears to exist at higher doses where nation of hydroxyl groups at the PHS becomes rate determining, similar to the mechanism for the negative resist. (From Ref. 69.)

sults can be compared with the development rate curves for the negative DUV resist (Fig. 26b and 27b). In this case, a moderately high DLS exists, and when compared with the i-line resist, it would be expected to coincide with worse lithographic performance. The Arrhenius plot shows a constant E_a and suggests that only one reaction mechanism governs development rate. Figure 26c and 27c show plots for the positive DUV resist. The DLS value is much greater than that for either the i-line or the negative resist. The Arrhenius plot also suggests a single dissolution mechanism, but a saturation of E_a appears to exist at higher doses. At these high doses, deprotonation of hydroxyl groups at the PHS becomes rate determining, as in the mechanism for the negative resist. Figure 28 shows the proposed dissolution model for the positive DUV chemically amplified resist. Figure 29a and 29b show development rate curves for a three-component positive DUV resist, which includes an additional dissolution inhibitor and various t-BOC protection levels and molecular weights [72]. Shown in Fig. 30 are plots of dissolution rate and log slope as a function of inhibitor concentration for a three-component PHS chemically amplified resist [73]. Increasing both the protection ratio and the inhibitor concentration results in higher R_{max}/R_{min} contrast and DLS values. Strong surface inhibition effects can limit the practical levels. The optimum protection ratio from Fig. 30 is on the order of 30–35% with an inhibitor concentration of 3%. PAG structure modification, molecular weight polydispersity, and polymer end groups can allow further improvements.

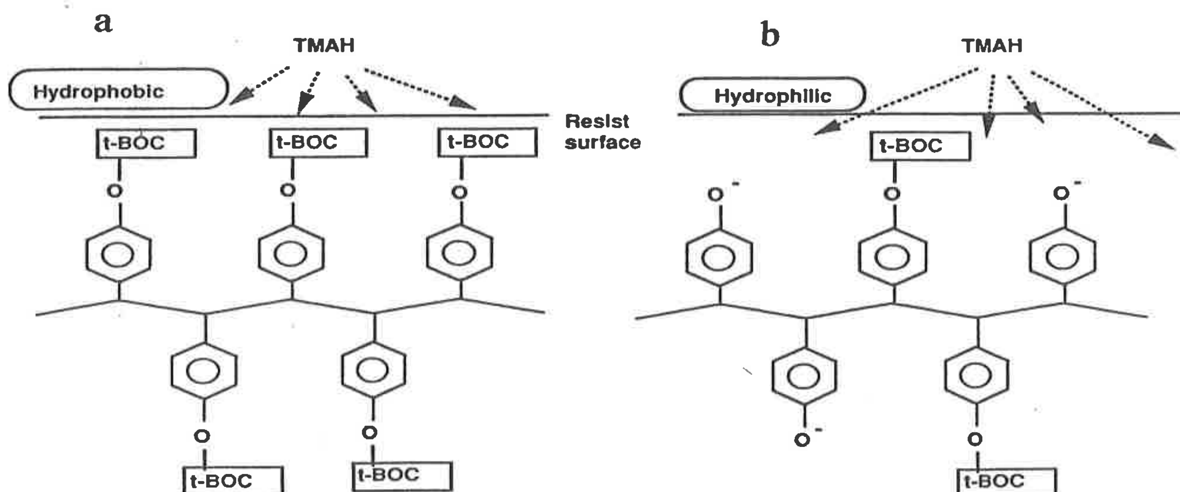

Figure 28 A proposed dissolution model for positive DUV chemically amplified resist derived from Arrhenius plot analysis. Two situations are considered: (a) before deblocking where TMAH penetration is prevented by strong hydrophobicity and (b) after deblocking. (From Ref. 69.)

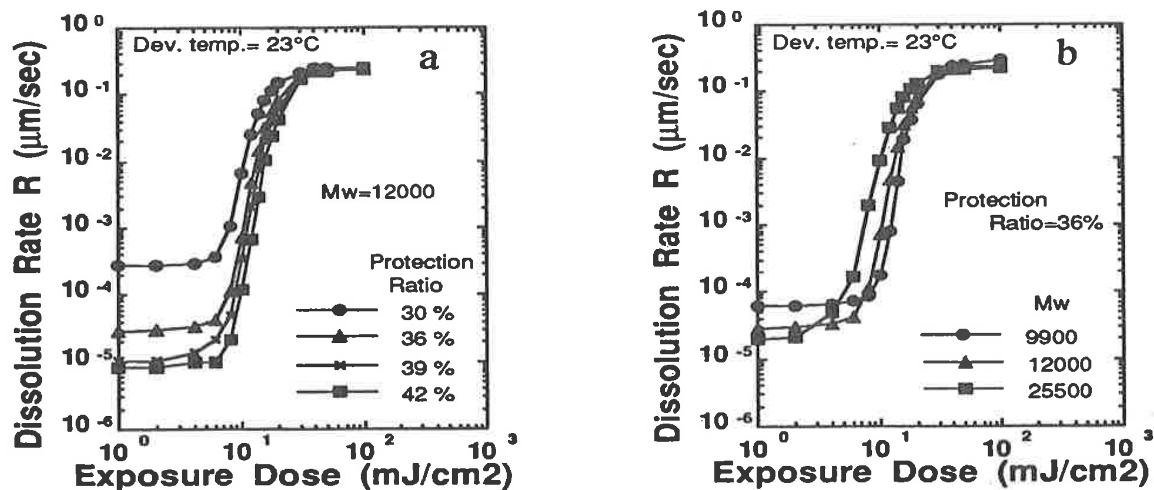

Figure 29 Development rate curves for a three component positive DUV resist, which includes an additional dissolution inhibitor and various t-BOC protection levels and molecular weights. (From Ref. 72.)

Preferential dissolution conditions for positive PHS chemically amplified resists can be summarized. A high R_{max}/R_{min} contrast is desirable, but not so high as to result in severe resolution of sidewall standing waves (some low contrast behavior is desired to reduce sensitivity to small oscillations in intensity at threshold levels). Since R_{max} is primarily a function of the polymeric resin, maximizing the R_{max}/R_{min} dissolution contrast ration generally involves reduction of

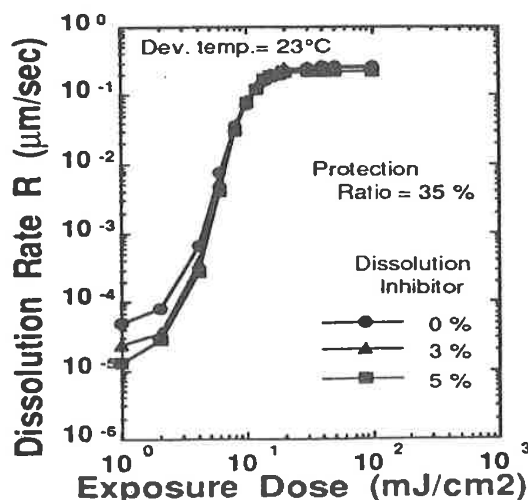

Figure 30 Plots of dissolution rate and log-slope plotted as a function of protection ratio for a three component PHS chemically amplified resist. (From Ref. 73.)

unexposed resist erosion. As shown earlier, a ratio above 10,000 is desirable but probably no greater than 50,000 should be expected. A large DLS is more important and can be controlled to some extent by the resin molecular weight.

9 E_0 AND CD SWING CURVE

Coherent interference resulting from substrate reflectivity will result in a swing of intensity distributed within a resist film. This will correlate to variations in clearing dose (E_0) and CD throughout a resist layer. The swing in E_0 is dependent only on the coherent interference of radiation within the film and can be predicted on the basis of knowledge of the coupling efficiency between the resist and the exposure variation. The only requirement for predicting the E_0 swing is that the distribution and conversion efficiency of the sensitizer reaction be known, making it independent of resist dissolution characteristics. In other words, only the photospeed of the resist influences the E_0 swing. Figure 31 shows the relationship between the E_0 swing ratio and exposure clearing dose (E_0) for several resist systems [74]. The swing ratio has been calculated from eq. 11. Since higher bleaching efficiency leads to higher resist sensitivities, the relationship shown in Fig. 31 makes sense from the standpoint of resist absorbance. Increased nonbleachable absorbance will lead to lower swing ratios, as can be demonstrated by adding a dye to a resist. Figure 32 is a plot of E_0 swing versus exposure-independent resist absorbance (B parameter). As resist absorbance increases, swing decreases.

The independence of E_0 swing on resist dissolution, along with the ease with which E_0 values can be measured, makes it an effective method for resist coat

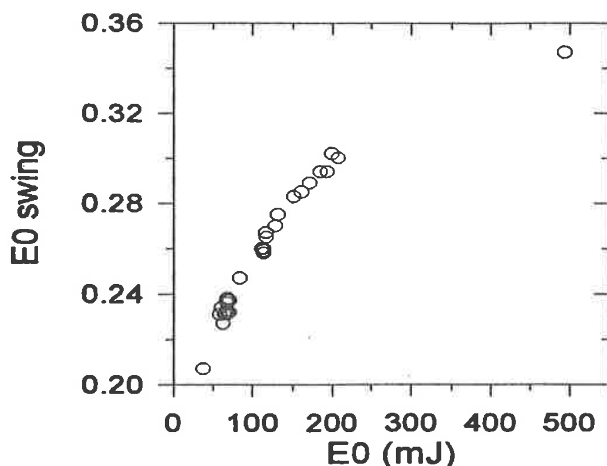

Figure 31 Plot of normalized E_0 verticle swing versus E_0 for several hypothetical resist systems. (From Ref. 74.)

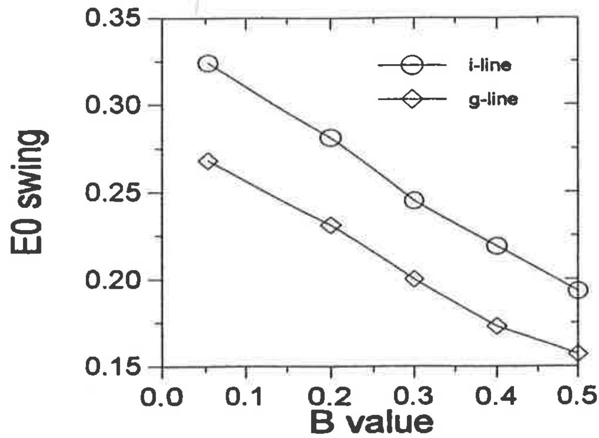

Figure 32 The effect of residual absorption (B parameter) on E_0 swing at constant sensitivity for g-line and i-line exposure. (From Ref. 74.)

characterization, as seen in Section 4. The swing in CD is not so straightforward, as it is influenced by the resist process and dissolution properties. Resist process exposure latitude (or the amount of allowable over- or underexposure) can have a significant influence on CD swing, which can be predicted from the relationship

$$\text{CD swing} = \frac{E_0}{E_L{}^x} \tag{17}$$

where E_L is exposure latitude and x is an empirically determined exponent, on the order of 2.5 for a reasonably fast photoresist.

Secondary swing effects are also present in a resist process. These include swings in resist contrast (γ) and surface contour effects. These secondary effects are a result of the spatial position of a standing wave node at the top surface of the resist. If there is a destructive interference node near the top surface of the resist, a surface induction effect will result, leading to an increase in γ. Figure 33 shows how this can be manifested. At resist thicknesses slightly greater than that corresponding to an optimum maximum exposure (1.18 μm), PAC concentration is increased at the top surface of the resist, resulting in T-top formation. This results in a significant loss of linearity, compared with the optimized condition. At thicknesses slightly less than 1.18 μm, there is a decrease in PAC concentration, resulting in top rounding. These surface effects occur at regular swing periods. The extent to which these secondary surface effects influence a resist process depends on how exposure requirements are affected. Surface effects influence clearing dose (E_0) more strongly than they influence dose to size ($E_{1:1}$) The exposure margin (EM), which is a ratio of these doses,

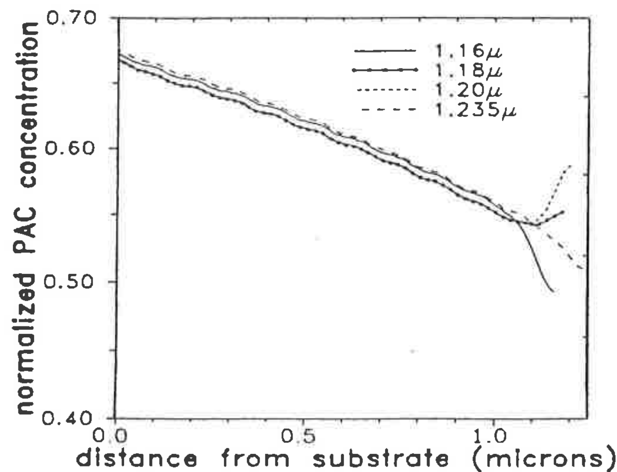

Figure 33 Calculated PAC distribution (at the mask edge) following PEB for four film thicknesses. (From Ref. 74.)

$$\mathrm{EM} = \frac{E_{1:1}}{E_0} \tag{18}$$

is a measure of the overexposure requirements for a resist and is a good indicator of mask linearity [75]. Surface-induced swings in E_0 lead to corresponding swings in EM. Resists that demonstrate large surface induction effects during development are most susceptible to these secondary swing effects.

10 POSTDEVELOPMENT BAKING AND RESIST TREATMENT

Postdevelopment baking is often utilized to remove remaining casting solvent, developer, and water within the resist. Baking above the resist's T_g also improves adhesion of the resist to the substrate. Because photosensitivity is no longer required, the baking temperature can be elevated toward the solvent boiling point (T_b), effectively eliminating the solvent from the resist and allowing maximum densification. For DNQ/novolac resist, any remaining DNQ can lead to problems in subsequent process steps. If the still sensitized resist is subjected to a high-energy exposure (such as ion implantation), rapid release of nitrogen can result from radiolysis of DNQ. In a densified resist film, the nitrogen cannot easily diffuse outward and may result in localized explosive resist popping, dispersing resist particles on the wafer surface. Baking above the DNQ T_d after development is therefor desired to volatilize the PAC.

Novolac resins generally suffer from thermal distortion (during subsequent high-temperature processes) more than PHS polymers. PHSs used for DUV resists have T_g values on the order of 140–180°C; the T_g values for novolac resins are in the 80–120°C range. Elevated baking temperatures also result in oxidation and crosslinking of the novolac, producing more "thermoset" materials with flow temperatures higher than the original resist T_g (and less well defined). The temperatures required to accomplish this, however, are above the resist T_g, allowing the flow of patterned features in the process. Novolac resins with T_g values above 130°C are now commonly used and higher T_g resists have been introduced [76].

To enhance the thermal properties of DNQ/novolac resists, the UV crosslinking properties of novolac can be utilized. Although the efficiency is quite low, novolac resin can be made to crosslink at DUV wavelengths. This is facilitated at high temperatures. The high optical absorbance of novolac at wavelengths below 300 nm (absorbance $\gg 1\ \mu m^{-1}$) prevents crosslinking to substantial depths. If patterned resist features are subjected to DUV exposure at temperatures above 150°C, a thermally stabilized surface crust can be formed. By elevating the temperature of the "DUV cure" process, oxidation of the bulk of the resist feature can be accomplished. The process is outlined in Fig. 34. The now networked re-

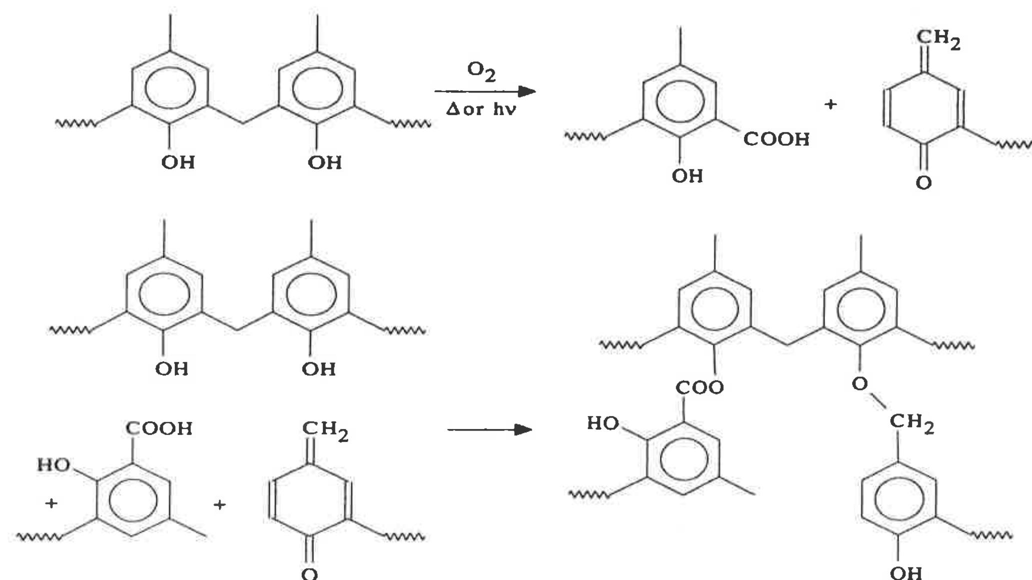

Figure 34 Radical reactions and oxidations induced in novolac from DUV curing. DUV hardening is effective in the presence of oxygen or with no oxygen (in nitrogen for instance) through self-oxidizing of novolac. Removal of DUV cured novolac can be difficult and particulate contamination can occur from rapid nitrogen outgassing at high exposure levels.

sist features can then withstand thermal processes up to 210°C without significant resist flow.

11 RESIST PROCESSING OUTLOOK

As improvements are made to existing resist technology, some process constraints may be reduced. In reality, however, the demand for reduction in geometry size will increase the requirements of process control. Optimum lithographic performance demands that resist processing factors be considered along with any optics-related advances, hence the process dependent "k" factor in the resolution scaling equation. As shorter wavelength technologies are considered, new resist materials need to be developed. The capability of these new resists cannot simply be comparable to that of existing materials but must allow performance that will scale with targeted resolution. Single-layer resist materials for 193-nm lithography have been under development for some time. Beyond this optical wavelength technology, little work has been done. Current i-line and DUV resist materials are impressive predecessors that will lead to extremely high process demands. The cost of ownership of new resist technologies is also an issue of great concern as DUV and 193-nm wavelength exposure is considered. The cost of resist materials and processing equipment may be the largest cost factor involved in a new lithographic technology. This leads to pursuit of not only methods for minimizing chemical materials and preparation costs but also methods for reducing the consumption of resist and processing materials. Resist volumes of less than 4 cm^3 for 200–300-mm wafers are desirable. Material and equipment methods for reducing volume to these levels will serve to reduce lithographic costs as well as impact on environmental safety and health (ESH).

At some point, it can be expected that single-layer resists may not be capable of meeting all needs. This is already seen with the application of antireflective layers to either the top or bottom surface of i-line and DUV resists. As optical and process-related solutions begin to fall short, alternative resist approaches such as top surface imaging may become more practical. Once implemented for manufacturing, these techniques will require a new set of process considerations. Bulk material properties become less of a concern and the demands of dry (plasma) processing may dominate. Regardless of future resist technology, there is assurance that current resists based on DNQ/novolac and chemically amplified PHS will remain in high volume for many years [77].

REFERENCES

1. Thompson, L. F., Wilson, C. G., and Bowden, M. J., *Introduction to Microlithography*, American Chemical Society, Washington, DC, 1994, Chapter 4.
2. Moreau, W., *Semiconductor Lithography*, Plenum, New York, 1988.

3. Dammel, R., *Diazonapthoquinone-Based Resists*, SPIE, Bellingham, WA, 1993, Chapter 5.
4. Moreau, W., *Semiconductor Lithography*, Plenum, New York, 1988, p. 49.
5. Katzisyma, L., *Russ. Chem. Rev.*, *35*, 388 (1966).
6. Asaumi, S., Futura, M., and Yokota, A., *Proc. SPIE*, *1672*, 616 (1992).
7. Hinsberg, W. D., et al., *Proc. SPIE*, *1925*, 43 (1993).
8. Huang, W., et al., *Proc. SPIE*, *2195*, 37 (1994).
9. Nalamasu, O., et al., *ACS Symp. Ser.*, *614*, 4 (1995).
10. Roschert, H., et al., *Proc. SPIE*, *1672*, 33 (1992).
11. Funhoff, D. J. H., Binder, H., and Schwalm, R., *Proc. SPIE*, *1672*, 46 (1992).
12. Nalamasu, O., et al., *J. Vac. Sci. Technol. B*, *10*(6), 2536 (1992).
13. Ito, H., et al., *J. Photopoly. Sci. Technol.*, *7*, 433 (1994).
14. Conley, W., et al., *Proc. SPIE*, *2724*, 34 (1996).
15. McDonald, S. A., *Proc. SPIE*, *1466*, 2 (1991).
16. van Zanten, J. H., Wallace, W. E., and Wu, W. L., *Phys. Rev. E.*, *53*, R2053 (1996).
17. Lyons, D., and Beauchemin, B. T., *Proc. SPIE*, *2438*, 726 (1995).
18. Bornside, D. E., Macosko, C. W., and Scriven, L. E., *J. Imag, Tech.*, *13*, 123 (1987).
19. Meyerhofer, D., *J. Appl. Phys.*, *49*(7), 3993 (1978).
20. Fujita, H., *Adv. Polym. Sci.*, *3*, 1 (1961).
21. Vrentas, J. S., *J. Polym. Sci. Polym. Phys. Ed.*, *15*, 403 (1977).
22. Pain, L., LeCornec C., Roilio, C., and Paniez, P. J., *Proc. SPIE*, *2724*, 100 (1996).
23. Rao, V., Hinsberg, W. D., Frank, C. W., and Pease, R. F. W., *Proc. SPIE*, *2195*, 596 (1994).
24. Frank, C. W., Rao, V., Despotopoulou, M. M., Pease, R. F. W., Hinsberg, W. D., Miller, R. D., and Rabolt, J. F., *Science*, *273*, 912 (1996).
25. Schlegel, L., Ueno, T., Hayashi N., and Iwayanagi T., *J. Vac. Sci. Technol. B*, *9*, 278 (1991).
26. Beauchemin, B., Ebersol, C. E., and Daraktchiev, I., *Proc. SPIE*, *2195*, 613 (1994).
27. Salamy, T. E., et al., *Proc. Electrochem. Soc.*, *90*(1), 36 (1990).
28. Dean, K. R., Carpio, R. A., and Rich, G. K., *Proc. SPIE*, *2438*, 514 (1995).
29. Chun, J., Bok, C., and Baik, K., *Proc. SPIE*, *2724*, 92 (1996).
30. Fields, E., Clarisse, C., and Paniez, P. J., *Proc. SPIE*, *2724*, 460 (1996).
31. Paniez, P. J., Rosilio, C., Monanda, B., and Vinet, F., *Proc. SPIE*, *2195*, 14 (1994).
32. Sinta, R., Barclay, G., Adams, T., and Medeiros, P., *Proc. SPIE*, *2724*, 238 (1996).
33. Paniez, P. J., Festes, G., and Cholett, J. P., *Proc. SPIE*, *1672*, 623 (1992).
34. Koshiba, M., Murata, M., Matsui, M., and Harita, Y., *Proc. SPIE*, *920*, 364 (1988).
35. Ito, H., et al., *Proc. SPIE*, *2438*, 53 (1995).
36. Dill, F. H., et al., *IEEE Trans. Electr. Dev.*, *ED-22*, 440 (1975).
37. Dammel, R., *Diazonapthoquinone-Based Resists*, SPIE Pres, Bellingham, WA, 1993, p. 19.
38. Sturdevant, J., Conley, W., and Webber, S., *Proc. SPIE*, *2724*, 273 (1996).
39. Shaw, J. M., and Hatzakis, M., *IEE Trans. Electr. Dev.*, *ED-25*, 425 (1978).
40. Brunner, T., Proc. SPIE 1463, 297 (1991).
41. Sturdevant, J., Holmes, S., and Rabidoux, P., *Proc. SPIE*, *1672*, 114 (1992).
42. Toukhy, M. A., and Hansen, S. G., *Proc. SPIE*, *2195*, 64 (1994).

43. Tanabe, T., Kobayashi, Y., and Tsuji, A., *Proc. SPIE*, *2724*, 61 (1996).
44. Pain, L., Le Cornec, C., Rosilio, C., and Paniez, P. J., *Proc. SPIE*, *2724*, 100 (1996).
45. Überreiter, K., and Asmussen, F., *J. Polym. Sci.*, *57*, 187 (1962).
46. Novembre, A. E., and Hartney, M. A., *Proc. SPE Photopolym. Conf.*, Ellenvile, New York (1985).
47. Huang, J. P., Kwei, T. K., and Reiser, A., *Proc. SPIE*, *1086*, 74 (1989).
48. Reiser, A., *Photoreactive Polymers*, Wiley Interscience, New York, 1989, pp. 211–223.
49. Shih, H., Yeu, T., and Reiser, A., *Proc. SPIE*, *2195*, 514 (1994).
50. Honda, K., Blakeney, A., and Hurditch, R., *Proc. SPIE*, *1925*, 197 (1993).
51. Itani, T., Itoh, K., and Kasama, K., *Proc. SPIE*, *1925*, 388 (1993).
52. Konnerth, K. L., and Dil, F. H., *IEEE Trans. Electron, Devices*, *ED-22*, 453 (1975).
53. Chowdhury, S. D., Alexander, D., Goldman, M., Kukas, A., Farrar N., Takemoto, C., and Smith, B. W., *Proc. SPIE*, *2438*, 659 (1995).
54. For instance, the Perkin Elmer Development Rate Monitor (DRM).
55. Arcus, R. A., *Proc. SPIE*, *631*, 124 (1986).
56. Dammel, R. R., et al., *Proc. SPIE*, *2195*, 542 (1994).
57. Shimomura, S., Shimada, H., Au, R., Miyawaki, M., and Ohmi, T., *Proc. SPIE*, *1925*, 602 (1993).
58. Flores, G., and Loftus, J., *Proc. SPIE*, *1672*, 328 (1992).
59. Henderson, C. L., et al., *Proc. SPIE*, *2724*, 481 (1996).
60. Henderson, C., et al., *Proc. SPIE*, *2724*, 481 (1996).
61. Honda, K., Blakeney A., and Hurdith, R., *Proc. SPIE*, *1925*, 197 (1993).
62. Garza, C. M., Szmanda, C. R., and Fischer, R. L., *Proc. SPIE*, *920*, 321 (1988).
63. Marriott, V., *Proc. SPIE*, *394*, 144 (1983).
64. Moreau, W., *Semiconductor Lithography,* Plenum Press, New York, Ch. 10, (1988).
65. Moreau, W. M., Wilson, A. D., Chiong, K. G., Petrillo, K., and Hohn, F., *J. Vac. Sci. Technol. B*, *6*, 2238 (1988).
66. Fadda, E., Amblard, G. M., Weill, A. P., and Prola, A. *Proc. SPIE*, *2195*, 576 (1994).
67. Yoshimura, T., Murai, F., Shiraishi, H., and Okazaki, S., *J. Vac. Sci. Technol. B*, *6*, 2249 (1990).
68. Damarakone, N., Jaenen, P., Van den Hove, L., and Hurditch, R. J., *Proc. SPIE*, *1262*, 219 (1990).
69. Itani, T., Itoh, K., and Kasama, K., *Proc. SPIE*, *1925* 388 (1993).
70. Thackeray, J. W., et al., *Proc. SPIE*, *1086*, 34 (1989).
71. Nalamasu, O., et al., *Proc. SPIE*, *1262*, 32 (1990).
72. Itani, T., Iwasaki, H., Fujimoto, M., and Kasama, K., *Proc. SPIE*, *2195*, 126 (1994).
73. Itani, T., Iwasaki, H., Yoshin, H., Fujimoto, M., and Kasama, K., *Proc. SPIE*, *2438*, 91 (1995).
74. Hansen, S. G., Hurdich, R. J., and Brzozowy, D. J., *Proc. SPIE*, *1925*, 626 (1993).
75. Hansen, S. G., and Wang, R. H., *J. Electrochem. Soc.*, *140*, 166 (1993).
76. Toukhy, M. A., Sarubbi, T. R., and Brzozowy, D. J., *Proc. SPIE*, *1466*, 497 (1991).
77. Smith, B. W., *Opt. Photon. News*, *8*(3), 23 (1997).

10

Multilayer Resist Technology

Bruce W. Smith

Rochester Institute of Technology
Rochester, New York

Maureen Hanratty

Texas Instruments
Dallas, Texas

1 INTRODUCTION

As higher resolution approaches to microlithography are pursued, conventional single-layer resist materials may fail to meet all process requirements. Multilayer resist techniques have been investigated for several years, but advances in single-layer technology have generally postponed their insertion into high-volume production operations. As long as single-layer resist materials can meet requirements for high-aspect-ratio resolution, photosensitivity, plasma etch resistance, planarization, depth of focus, reflection control, and critical dimension (CD) control, they will be preferred over most multiple-layer or pseudo-multiple-layer techniques. This becomes increasingly difficult and, at some point, the lithographer needs to consider the advantages of dividing the functions of a single-layer resist into separate layers. The fewer layers the better, and the ultimate acceptance of any multilayer technique will be determined by the simplicity of the overall process.

In order to understand the potential advantages of multiple-layer lithographic materials and processes, the general requirements of a photoresist should first be addressed. Although most resist requirements have existed for many generations of integrated circuit processing, the importance of a number of issues has recently increased dramatically.

IPR2016-01378 Page 0054

1.1 Resist Sensitivity

Because resist sensitivity directly affects process throughput, it is a fundamental consideration for the evaluation of resist process capability. In general, resist sensitivity can be shown to be proportional to thickness. For a direct photochemical (not chemically amplified), nonbleaching resist material, this is an exponential relationship, determined by resist absorption and chemical quantum efficiency. However, as resist bleaching mechanisms are considered (as with the photochemical conversion of diazonapthoquinone to indene carboxylic acid), dynamic absorption exists, which introduces some additional considerations to this exponential decay. With chemically amplified resists, quantum efficiency is sufficiently high that the dependence of sensitivity on resist thickness becomes less of an issue and other considerations become more of a concern.

1.2 Depth of Focus

The dependence of depth of focus on lens numerical aperture and wavelength can be expressed as

$$\mathrm{DOF} = \pm\, k_2 \frac{\lambda}{\mathrm{NA}^2} \tag{1}$$

where λ is wavelength, NA is numerical aperture, and k_2 is a process-dependent factor, determined by process specification and requirements (a typical value for k_2 for a single-layer resist may be near 0.5, as shown in Chapter 9). As optical lithographic technology is pushed toward sub-200 nm wavelengths at numerical apertures greater than 0.6, DOF may fall below 0.5 μm. This presents an interesting challenge for substrate topography and photoresist thickness issues. With such a small useful DOF and without the use of some method of planarization, it is not easily predictable just how large a fraction of this range could be consumed by photoresist thickness.

1.3 Limitations of Resist Aspect Ratio

The physical and chemical nature of a polymeric resist material will determine its limitations for high-aspect-ratio patterning. In addition, the complex nature of development and process chemistry will influence limitations. An aspect ratio less than 3:1 is common for conventional single-layer resists. The limit to how fine the resolution can be for a single-layer resist of a given thickness is influenced to a large extent by polymer flow properties including glass transition temperature (T_g) and melting point (T_m). Because thermoplastic polymeric behavior is desired during processing, in which photoresist materials can go through cycles of heating, flowing, and cooling, they generally possess T_g val-

ues in the 70 to 180°C range. Materials of lower T_g will inherently be capable of lower aspect ratio imaging.

1.4 Reflection and Scattering Effects

Imaging over reflective substrates such as metal or polysilicon can allow significant intensity variation within a resist film. High levels of reflectivity can produce overexposure, manifested not only as a bulk effect over the entire imaged field but also at pattern-specific locations such as line boundaries and corners. This is often referred to as reflective line notching or necking, which is a result of the scattering of radiation to unwanted field regions. Substrate reflection will affect the overexposure latitude and ultimately lead to a reduction in focal depth by limiting the amount of tolerable image degradation. To understand the impact of exposure latitude on depth of focus, consider imaging a feature with poor modulation. If a resist process is capable of resolving such a feature, it is likely to be possible only within a limited range of exposure dose. For a positive resist, overexposure can result in complete feature loss and underexposure can result in scumming. There is an intimate relationship, therefore, between depth of focus and exposure latitude. Decreasing the demands on focal depth increases exposure latitude. For a reflective substrate, if a large degree of overexposure latitude must be tolerated, the useful depth of focus will be reduced significantly. It is desirable to reduce any reflected contribution to exposure in order to eliminate feature distortion from scattering and to reduce detrimental effects on focal depth. This can be accomplished in a single-layer resist by several methods. First, because absorption is dependent on resist thickness, a thicker absorbing resist layer will decrease the impact of reflection. Other requirements drive resist toward thinner layers, however, reducing the practicality of this method. A second alternative would be to increase the absorption of the resist so that little radiation is allowed to penetrate to the resist-substrate interface and be reflected back through the resist. The addition of dyes into a resist will accomplish this, but at the cost of resist sidewall, sensitivity, and resolution. The beneficial dynamic bleaching mechanism of the diazonaphthaquinone (DNQ)/novolac materials is undermined by the addition of an absorbing dye that makes no direct contribution to the photochemical process. An alternative approach to reduction is the use of a multilayer resist system, incorporating a separate antireflective layer.

1.5 Reflective Standing Wave Effects

An additional reflection phenomena that deserves consideration is the resist standing wave effect. This is an exposure variation within a resist layer resulting from coherent interference between incident and reflected radiation. The situation is described in detail in Chapters 2 and 9 and has significant impact on

exposure, CD control, depth of focus, and coating uniformity requirements. Minimization of standing wave is generally desired. The addition of a resist dye can help in reducing standing wave effect, but the impact on resist sidewall angle can be significant as the top to bottom resist film attenuation increases.

1.6 Plasma Etch Resistance

Post-lithographic processing operations ultimately dictate the minimum acceptable resist thickness after development. For example, resist erosion during etch processing will increase any lithography-related thickness requirements. Furthermore, as new materials are considered for short wavelength exposure application, their etch resistance in halogen-based plasma etch processes may be reduced. Postlithographic processes may place the most restrictive demands on resist performance and may preclude any consideration of thinner single-layer resists.

1.7 Planarization

Because the lithography operations involved with integrated circuit (IC) fabrication are rarely performed over a flat substrate, planarization of topography is a fundamental function of a resist material. The degree of planarization required for a specific level will be determined by step height, feature size and density, and substrate surface properties. Material properties of a resist, including polymer molecular weight, solids content, solvent type, coating spin speed, acceleration, temperature, and exhaust, will contribute to the extent of substrate smoothing. Polymeric materials with low molecular weight and a high solids content are generally employed for maximum results [1]. A fluid dynamics approach can be used to demonstrate the relationships between process factors and planarization:

$$P \propto \frac{t\gamma h_0^3}{\eta w^4} \tag{2}$$

where t is leveling time, γ is surface tension, h_0 is initial film thickness, η is solution viscosity, and w is feature width. This relationship suggests that several factors can be modified to affect net results. Planarization of close-proximity features (local geometry) and of widely spaced features (global geometry) may be required, depending on substrate characteristics and process needs. Figure 1 illustrates that planarization by a polymeric material may be suitable for both situations. The extent of planarization can be quantified by considering the initial step height (z_0) and the final effective step height after smoothing (z_1) and determining the normalized ratio:

$$\text{Effective planarization} = \frac{z_0 - z_1}{z_0} \tag{3}$$

which can be calculated for local and global features [2].

IPR2016-01378 Page 0057

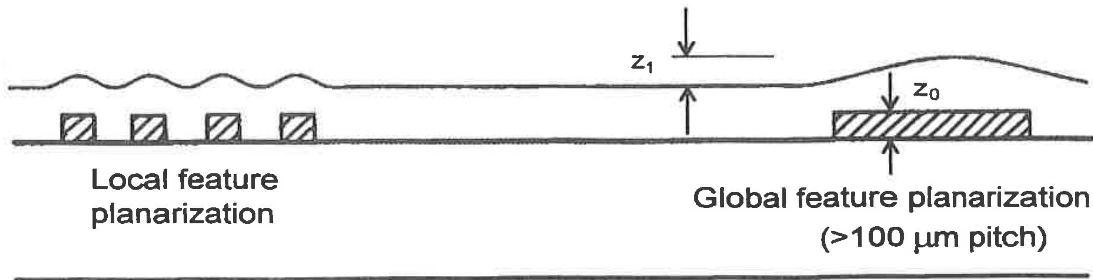

Figure 1 Polymeric planarization of local and global topography. The extent of planarization can be determined from measurement of initial and final step heights (z_0 and z_1).

Planarization can be accomplished by means of substrate overcoating (generally with an organic polymeric film), etch back processing, or polishing of a topographic substrate to reduce step height. Techniques of chemical mechanical polishing (CMP) are becoming widely accepted as alternatives to additive planarization methods, reducing constraints on resist processing and requirements for focal depth [3]. Methods of CMP can allow global planarization of both insulator and conductor layers in multilevel metallization interconnect structures and of both deep and shallow trench isolation materials. These techniques have become a critical path for both logic and memory production and a number of issues are receiving careful attention, including optimization of process techniques, cleaning considerations, and defects.

1.8 Multilayer Resist Processes as Alternatives to Conventional Resist Patterning

The appeal of multilayer resist processes and surface imaging resist (SIR) technology has increased because of the resolution enhancement they provide for the current optical exposure tools, as well as the potential application for newer exposure systems such as 193 nm or extreme ultraviolet (EUV, 13–40 nm). At the shorter exposure wavelengths, conventionally developed resists are either unavailable or lack sufficient performance. With surface or near-surface imaging, photochemical modification necessary to effect the pattern transfer is restricted to a thin upper portion of the resist layer. Ideally, the imaging layer should be as thin and as planar as possible. In this way, maximum resolution can be obtained and optimum use can be made of the entire available focus range of the exposure tool. The resist image is free from the effects of device topography and substrate reflection, an advantage that becomes increasingly important as optical tools move to shorter wavelength sources where the reflectivity of many materials increases. In addition, the high CD tolerances demanded by advanced IC designs require high-performance patterning, which multilayer and surface imaging resist systems can provide.

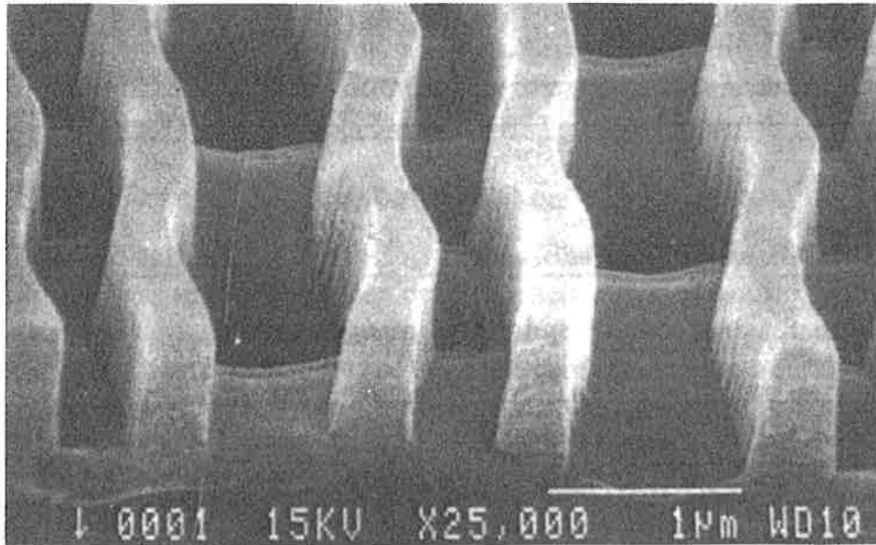

Figure 2 SEM micrograph of 0.35 μm DRAM gate structures patterned over 0.6 μm of topography using surface imaging techniques.

Multilayer techniques or single-layer surface imaging resist processes provide an advantage in application in which the substrate reflectivity is high or topography is severe. Patterning of DRAM gates, such as the one pictured in Fig. 2, often provides just such a challenging scenario. In this case, where 0.35-μm gates were patterned over 0.6 μm of topography, surface imaging resist techniques ensured constant critical dimension control even over large step heights. Particularly in instances in which the design dimensions challenge the resolution capability of the exposure tool and the resist, near-surface or surface imaging techniques can play an important role.

A large number of polymeric multilayer systems have been developed and utilized for several decades. Multilayer schemes can be divided into four basic categories, with some overlap in function. Specifically, approaches have allowed planarization, reduction of reflection, contrast enhancement, and surface imaging. These categories are not necessarily clearly divided, as a single multilayer approach can accomplish several objectives. Details of these approaches will be explored in this chapter.

2 MULTILAYER PLANARIZING PROCESSES—WET DEVELOPMENT APPROACHES

Various multilayer techniques have been introduced that employ polymeric planarization layers to reduce substrate topography and allow the use of a thin topcoated imaging resist layer, as depicted in Fig. 3 [4]. Methods have included a

BILAYER SYSTEMS

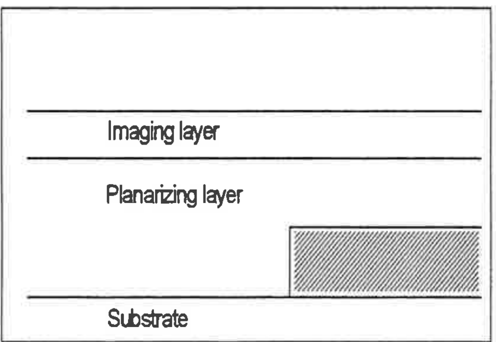

TRILAYER SYSTEM

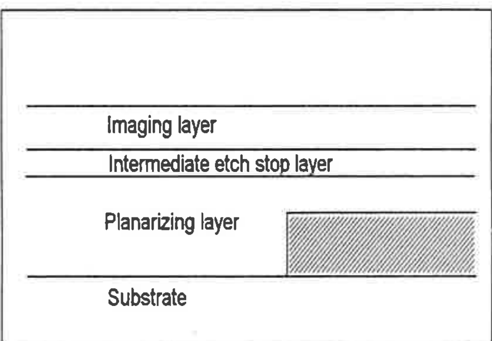

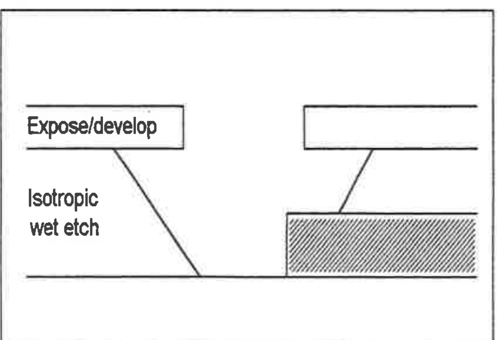

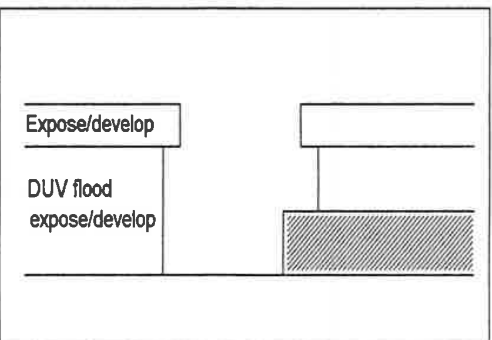

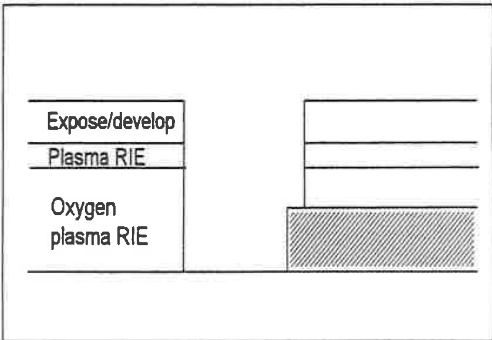

Figure 3 Multilayer approaches utilizing polymeric planarization layers. (a) A wet etch bilayer system using isotropic dissolution of the planarization layer; (b) a bilayer system with blanket DUV exposure of a photosensitive planarization layer masked by a patterned DNQ/novolac layer; (c) a typical trilayer resist system utilizing a planarizing layer, an etch stop layer, and an imaging layer.

wet-processed thick planarization layer [5], a two-layer portable conformable mask (PCM) [6], and a three-layer plasma transfer process [7]. The wet-processed approach leads to isotropic dissolution of an underlying planarizing layer, limiting application generally to non–integrated circuit use. The PCM process employs a deep ultraviolet (DUV)-sensitive planarizing layer, typically poly(methyl methacrylate), PMMA [8], or poly(dimethylgluterimide), PMGI [9], and a DNQ/novolac imaging layer. Because the DNQ/novolac is highly absorbing at wavelengths below 300 nm, once imaged it acts as a surface contact mask over the bottom resist layer. DUV flood exposure and development of the bottom layer allow pattern transfer through the entire multilayer stack. This technique can be limited by interfacial mixing of the two resist layers, which is minimized when using PMGI materials. Poor contrast of the DUV planarizing layer and reduced process control of this two-layer technique has limited resolution, making sub-0.5 μm imaging difficult.

Variations on the multiple-resist approach have also been used for electron beam T-gate fabrication [10, 11]. Three resist layers may be used to allow specific feature shaping through the depth of a resist stack. For example, a bottom layer of PMMA is overcoated by a layer of a methyl methacrylate–methacrylic acid copolymer (PMMA-MAA), followed by a top coat of PMMA. Exposure and wet development lead to larger pattern widths in the more sensitive PMMA-MAA layer, allowing the formation of T-shaped metal gate structures through a subsequent additive liftoff process.

3 WET DEVELOPMENT/DRY PATTERN TRANSFER APPROACHES TO MULTILAYERS

Anisotropic pattern transfer can allow significant improvement over the isotropic processing of wet-etched multilayer approaches. Through the use of a plasma reactive ion etch (RIE) pattern transfer process, near anisotropy can be approached, allowing high-aspect ratio, fine feature resolution [12, 13]. The three-layer schemed depicted in Fig. 3 makes use of a polymeric planarizing layer (such as novolac resin or polyimide) and a thin intermediate etch stop layer. This etch stop layer can be a spin-on organosilicon compound (spin on glass), a low-temperature oxide, a silicon oxinitride, or a metallic layer, which provide oxygen etch resistance. A thin resist imaging layer is coated over this etch stop, exposed, and wet developed. Pattern transfer into the intermediate etch-stop layer can be achieved with wet etch or dry plasma techniques with suitable chemistry. Anisotropic pattern transfer through the thick polymeric planarizing layer can be achieved via an oxygen RIE process. Variations on this technique have been used for both optical and electron beam applications [14].

The importance of polymeric planarization approaches historically has declined as single-layer resists and CMP techniques have steadily improved. As

shorter wavelength exposure technologies are pursued, however, it is likely that application of multilayer approaches will become more viable. A bilayer resist technique that allows planarization, etch resistance, and reflection control with a thin imaging layer has many attractive properties. Such schemes will be addressed in detail as silicon-containing resists and top-surface imaging techniques are addressed.

4 RESIST REFLECTIVITY AND ANTIREFLECTIVE COATINGS

Reflection at resist/substrate interfaces has been a concern for many IC generations. The impact is most pronounced when using high-contrast resists, a result of increasing exposure thresholding effects. Shown in Fig. 4 is the effect that varying resist film thickness has on feature size (CD swing curves) for an i-line resist imaged over polysilicon and aluminum films. The reflectance from a resist-polysilicon interface at 365 nm can be above 30% and at 248 nm above 38%. Resist over aluminum can produce reflectivity values of above 86% at 365 nm and above 88% at 248 nm. Interface reflectance can be determined from a Fresnel relationship for two media at normal incidence as

$$R = \left| \frac{n_2^* - n_1^*}{n_2^* + n_1^*} \right|^2 \tag{4}$$

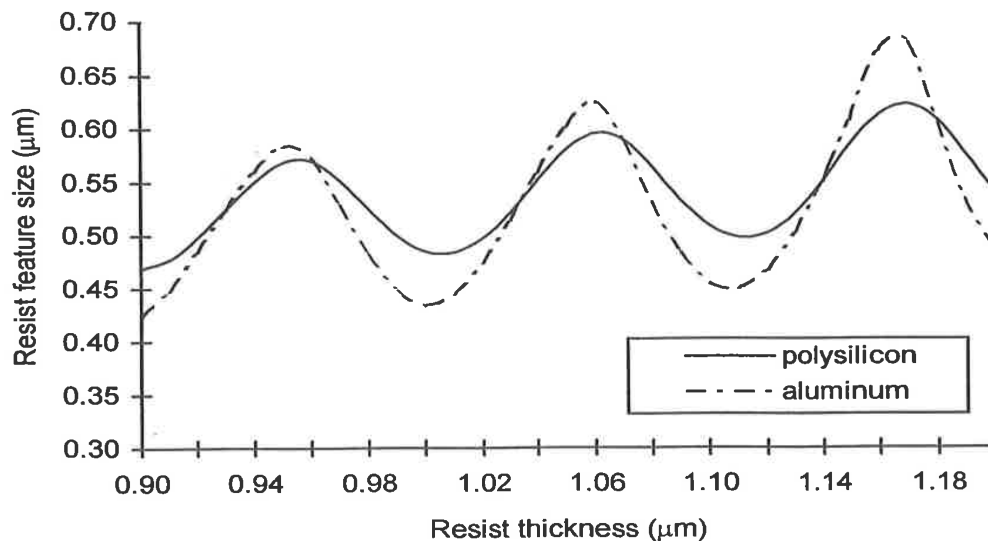

Figure 4 A CD swing curve showing the effect of resist thickness variation on resist linewidth. Results for polysilicon and aluminum substrates are shown at 365 nm using a resist with a refractive index of 1.7.

Here n^* is the complex refractive index or n-ik, where n is the real refractive index and k is the extinction coefficient. For nonabsorbing materials, $k = 0$ and $n^* = n$ simplifying Eq. 4. For nonnormal incidence, a additional cos θ term is required, where θ is the angle of incidence. Inspection of the optical constants for materials in Table 1 gives an indication of the need to incorporate methods of reflectance control.

If the materials that make up the lithographic substrate are nonabsorbing or possess low absorbance, reflectance values at each interface must be uniquely considered to determine the net reflectance through the film stack. Figure 5 shows an example of a resist film over an SiO_2/Si substrate. Here, the contribution from the oxide-resist interface is low compared with the contribution from the silicon underlying material. In this case, the thickness of the SiO_2 film can be adjusted to minimize total reflectivity through destructive interference (the use of quarter-wave approaches for inorganic antireflection materials will be discussed in detail in Section 4.1).

Control of reflectivity at the resist-substrate interface to values near a few percent is generally required for critical lithography levels, leading to the need for some method of control. The situation becomes more critical as lithographic methods incorporate shorter wavelength sources, a smaller spectral bandwidth, and more transparent resists. Reduction of reflection to values below 1% will probably be needed for next-generation lithography. Dye incorporation into a resist can reduce the coherent interference effects but at the cost of exposure throughput and sidewall angle, leading ultimately to resolution loss. Dyed resists are therefore generally limited to noncritical reflective levels at which the highest resolution is not necessary.

Instead of reducing reflection effects through modification of a resist material, methods that reduce reflectivity at resist interfaces can provide control with minimal loss of resist performance. This can be accomplished through manipu-

Table 1 Optical Constants (n and k) for Several Materials at 436, 365, 248, and 193 nm

	193		*248*		*365*		*436*	
	n	k	n	k	n	k	n	k
Silicon	0.960	2.88	1.58	3.60	6.41	2.62	4.79	0.175
SiO_2	1.56	0.00	1.51	0.00	1.47	0.00	1.47	0.00
Si_3N_4	2.65	0.18	2.28	0.005	2.11	0.00	2.051	0.00
Aluminum	0.117	2.28	0.190	2.94	0.407	4.43	0.595	5.35
Polysilicon	0.970	2.10	1.69	2.76	3.90	2.66	4.46	1.60
DNQ/novolac					1.70	0.007	1.67	0.007
PHS CAR			1.76	0.007				

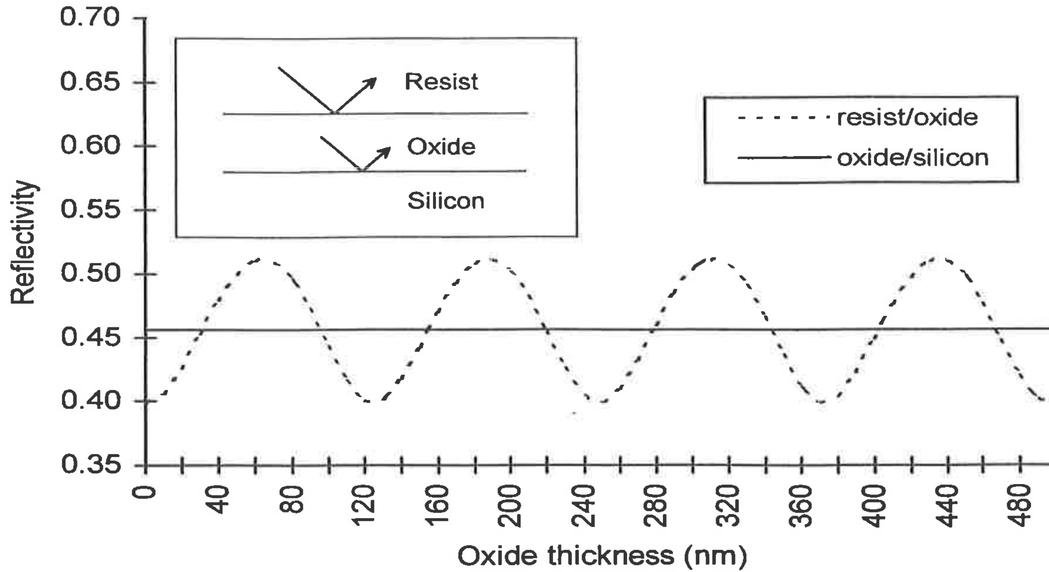

Figure 5 Reflection contribution at resist/oxide and oxide/silicon interfaces with increasing silicon dioxide thickness at a 365 nm wavelength using a resist with $n = 1.7$ and $k = 0.007$. Minimum reflectivity occurs at quarter wave oxide thicknesses.

lation of thin-film optical properties and film thicknesses and by careful matching of the optical properties of each layer in an entire resist/substrate stack.

4.1 Control of Reflectivity at the Resist-Substrate Interface: Bottom Antireflective Coatings

To reduce the reflectivity at the interface between a resist layer and a substrate, an intermediate film can be coated beneath the resist. This is known as a bottom antireflective coating (BARC). Inspection of Eq. 4 suggests one approach where the refractive index of this layer could be close to that of the resist at the exposing wavelength. To reduce reflectivity, the film could then absorb radiation incident from the resist film. Thin-film absorption (α) is related to the optical extinction coefficient (k) as

$$\alpha = \frac{4\pi k}{\lambda} \tag{5}$$

and transmission through an absorbing film is

$$T = \exp(-\alpha t) \tag{6}$$

where T is transmission and t is film thickness. A high extinction coefficient may therefore be desirable, leading to high absorption and low transmission

through the BARC layer. As k is increased, however, reflectivity at the resist/BARC interface is increased, as seen also from Eq. 4. An extinction coefficient value in the range of 0.25 to 1.2 may be reasonable, based on these considerations and depending on resist material and film thickness demands. Shown in Fig. 6 is a series of plots showing substrate reflectance versus BARC thickness for real-index matched materials with extinction coefficient values from 0.1 to 1.2. Since the BARC layer needs to accommodate pattern transfer (using either a wet or dry plasma etching approach), minimum thickness values are desirable. For these layer combinations, a BARC thickness between 500 and 800 produces a first reflectance minimum. These minima occur as reflectance from the BARC-substrate interface interferes destructively with the reflection at the resist-BARC interface. This interference repeats at intervals of $\lambda/2n$ which can be explained by examining Fig. 7. Here, radiation passes twice through the BARC layer with wavelength compression corresponding to its refractive index (λ/n_i). Two passes through a quarter wave thickness ($\lambda/4n$) results in a half-wave phase shift directed toward the resist-BARC interface. This phase-shifted wave will then interfere with the reflected wave at the resist. Complete destruction will occur only if the amplitude values of the waves are identical,

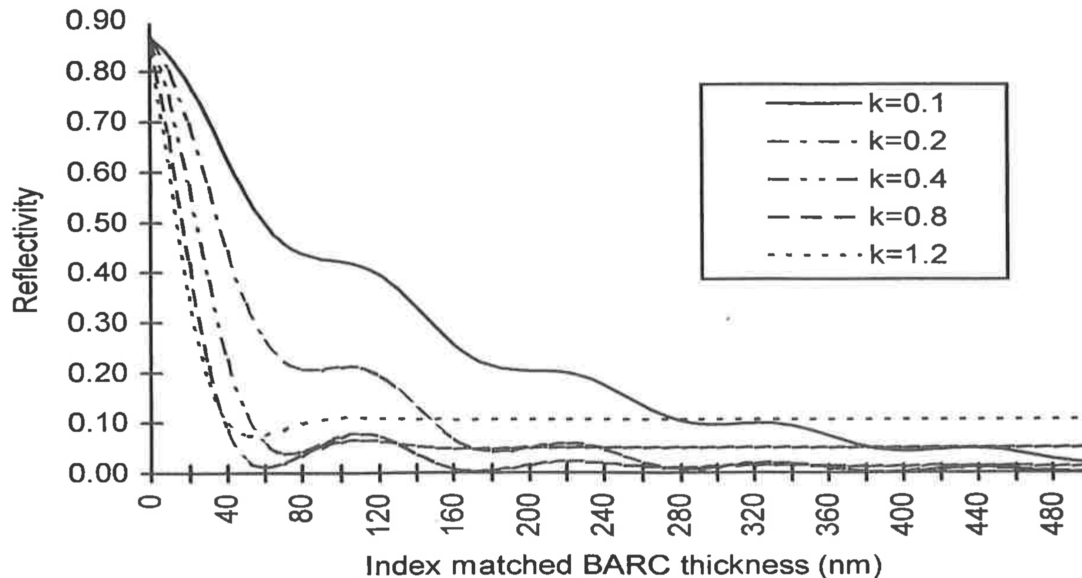

Figure 6 Substrate reflectivity vs. bottom ARC thickness for real index matched materials (n = 1.7 at 365 nm) and extinction coefficient values from 0.1 to 1.2. The best performance for a thin BARC layer may be possible with k values near 0.8.

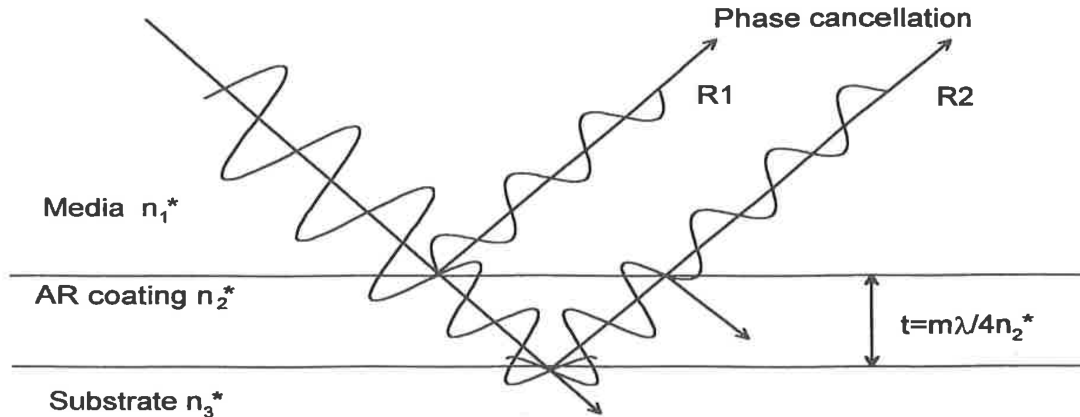

Figure 7 Diagram of the principle of a quarter wave AR layer between two media. A thickness of the AR coating is chosen to produce destructive interference between reflected components, R_1 and R_2. The ideal refractive index is $\sqrt{n_1^* n_3^*}$.

which is possible only if the reflectance at the resist-BARC interface is exactly equal to the reflectance at the BARC-substrate interface or if:

$$n_{\text{arc}} = \sqrt{n^*_{\text{resist}} \times n^*_{\text{substrate}}} \tag{7}$$

This leads to a more complex route toward reflection reduction with a bottom ARC using both absorption and interference considerations.

Reflection control and aspect ratio requirements need to be considered to determine optimum ARC film thickness values. A first reflectance minimum corresponding to a relatively thin film may be chosen for fine feature pattern transfer. If thicker layers can be tolerated, further reduction in reflectivity may be achieved by increasing the BARC film thickness. There is an exponential trend in reflection reduction with increasing thickness and BARC absorption. As extinction coefficient values increase toward 0.8, reflection begins to increase, and for values above 1.2, reflectivity below a few percentage becomes difficult. Figures 8 and 9 are a series of contour plots of substrate reflectivity for BARC films with extinction coefficient values from 0.0 to 0.9 and refractive index values from 1.8 to 2.7.

Organic BARCs

Organic bottom ARC materials have been used for some time, typically in the form of spin-on polymeric materials [15]. These polymers contain highly absorbing dyes introduced at levels to deliver appropriate extinction coefficient values. Several classes of materials can be used, depending to a large extent on the pattern transfer requirements of a process [16–19]. Wet developable organic BARCs based on partially cured polyamic acids (polyimide precursors) have been utilized for large feature geometry. These materials, with refractive index

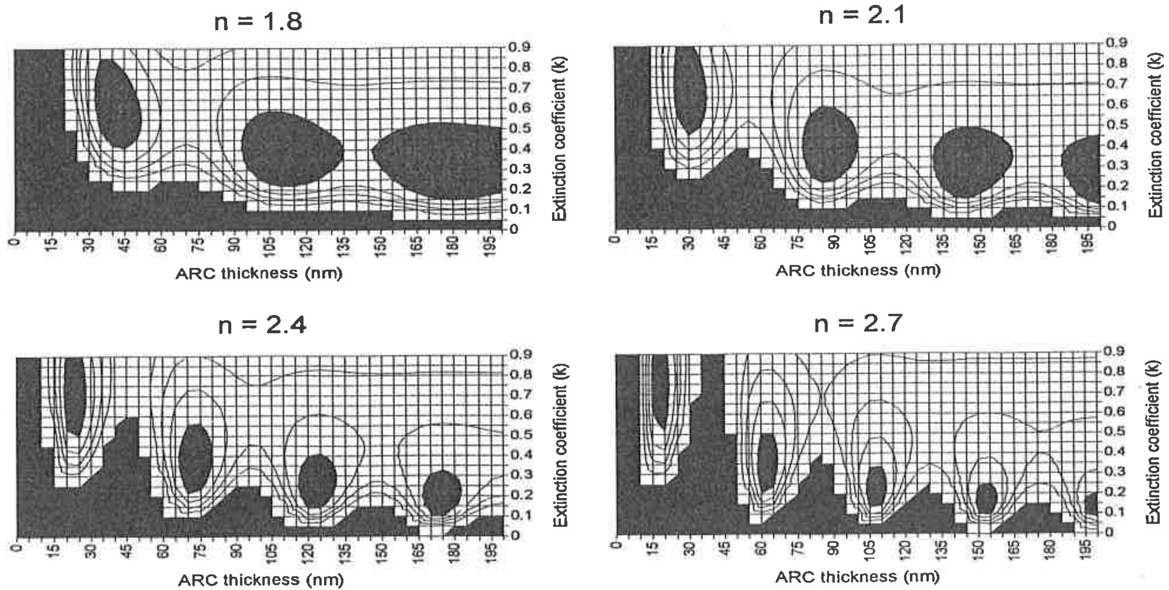

Figure 8 Contour plots of substrate reflectivity (over silicon) at 248 nm as a function of bottom ARC thickness for materials with refractive indices between 1.8 and 2.7 and extinction coefficient values to 0.9. Central contour areas correspond to 0-2% reflectivity and 2% constant contours are shown. Results beyond 10% reflectivity are shown in black [$n_{resist}(248) = 1.75$].

values near 1.7 and extinction coefficients near 0.3, are coated and partially cured prior to resist application. Partial curing of the dyed polyamic acid allows tailoring of the alkaline solubility of the layer to match that of exposed resist. Bottom ARC materials made of dyed triazine derivatives have also been introduced [17].

As shown in Fig. 10, exposure and development of an aqueous base–soluble resist layer exposes the underlying BARC material, which is also base soluble if cured appropriately. Materials have been formulated that provide a high degree of bake latitude (as high as ±20°C) [20] and exhibit a very low degree of interfacial mixing. The inherent problem with this approach for antireflection is the isotropy of wet pattern transfer. With no preferential direction for etching, undercutting results to the full extent of the BARC thickness. As shown in Fig. 10, resist features are undercut by twice the BARC thickness, limiting application of wet-developed organic materials to a resolution above 0.5 μm.

Dry etch compatible organic BARC materials can allow control of the etch profile through use of plasma RIE methods of pattern transfer. The requirements then become one of resist to BARC etch selectivity to minimize resist erosion and the accompanying loss in process and CD control. Initial candidate

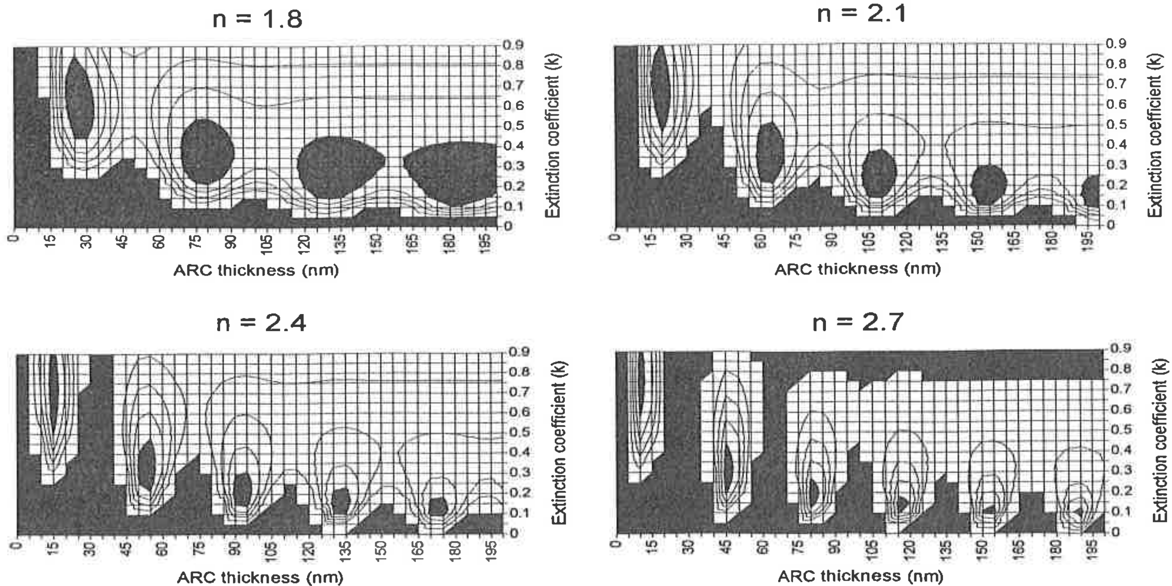

Figure 9 Contour plots of substrate reflectivity (over silicon) at 193 nm as a function of bottom ARC thickness for materials with refractive indices between 1.8 and 2.7 and extinction coefficient values to 0.9. Central contour areas correspond to 0-2% reflectivity and 2% constant contours are shown. Results beyond 10% reflectivity are shown in black. Resist refractive index is 1.6.

materials for use as dry etch BARCs may be polymers that undergo efficient scissioning with plasma exposure, leading to increased volatility. For instance, dyed polyolefin sulfone materials (frequently employed as electron beam resists) [21] could allow relatively high oxygen-based RIE etch selectivity to novolac or polyhydroxystyrene (PHS) resist materials. Several dry-etch materials have been introduced [22, 23] for use in 248 nm and i-line application. Figure 11 shows

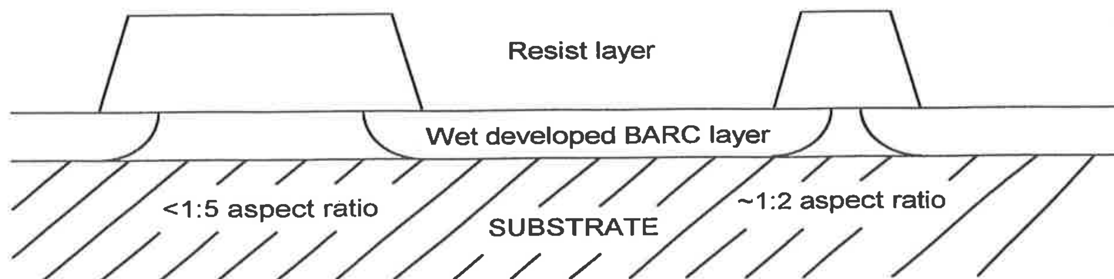

Figure 10 Process schematic for an aqueous base developed bottom ARC. Exposure and development of a top resist layer allow development to continue through a suitably baked AR film. Isotropic pattern transfer limits this approach.

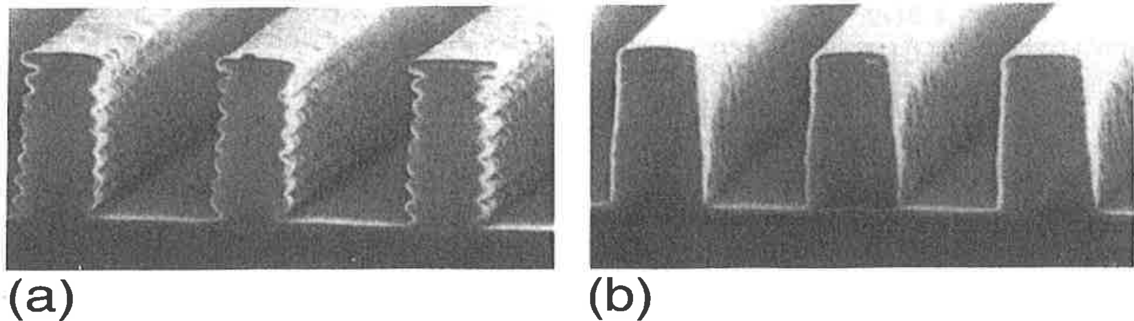

Figure 11 Comparison of reflective standing wave reduction through use of a dry etch bottom ARC: (a) without a bottom ARC; (b) with a bottom ARC.

lithographic results and reduction of reflective standing wave effects with use of a dry-etch BARC material.

A potential problem with spin-on organic BARC materials is their planarizing nature. As seen in Figs. 8 and 9 control of film thickness to a few tens of angstroms may be required for suppression of substrate reflectivity. If a polymeric material is spin coated over severe topography, film thickness can deviate substantially from a targeted value. The film is generally not conformal, which leads to significant variation in reflection reduction across a field. To increase the conformal properties of a BARC layer, alternative deposition methods can be explored. Also, through elimination of the polymeric nature of the BARC material, planarization can be further reduced. This leads to a class of inorganic antireflective materials that can be coated using chemical vapor or vacuum deposition methods.

Inorganic BARCS

Vapor-deposited ARC materials were first proposed for use over aluminum [24] and have since been applied over a variety of reflective substrate layers. The optical requirements for an inorganic layer are generally the same as for organic films. This is, however, a more difficult task with inorganic dielectric materials than it is with organic polymers as practical material choices are generally limited to those that allow process compatibility. The challenges for organic and inorganic materials can therefore differ. For inorganic films, the flexibility of optical constants is made possibly to some extent through material selection and variation in stoichiometry. Deposition thickness and uniformity can be controlled accurately to the nanometer level and films are generally conformal to the underlying topography. The choice between inorganic or organic BARC materials therefore depends in part on the underlying substrate and processing that will

be encountered. Titanium nitride [25], silicon nitride, silicon oxinitride [26], amorphous carbon [27], tantalum silicide [28], and titanium tungsten oxide [29] films have been used as inorganic antireflection layers at 365, 248, and 193 nm [30]. Substrate-resist interaction effects for 248-nm chemically amplified resists also need to be considered as candidates are evaluated, which may reduce the attractiveness of some materials for some ARC applications [31].

For nonstoichiometric materials such as silicon oxinitride, modifications in stoichiometry can be used to tailor optical properties. Traditionally, a chemical compound is thought of as having a fixed atomic ratio and composition. A wider range of properties is possible by relaxing this stoichiometric requirement. By controlling the ratios of material components during deposition, optical behavior can be modified. It is not immediately obvious that nonstoichiometric composite films of metal, insulator, or semiconductor combinations will exhibit predictable optical properties. Through analysis of the atomistic structure of materials and by relating optical material properties to electrical properties, some conclusions can be drawn [32]. Optical constants can be related to electrical properties by neglecting material structure and considering macroscopic material quantities only:

$$n^2 = \tfrac{1}{2}\left(\sqrt{\varepsilon_1^2 + \varepsilon_2^2} + \varepsilon_1\right) \tag{8}$$

$$k^2 = \tfrac{1}{2}\left(\sqrt{\varepsilon_1^2 + \varepsilon_2^2} - \varepsilon_1\right) \tag{9}$$

where ε_1 and ε_2 are real and imaginary dielectric constants, respectively. In order to account for material structure, Drude analysis of optical and electrical constants describes free electron or metallic behavior quite well in the visible and infrared (IR) region [33]. Equations 10 and 11 are Drude equations for optical and electrical constants, related to material plasma frequency (ν_1) and damping frequency (ν_2).

$$n^2 - k^2 = \varepsilon_1 = 1 - \frac{\nu_1^2}{\nu^2 + \nu_2^2} \tag{10}$$

$$2nk = \varepsilon_2 = \left(\frac{\nu_2}{\nu}\right)\frac{\nu_1^2}{\nu^2 + \nu_2^2} \tag{11}$$

To account for optical properties at shorter wavelengths, bound electron theory needs to be utilized. For dieletric materials, no intraband transitions exist because of filled valence bands. Interband transitions are also limited in IR and visible regions because of large band gap energies. Bound electron theory alone is sufficient to describe classical dielectric behavior. Characterization of metal-

lic and noninsulating materials in UV and visible regions requires use of both free electron and bound electron theory. By assuming a given number of free electrons and a given number of harmonic oscillators, optical properties over a wide wavelength range can be described. Using bound electron or harmonic oscillator theory, relationships for optical and electrical constants can be determined from the following equations:

$$\varepsilon_1 = 1 + \frac{4\pi e^2 m N_a (\nu_0^2 - \nu^2)}{4\pi^2 m^2 (\nu_0^2 - \nu^2)^2 + \gamma' \nu^2} \quad (12)$$

$$\varepsilon_2 = \frac{2e^2 N_a \gamma' \nu}{4\pi^2 m^2 (\nu_0^2 - \nu^2)^2 + \gamma' \nu^2} \quad (13)$$

where γ is the damping factor, N_a is the number of oscillators, m is electron mass, and e is electron charge. From this analysis, it can be shown that the optical properties of a material can be described by metallic behavior combined with dielectric behavior. Shown in Fig. 12 are plots of optical constants for a metallic film using the Drude model for free electron motion and metallic-dielectric composite films using combined free and bound electron models. These results suggest that the optical properties of a composite material can be modified by controlling the ratio of its components. It is expected, therefore, that the optical properties of nonstoichiometric materials would fall somewhere between those of their stoichiometric elemental or compound constituents.

Silicon nitride (Si_3N_4) possesses optical constants that may be a good starting point for use as an ARC at several wavelengths. Optical constant data for silicon nitride, silicon dioxide (SiO_2), and silicon at 436, 365, 248, and 193 nm are contained in Table 1 [34]. By adjusting the deposition parameters during

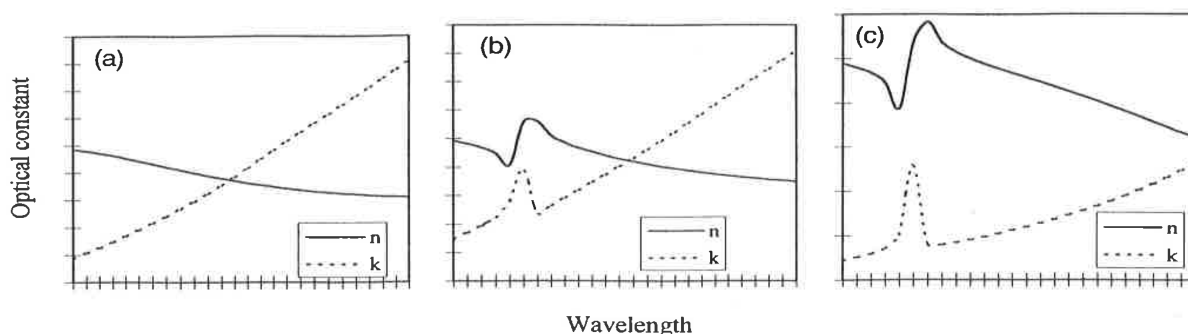

Figure 12 Plots of optical constants for a metallic film using the Drude model for free electron motion and metallic-dielectric composite films using combined free and bound electron models. (a) A metallic film; (b) a dielectric film; and (c) a dielectric composite film with increasing metallic content.

film formation (gas flow ratios for CVD and power, pressure, and gas flow for sputtering, for instance), thin-film materials can be produced with optical properties defined by these constituents. Figure 13 shows the reflectivity at the substrate interface for several 248 nm SiON ARC materials under a resist with a refractive index of 1.76. Shown also in Fig. 14 are the optical constants (n and k) for a variety of materials at 193 nm [35]. From these data together with compatibility and process requirements, potential ARC films for 193 nm can also be identified.

An additional advantage from the use of inorganic ARCs is the ability to grade the indices of materials to best match requirements of resist and substrate layers [36]. This is possible through control of process parameters during deposition. To achieve similar results with organic spin-on ARCs, multiple layers would be required. Pattern transfer for inorganic antireflective layers can also result in higher selectivity to resist, made possible, for instance, if fluorine-based etch chemistries are used. Shown in Fig. 15 is a comparison of pattern transfer processes through an organic spin-on ARC and an inorganic ARC with high resist selectivity [37]. Minimum resist erosion during the etch process with the inorganic material can result in an increase in CD control. A major trade-off when using inorganic materials is the increased complexity of deposition processes over spin coating. Process trends and requirements will probably lead to incorporation of both approaches for various lithographic operations.

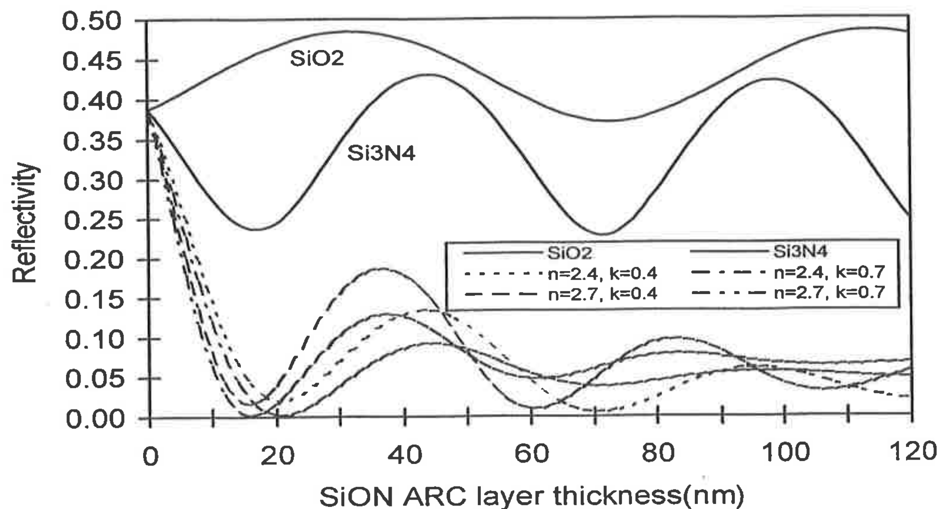

Figure 13 Reflectivity at the resist/substrate interface for several 248 nm understoichiometric SiON ARC materials under a resist with a refractive index of 1.76. The underlying substrate is polysilicon. Reflectivity for stoichiometric SiO_2 and Si_3N_4 are also shown.

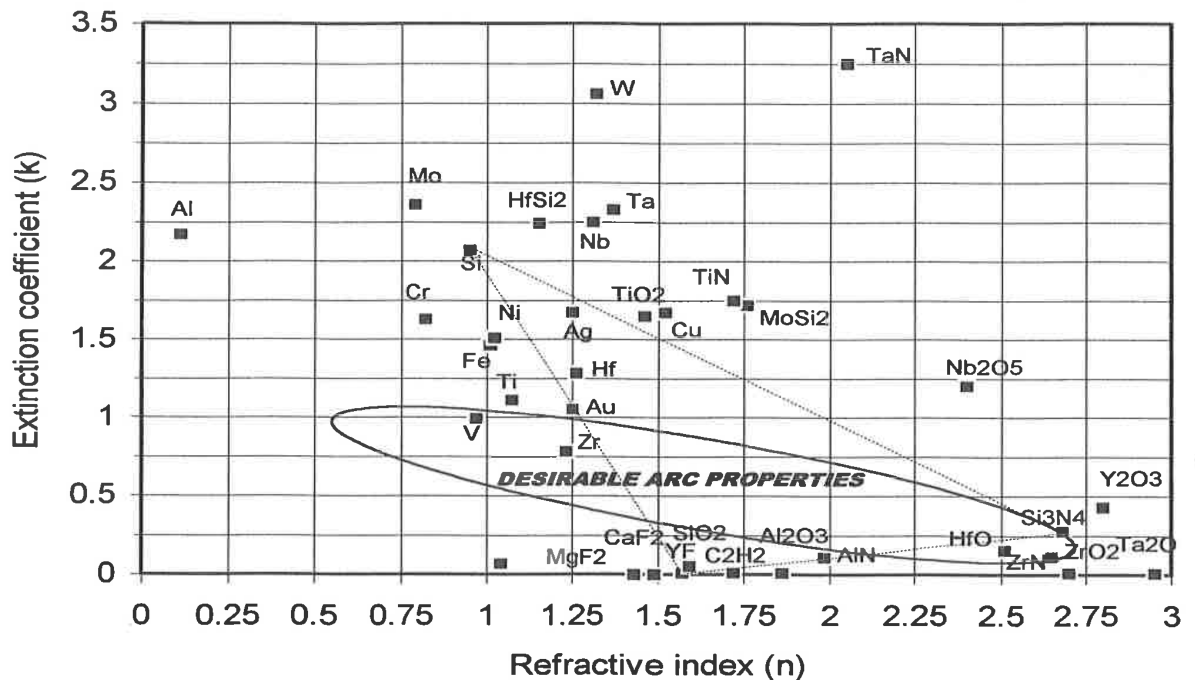

Figure 14 A plot of the optical constants (n and k) for various materials at 193 nm. A window of desirable ARC properties is shown, as also described in Figure 9. An understoichiometric SiON film would also suffice for use at 193 nm, with properties falling within the area defined by dashed lines.

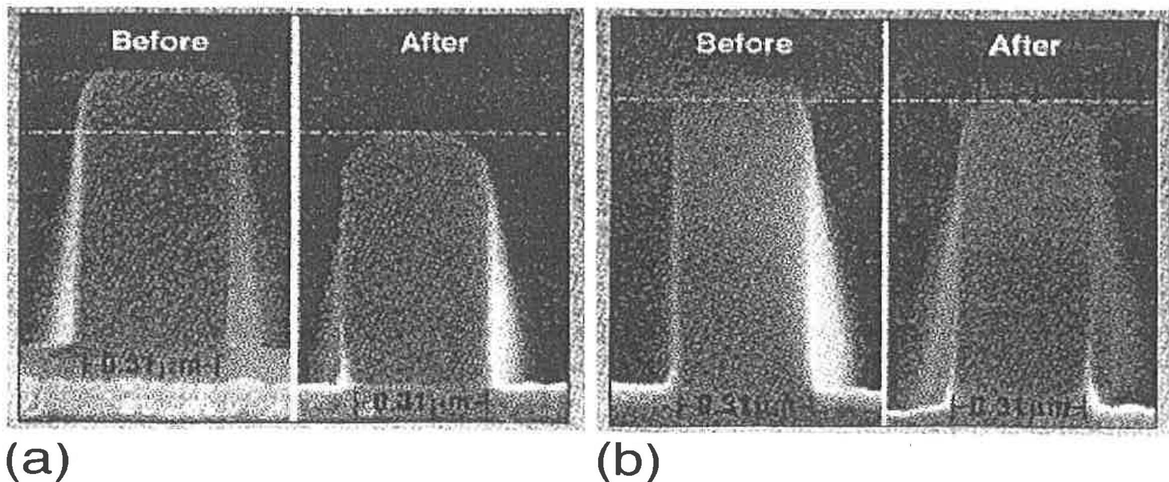

Figure 15 A comparison of resist loss during pattern transfer to bottom ARC layers. (a) Organic spin-on ARC; and (b) dielectric inorganic ARC. [From C. Bencher, C. Ngai, B. Roman, S. Lian, and T. Vuong, *Solid State Technol.*, *111*, (1997).]

4.2 Top Antireflective Approaches

The bottom antireflective approach leads to reflection reduction at the interface between a resist material and the substrate. Reflection also occurs at the top of the resist, at the resist-air interface, as shown in Fig. 16. This leads to a situation similar to that of a Fabry-Perot etalon. An expression for the reflective swing ratio can be utilized to address reflection effects within an entire resist film stack [38]:

$$\text{Swing} = 4\sqrt{R_1 R_2}\,\exp(-\alpha t) \tag{14}$$

where R_1 is the reflectivity at the resist-air interface, R_2 is the reflection at the resist-substrate interface, α is resist absorbance, and t is resist thickness. Here the swing is the ratio of the peak-to-valley change in intensity to the average intensity, which is desired to be a minimum. A decrease in R_2 via a BARC layer can be used to accomplish this, as can an increase in absorption (through use of a resist dye, for instance) or an increase in resist thickness. A reduction in R_1 is also desirable, which can be addressed through the use of a top antireflective coating (TARC) [39]. Because there is a mismatch between refractive indices of the resist material and air, R_1 can be on the order of 7%. This can lead to resist exposure and CD control problems, encountered as a result of internal reflectance via multiple interference effects, scattered light, and reflective standing wave. An exposure tool alignment signal detection can also be degraded from top surface reflection effects [40]. Like conventional AR coatings for optical applications TARC films are not absorbing materials but instead transparent thin-film interference layers that utilize destructive interference to eliminate reflectance. The ideal refractive index for such a film coated over a resist material is that which produces equivalent reflectance of from the air and from the resist side of the interface. This leads to an optimum index of

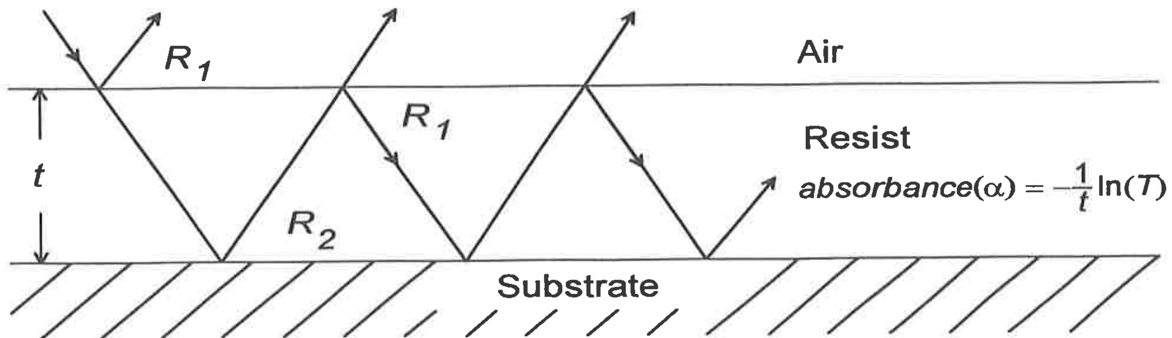

Figure 16 Diagram of reflection contribution from resist/substrate and resist/air interfaces.

$$n^*_{\mathrm{AR}} = \sqrt{n^*_{\mathrm{air}} \times n^*_{\mathrm{resist}}} \quad (15)$$

If a film of this index is coated to a quarter-wave thickness ($\lambda/4n_{\mathrm{ARC}}$), complete destructive interference can occur. For i-line resist materials with a refractive index of 1.70, an ideal TARC material would have an index of 1.30 and would be coated at 700 Å. Figure 17 shows the reduction in reflection for a quarter-wave top AR layer when the refractive index is varied from 1.1 to 1.5. For refractive index values below 1.3, there is a larger contribution to reflection from the resist-TARC interface. At values above 1.3, the contribution from the air-TARC interface is larger.

The refractive index and reflectance properties of several TARC materials are given in Table 2. As the refractive index of a material approaches the ideal value of $\sqrt{n^*_{\mathrm{air}} \times n^*_{\mathrm{resist}}}$, the reflectances at the resist and air interfaces are equivalent, allowing destructive interference at a quarter-wave thickness. Residual reflectances results as TARC indices deviate from the ideal. To achieve refractive index values near the ideal 1.3, polyfluoroalkylpolyethers and polytetrafluoroethylene-based materials cast in solvents that do not dissolve novolac resist materials have been utilized at TARC layers [41, 42]. These fluorinated polymers require removal with chlorofluorocarbons prior to development and have been replaced by water-based and water-soluble materials to improve process compatibility [43]. Although these materials do not possess a refractive index

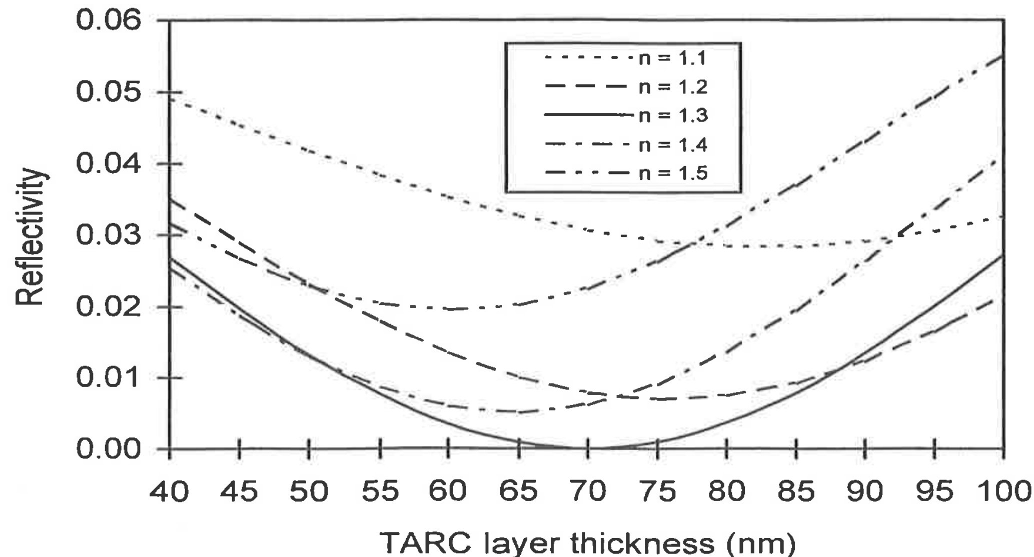

Figure 17 The reduction in surface reflection through use of a TARC material at 365 nm. Reflection can be eliminated through use of a quarter wave thickness (700 Å) of a material with a refractive index of 1.3.

Table 2 Refractive Index and Reflectance Properties of Several TARC Candidates

	Refractive index n(365nm)	*Departure from ideal*	*Quarter wave thickness at 365 nm*	*Reflectance at air interface*	*Reflectance at resist interface*
Polyvinyl alcohol	1.52	0.32	600 Å	4.26%	0.3%
Polyethylvinylether	1.46	0.16	625 Å	3.5%	0.6%
Polyfluoroalkylpolyether	1.27	0.02	713 Å	1.5%	2.0%
Aquatar [12]	1.41	0.11	647 Å	2.9%	0.9%
Ideal*	1.30	—	702 Å	1.8%	1.8%

*Assuming a resist refractive index of 1.70.

as close to the ideal values for use with DNQ/novolac resists at 436 and 365 nm, (the refractive index is 1.41 at 365 nm), the reduced process complexity makes them a more attractive choice over solvent-based systems. Figure 18 shows the reflectivity of a resist film stack as resist film thickness is varied. Reflectivity varies by over 20% for resist over polysilicon over one swing period. This is reduced significantly with the addition of an water-soluble TAR coated to a quarter-wave thickness. Exposure and focus latitude improvement has also been demonstrated with these materials.

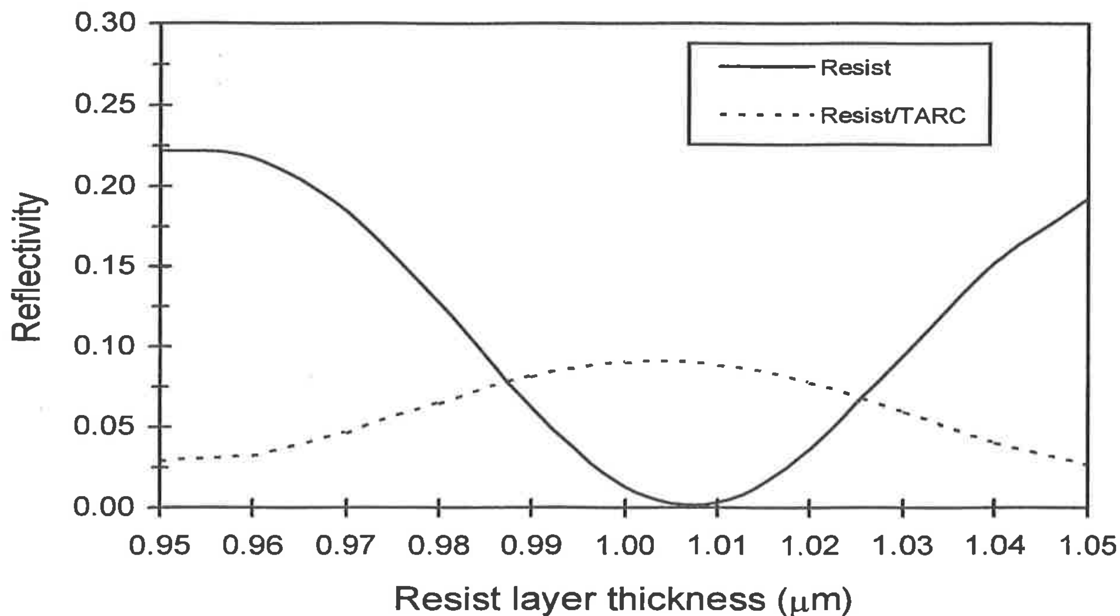

Figure 18 Reflective at the top surface of a resist material as a function of resist thickness with and without a TARC. Results are for 365 nm and a polysilicon substrate. The refractive index of the TARC is 1.41 and its thickness is 647 Å.

5 THE IMPACT OF NUMERICAL APERTURE ON REFLECTANCE EFFECTS

In Eqs. 4 and 14 the assumption of normal incidence is made. In projection imaging, the incident angle of illumination is a function of the numerical aperture (NA) of the optical system. Reflectance at an interface is a function of the angle of incidence (in air) I_1 and the angle of refraction I_2 as

$$R = \frac{1}{2}\left[\frac{\sin^2(I_1 - I_2)}{\sin^2(I_1 + I_2)} + \frac{\tan^2(I_1 - I_2)}{\tan^2(I_1 + I_2)}\right] \tag{16}$$

The first term in this equation corresponds to the reflection that is polarized in the plane of incidence and the second term corresponds to the reflection in the perpendicular plane. The effective film thicknesses for resist, AR layers, and underlying dielectric films are also scaled by the angle of incidence as $t \cos(\theta)$, where t is the thickness of the film at normal incidence. Large angles of incidence (with high-NA optics) have been shown to contribute to reducing the reflective swing ratio [44].

6 CONTRAST ENHANCEMENT MATERIALS

Resolution is generally limited in optical lithographic processes by the inability of a resist material to adequately utilize a degraded aerial image. Optical improvement techniques including the use of lenses with a higher numerical aperture, shorter wavelength exposure sources, modified illumination, or phase shift masks can be employed to improve aerial image integrity through a sufficiently large focal depth. In addition, the use of a thinner, higher contrast resist over a low-reflective substrate can best record aerial images of limited modulation. The concept of a contrast enhancement material (CEM) coated over a resist allows an alternative to these approaches, making use of an intermediate image capture step prior to image transfer into photoresist. Contrast enhancement is based on the use of photobleachable materials that are opaque prior to exposure but become transparent after photoabsorption [45–47]. The process is illustrated in Fig. 19. Here, an aerial image of low modulation is incident on a thin CEM layer coated over resist. During exposure of the CEM, its transparency increases until the resist interface is reached, at which time resist exposure begins. If the dynamic photobleaching rate of the CEM is low compared with the exposure rate of the underlying resist, the CEM image becomes an effective contact masking layer. This masking layer transfers the image into the underlying resist. The net effect is to increase the effective contrast of the resist process.

To be applicable for a microlithographic process, CEM materials must exhibit optical absorbance values above 2 at thicknesses on the order of minimum fea-

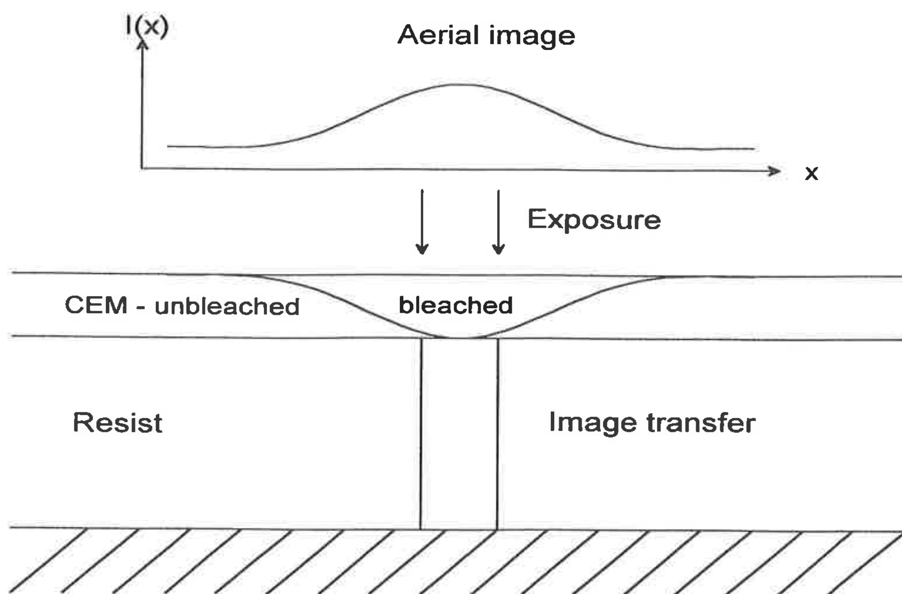

Figure 19 Schematic of a photobleachable CEM process. The CEM material acts as a contact mask for exposure of an underlying resist.

ture sizes. Figure 20 shows the spectral characteristic of a 365-nm water-soluble material consisting of an inert polymer film and an organic dye. Upon exposure, photoisomerism of the organic dye increases transparency near 365 nm. Several materials have also been introduced for exposure wavelengths of 436, 365, and 248 nm [48–50].

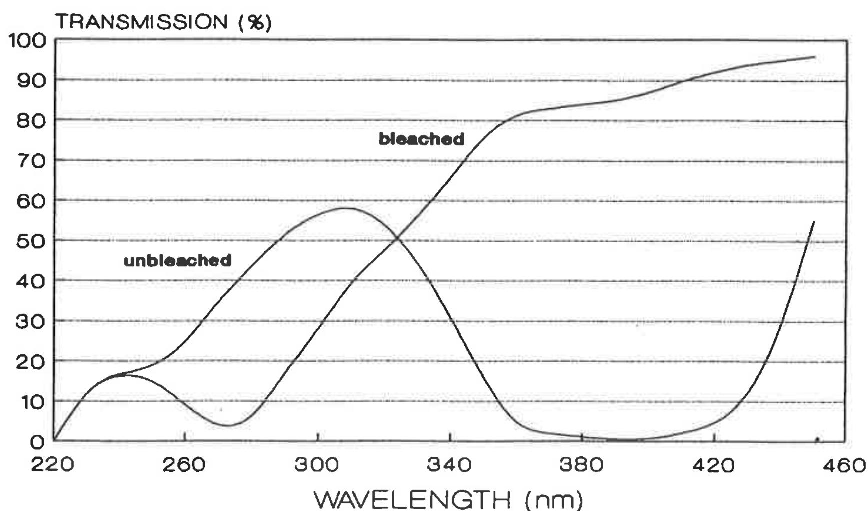

Figure 20 Transmission characteristics of a water soluble CEM material for use at 365 nm.

7 SILICON-CONTAINING RESISTS FOR MULTILAYER AND SURFACE IMAGING RESIST APPLICATIONS

Multilayer resist techniques have long been used to ease requirements for resist performance [51–56]. This goal is achieved by using physically distinct layers to separate the imaging function from the etch resistance, planarization, and reflection suppression functions. Trilevel resists have demonstrated enhanced resolution compared with single-layer resist processing. The trade-off for this resolution, however, is additional processing difficulty as the deposition and patterning of three layers must now be simultaneously controlled. Although excellent results have been obtained, the processing complexity has been the major obstacle for the widespread application to production of integrated circuits.

An obvious simplification of the original multilayer technique is to incorporate the patterning and etch resistance into one layer and require only one additional layer for planarization. Eliminating the middle layer requires that the top layer have sufficient etch resistance and that there are no detrimental interactions between the top and bottom resist layers. The use of resists containing organosilicon and organometallic polymers on top of a thick organic planarizing layer has been reported [57]. The top resist layer is developed using standard wet development techniques and the image is transferred to the bottom resist layer with an oxygen plasma etch. A refractory oxide, which is highly etch resistant, is formed in the top resist layer during the oxygen plasma etch [58,59]. Taylor et al. [60,61] demonstrated the selective introduction of silicon into the resist polymer following exposure of the resist. During the oxygen plasma development, a protective SiO_2 coating is formed on the polymer surface that is resistant to etching [62].

7.1 Bilayer Process with Silicon-Containing Resists

Silicon-containing resists for use in bilayer imaging processes are an ideal choice because of the compatibility with silicon semiconductor processing [63–65]. Many variants of silicon-containing polymers for use as resists were developed; however, early polymers required organic solvents for development and did not possess either sufficient resolution or sensitivity [66,67]. Addition of fluorescence quenchers improved the photosensitivity for polysilanes by a factor of 5, although development of the sub-0.5 mm features patterned with a 0.35 NA, 248-nm stepper was still performed in an organic solvent [68]. For aqueous development of silicon-containing resists, loss of resolution is often observed because the silicon-containing groups that are incorporated in the resists interfere with the development process by significantly altering the resist hydrophilicity.

Silicon-containing bilayer resists have received renewed attention for use at an exposure wavelength of 193 nm. A silicon-containing bilayer process capa-

ble of imaging 0.175-nm equal lines and spaces with a 193-nm, 0.5 NA stepper has been demonstrated [69]. This silicon-enriched methacrylate-based top imaging layer can be developed in standard tetramethylammonium hydroxide solution. Interestingly, the top imaging layer is relatively thick (2500 Å), suggesting that even finer resolution could be achieved if a thinner imaging layer could be used.

Si-CARL Process

A variation of the silicon-containing bilayer scheme known as Si-CARL (silicon chemical amplification of resist lines) [70,71] is illustrated in Fig. 21. Si-CARL is a typical bilayer process in that a thin imaging layer is applied on top of a thick planarizing layer. A strongly cross-linked novolak resist film of sufficient thickness to suppress substrate reflections and standing waves is used as the bottom layer. The top resist contains an anhydride, which is converted via acid-catalyzed hydrolysis to a soluble carboxylic acid . The Si-CARL process incorporates silicon into the resist after the top film has been exposed and

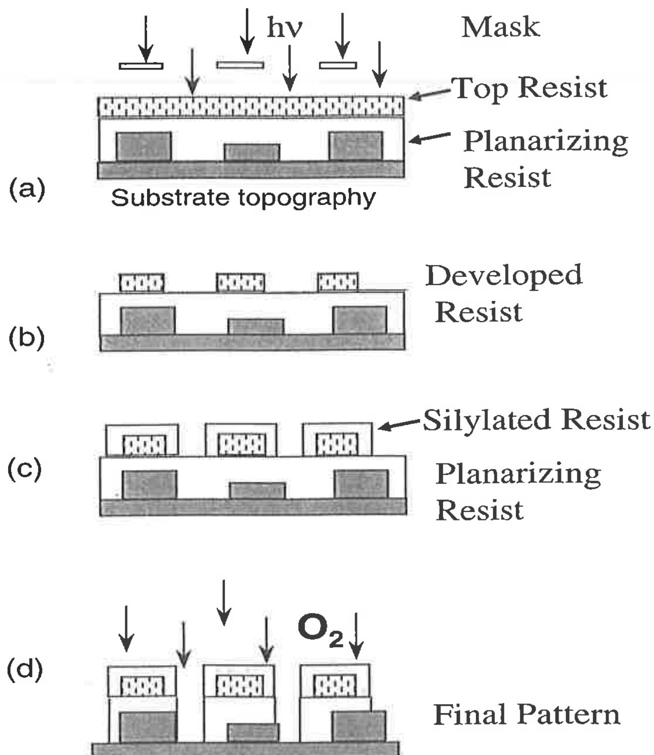

Figure 21 Illustration of the Si-CARL process. (a) Exposure of top resist; (b) aqueous development of top layer; (c) silylation of top pattern resulting in linewidth increase; (d) dry etch transfer of image to bottom layer.

developed. An amino-containing siloxane such as bis-diaminoalkyl-oligo-dimethylsiloxane reacts chemically with the anhydride and provides the etch resistance for the top resist layer during the subsequent plasma etching of the bottom layer.

The silicon incorporation in the Si-CARL process is typically performed in solution using conventional track equipment, but the dry development step is carried out using a plasma reactor. The bifunctional oligomers used for silicon delivery, so-called CARL reagents, have a reactive amine group at each end of the chain and incorporate multiple silicon atoms at each binding site in the resist polymer. These diamines can also react with different polymer chains to cause cross-linking in the resist polymer. A very high silicon content in the resist, up to 20–30% (by weight), can be achieved. After inclusion of these oligomers, the additional organic material incorporated in the resist is responsible for the swelling (i.e., amplification) of the original resist pattern. This increase in film thickness is reportedly linear in silylation time and does not appear to be inhibited by increasing cross-linking. In addition, the corresponding line width increase is independent of feature size [72]. Depending on the time during which the resist is exposed to the CARL reagent, the resulting pattern can be either the same size as the mask dimensions or the space can be reduced beyond the design size. Thus, depending on dose and aqueous silylation time, it is possible to introduce a process bias to pattern subresolution spaces. Interestingly, no observed pattern deformation or distortion has been reported with this process [72]. It is important to note that in the Si-CARL process the entire surface of the developed resist feature incorporates silicon and therefore is resistant to sizing changes during the plasma patterning of the bottom layer of resist. Very high aspect ratio patterns have been demonstrated with these methods [70].

A top surface imaging variant of this process, called simply Top-CARL, can be implemented as a single-layer process in which exposure to the CARL reagents and selective silicon uptake occur in the exposed area before development has taken place [70]. However, the Si-CARL bilayer process has a larger process latitude and greater etch resistance. Changes in the photoactive compound and matrix resin have been used to tailor the CARL and Si-CARL process for g-line, i-line, 248-nm, 193-nm lithography and e-beam lithography. Both positive and negative tone systems have been developed [73].

The Si-CARL process has the advantages of a bilayer technique (topographic invariance, reflection suppression, enhanced resolution) and can allow the optical exposure tools to operate in a more linear sizing regime. This can be advantageous for levels such as contacts, which are notoriously difficult to pattern. Another advantage of the Si-CARL process is the use of an aqueous-based, room temperature silylation scheme that can be performed on a conventional resist development track.

Other Bilayer Techniques Involving Silicon Incorporation

The silicon-added bilayer resist or SABRE process [74] is very similar to the Si-CARL technique except that silicon is introduced into the patterned top layer using a gas-phase process. In the SABRE process, conventional novolac-based g-line resists are silylated using bifunctional silylating agents to prevent resist flow and deformation. A major drawback of the SABRE process is that the silicon incorporation step is extremely slow, reportedly requiring 5 to 90 minutes, depending on the silylating agent [74].

The difficulties in formulating a single-layer resist with sufficient transparency and etch selectivity for patterning at 193 nm and even shorter wavelengths have intensified investigations of various bilayer schemes, particularly those involving introduction of silicon into the resist after it has been exposed. A bilayer approach has been demonstrated that incorporates silicon after exposure of the top resist layer by DUV (248 nm) or extreme ultraviolet (EUV; 13.5 nm) wavelengths [75,76]. As illustrated in Fig. 22, cross-linking induced by the photogenerated acid and the subsequent postexposure bake provides differential silicon permeability in the exposed and unexposed areas of the imaging layer. Silicon is

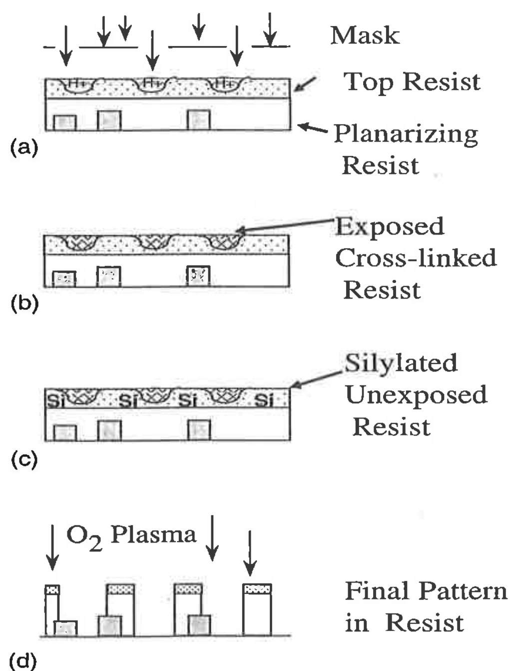

Figure 22 A silylated bilayer approach for using chemically amplified resists. (a) Exposure and generation of photoacid; (b) post-exposure bake and cross-linking of exposed resist; (c) silicon incorporation into unexposed resist; and (d) dry etch transfer of image.

preferentially incorporated in the unexposed resist from a gas-phase reagent after the exposure and bake steps. As with the Si-CARL process, some increase in resist volume accompanies the silicon incorporation. Further improvements in the process are achieved by introducing small amount of a difunctional disilane to control the resist swelling and to improve both the selectivity of the silicon inclusion step and process resolution [75]. Exposure to an oxygen-containing plasma for the all dry development step produces an etch resist silicon oxide mask in the unexposed regions resulting in a positive tone pattern.

The silylated bilayer system depicted in Fig. 22 employs chemical amplification, which, because of the low exposure dose requirements, is compatible with the limitations for the present 193-nm and EUV exposure tools. The difficulty with these systems is providing sufficient silicon incorporation into the resist while maintaining adequate contrast between the exposed and unexposed portion of the resist [76].

The use of unique materials as top imaging layers is also being explored. For instance, a bilayer process has been developed in which an imaging layer is formed by plasma-enhanced chemical vapor deposition (PECVD) from tetramethylsilane deposited on a PECVD planarizing layer. The PECVD process allows a very thin conformal top imaging layer to be applied [77].

Although the bilayer processes show some of the advantages of surface imaging, they are limited primarily by process complexity. Not only are two separate resist applications necessary, but also in most schemes both conventional wet development and dry development equipment is needed. This complexity generally translates into higher final costs that have kept many systems from becoming widely adopted. Defect and particle generation and problems with pinholes in the top imaging and barrier layers are additional problems with multilayer techniques [78,79]. With the notable exception of the Si-CARL and CARL processes, bilayer approaches are generally viewed as a method for extending the exposure tool capability and for research applications but not as manufacturable processes.

8 SILYLATION-BASED PROCESSES FOR SURFACE IMAGING

Instead of applying two distinct layers for patterning, the concept of selectively incorporating an inorganic or organometallic substance into either the exposed or unexposed regions of a single resist layer was demonstrated by Taylor et al. [60,61]. Effectively, silicon-containing bilayer was achieved post patterning by the reaction of $SiCl_4$ with the photochemically altered resist, a process termed gas-phase functionalization. In a similar vein, MacDonald et al. [80,81] used photogenerated OH reactive groups in the exposed photoresist to react with a silicon-containing amine to achieve silicon incorporation into the resist polymer.

Selective diffusion of silicon into the imaged resist gained widespread attention with the DESIRE process introduced by Roland and co-workers [82,83]. Many derivative processes were later developed and given suitable acronyms such as PRIME [84], SUPER [85], and SAHR [86]. All are single-layer patterning techniques that depend on preferential incorporation of a silicon-containing compound into the photoresist after the exposure step. Silicon incorporation in the resist was initially achieved by diffusion from the gas phase; however, Shaw et al. [87] introduced the use of a wet silylation process to produced an etch-resistant top resist layer. LaTulipe et al. [88,89] also used a liquid silylation process for surface imaging of a novolac resist. Silicon functionalization of a single-layer resist after exposure offers the attractive potential of simplifying both the resist processing sequence and the resist formulations. Although the various techniques differ in the exact mechanism of creating the contrast between the areas of silicon incorporation and silicon exclusion, many of the general characteristics are similar. Therefore, a detailed consideration of one of these schemes will serve to illustrate the major process parameters and concerns for this type of process.

8.1 The Desire Process

DESIRE, which is an acronym for diffusion-enhanced silylated resist, was the first commercialized surface imaging process [90–92]. Formulated originally for g-line exposure (436 nm), the technique is readily adaptable for I-line (365 nm) [93] as well as DUV (248 nm) [94,95] exposure. The DESIRE process, illustrated schematically in Fig. 23, consists of four interdependent steps: (1) exposure and formation of the latent image, (2) presilylation bake, (3) formation of silylated image, and (4) dry etch transfer of the pattern. Successful patterning of the resist will depend on having optimized parameters for all four steps.

The Exposure Step

During the exposure step, the photoactive compound, a naphthoquinone diazide, undergoes photochemical decomposition. Since the unexposed photoactive compound is a diffusion inhibitor, the exposed resist is more susceptible to silicon diffusion. The exposure dose and shape of the projected image to a large degree determine the ultimate depth and lateral dispersion of the silicon incorporation into the resist.

The Presilylation Bake

The presilylation bake (step 2, Fig. 23) is extremely important for selective incorporation of the silicon into the exposed regions. During this high-temperature bake, phenol ester formation by the unexposed photoactive compound forms a cross-linked and hence less permeable resist [91]. This thermally induced cross-linking of the unexposed resist in conjunction with the photochemical decom-

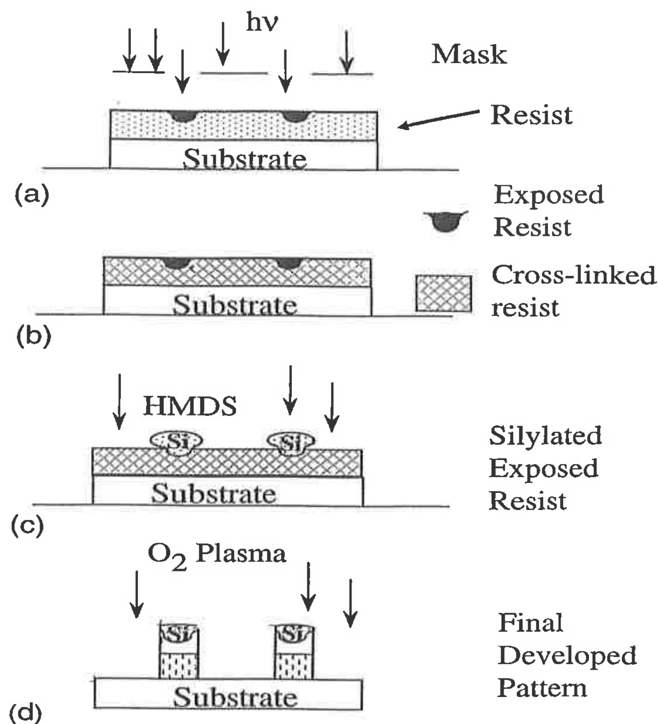

Figure 23 Schematic illustration of the DESIRE surface imaging process. (a) Exposure; (b) presilylation bake and cross-linking; (c) silicon incorporation; and (d) oxygen plasma development.

position of the sensitizer in the exposed area leads to preferential silicon incorporation into the exposed areas. The temperature and duration of the presilylation bake and the silicon exposure steps are important for defining the contrast between the exposed and unexposed region [96].

Silicon Incorporation Step: Vapor Phase Silylation

Incorporation of silicon is typically performed by vapor-phase introduction of a suitable silicon-containing reagent such as hexamethyldisilazane (HMDS). The mechanism for diffusion of the gas-phase silylation agent has been widely investigated. The unexposed naphthoquinone diazide can act as a diffusion inhibitor for HMDS in a phenolic resin, while the exposed naphthoquinone diazide will increase the diffusion rate [97,98]. Generally, the resin must provide sufficient binding sites and the diffusion of the silicon must allow 8–10% silicon incorporation, by weight, to provide sufficient etch selectivity [91]. Thermal cross-linking of the resist, initiated by the presilylation bake, continues during the silylation bake and determines the permeability of the silicon delivery agent and, hence, selectivity. The presilylation and silylation bake

parameters of temperature and time are sensitive controls for silicon incorporation. In addition, the chemical structure of the silylation agent will influence the diffusion rate and the total amount of silicon introduced into the resist. Early versions of the resist for the DESIRE process exhibited pattern deformation due to the volume change upon inclusion of the silylating agent in the resist. Changes in the resist polymer and optimization of the silylating agent have eliminated this problem [99,100].

Although HMDS is the most readily available silylating agent in semiconductor purity and was used most often for silylation processes, interesting alternative silylation agents have been investigated [93]. Small silylating agents such as dimethylsilyl dimethylamine (DMSDMA) and tetramethyldisilazane (TMDS) require relatively low temperatures (80–120°C), but silylating agents containing bulky groups such as 1,3-diisobutyl-1,1,2,2,-tetramethyldisilazane proved too bulky to provide sufficient silylation. For the smaller silicon delivery agents, it is important to decouple the presilylation bake from the silylation in order to obtain sufficient cross-linking and selectivity. Polyfunctional silylating agents have proved to be very attractive in certain applications [74,101].

Liquid-Phase Silylation

Although the silylating agent is usually introduced in the gas phase, liquid-phase silylation processes for DESIRE have been reported [102]. Liquid-phase silylation is carried out using a three-component system containing an inert carrier solvent (xylene), a diffusion promoter (*N*-methylpyrrolidone or propyleneglycol monomethyl ether acetate), and a silylating agent. Hexamethylcyclotrisilazane (HMCTS), a trifunctional cyclic amine, is generally used as the silylation agent [87,89,103], although monofunctional silylating agents such as bis(dimethylamino)dimethylsilane have also been used [102]. HMCTS induces cross-linking of the resin, which can reduce the silicon diffusion rate and ultimately limit the total silicon uptake. However, the cross-linking is beneficial because it prevents lateral swelling and pattern deformation as well as out-diffusion of silicon, problems that occur under certain conditions with gas-phase silylation [99,100,104].

Unlike gas-phase silylation, the liquid-phase silicon uptake exhibits a nonlinear response to exposure dose. There is a threshold behavior with exposure dose that should favor a more selective silylation process. The amount of silicon incorporated into the film for liquid-phase silylation (~25%) is much higher than in the gas-phase process (~10%). Hence, the dry etch selectivity of these films is also higher [105]. The reason for the higher silicon content in the liquid silylation systems is not certain. Because the amount of observed silicon added to the resist corresponds to an average of two silicon atoms for each OH group, it is proposed that some polymerization, perhaps growth of polysiloxane chains on the phenolic OH group, occurs [105].

IPR2016-01378 Page 0086

Liquid silylation techniques have been applied to other surface imaging techniques [88,89] and hold promise for improved silylation processes. For implementation in device manufacturing, an aqueous-based solution such as that used for the CARL process is much preferred to a xylene-based system from the standpoint of compatibility with existing resist processes and environmental concerns.

Dry Etch Development

Dry etch pattern transfer in the DESIRE process involves the use of an O_2 plasma to remove the unprotected resist while forming an etch-resistant silicon oxide covering in the silicon-containing areas. The dry development etch is generally carried out in a high-density plasma containing either pure oxygen or oxygen and a fluorocarbon gas [106]. Anisotropy of the etch is ensured by using very low pressures and by applying a DC bias to the wafer. Etch conditions must maintain a balance between the chemical component of the etch and physical sputtering. If care is taken to minimize the isotropic components of the etch, the resultant resist profile will depend to a large extent on the silylated profile.

Successful pattern definition during dry development involves a combination of etching of any unprotected resist and sputtering away of the silylating region [107–109]. For understanding the etch process, models that assume some competition between SiO_2 formation and sputtering of the film by ion bombardment can be applied [110,111]. Evidence for formation of a silicon oxide hard mask in the silylated regions comes from x-ray photoelectron spectroscopy (XPS) investigations of silylated resist samples before and after plasma exposure, which reveal that the silicon content of the surface does not change appreciably while there is a dramatic increase in the oxygen level. Both carbon and silicon XPS peaks are shifted to higher energy, indicating extensive oxidation [86]. For the unprotected resist, the etching mechanism involves both chemical and ion-induced etching. Clearly, oxygen atomic concentration, ion flux, and energy are important parameters for the etch. In addition, the glass transition temperature for the silylated resist polymer (T_g) has been shown to be important [112]. At higher temperatures silicon diffuses out of the exposed, silylated region, thus preventing adequate hard mask formation. This is confirmed by silicon profiling studies and correlates with a dramatic decrease in the observed etch selectivity (initially silylated vs. unsilylated areas) with increasing wafer temperature during plasma development. Improvements in etch anisotropy with the use of very low temperatures (−70°C) [113,114] and SO_2 in the plasma have been reported [115,116].

Initial attempts at dry development of silylated resists were plagued by severe problems with residue between patterned features and with line edge roughness. Residue, sometimes referred to as "grass," can arise from two

IPR2016-01378 Page 0087

sources: unintentional masking of resist during the plasma etch due to unwanted silicon incorporation in these areas and sputtering and redeposition of materials. Residue caused by unintentional silylation is usually distributed equally throughout the pattern, in some instances appearing in greater abundance in large open areas. In contrast to this, residue from sputtering and redeposition is located almost exclusively between features that should be very well resolved by the exposure tool. An example of severe grass formation caused by parasitic silylation is illustrated in Fig. 24.

Residue resulting from unintentional silicon incorporation can be minimized by optimizing the silylation and bake conditions to improve the selectivity of the silylation step. This usually involves changes in the bake time, temperature, pressure, or silylating agent. Alternatively, the dry development step can take care of the unwanted silicon inclusion by extending the over-etch time (i.e., overdevelopment) or by introducing an initial nonselective etch step to remove a certain amount of resist uniformly from the wafer. The latter step, often referred to as a "descum," involves the use of a fluorine-containing plasma or a high-energy ion bombardment step [117,118]. Usually, an initial step with low selectivity for silylated resists is followed by a second, more selective, etch [106]. A two-step oxygen etch, in which the initial step has a high ion energy, can also be used [117]. The disadvantage of either alteration of the dry development step is loss of resist thickness in the final pattern. This requires a thicker hard mask,

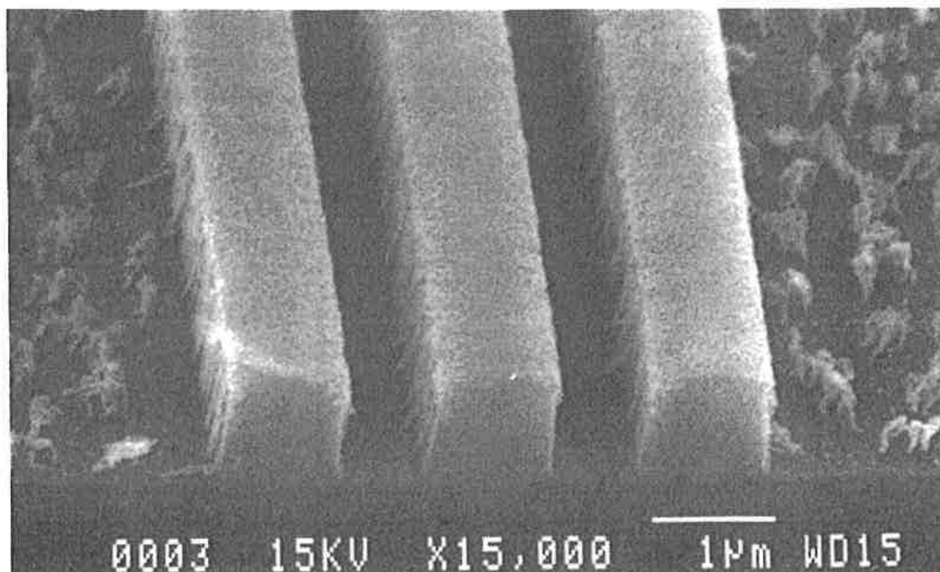

Figure 24 Examples of residue caused by unintentional silicon incorporation into exposed resist areas.

which usually translates into higher required exposure doses and longer processing times. Residue resulting from sputtering of the hard mask is eliminated by reducing the ion bombardment energy in the plasma development step.

Edge roughness for the dry developed resist can be a serious concern, particularly as the dimension of the line edge roughness become a significant percentage of the line width dimension. Extreme edge roughness is observed if the silicon content is insufficient to withstand the plasma dry development and breakdown of the etch mask occurs. The resist line roughness will most likely transfer into the underlying substrate during the subsequent etch step, causing variations in the pattern sizing. Severe edge roughness as illustrated in Fig. 25 can be caused by insufficient silicon hard mask protection of the underlying resist, low selectivity in the dry development etch, or both. Therefore, the silylation conditions and the dry etch parameters must be optimized in concert to minimize the line roughness.

Hard mask breakdown can also be observed when there is a lack of contrast in the exposed image. This can happen near the resolution limit of the exposure tool or if the exposed image is severely defocused. Edge roughness is of special concern at 193 nm and shorter exposure wavelengths due to very shallow absorption depth of the resist coupled with the small targeted line widths. Staining techniques that decorate the silylated resist profiles have verified the shallow silylated layer for these exposure wavelengths [75]. Any thinning of the silylated image near the edges of the silylated profile will result in an increase in line edge roughness. Shown in Fig. 26 is a section of a silylated grating pat-

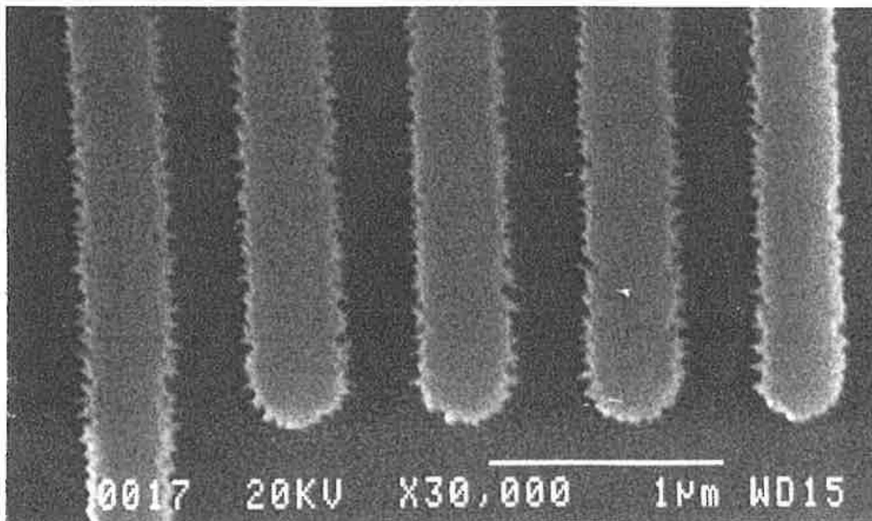

Figure 25 Line edge roughness resulting from hardmask breakdown during dry development of the resist.

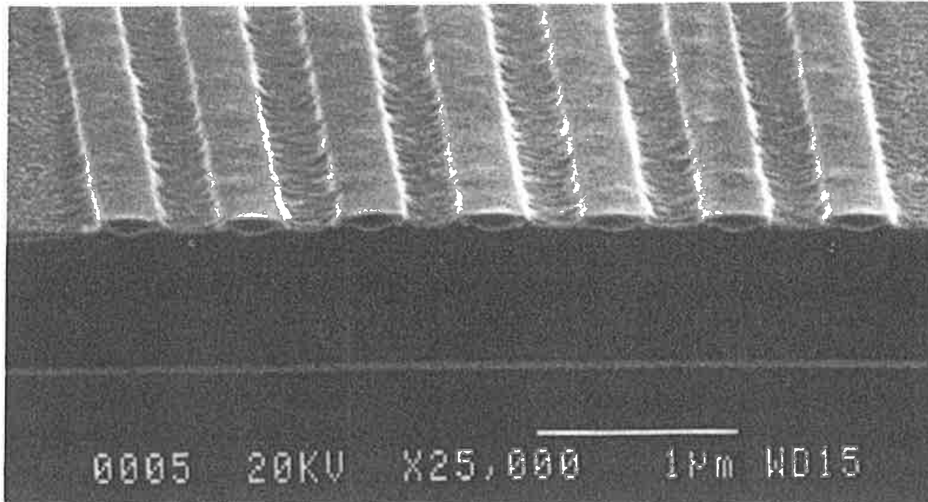

Figure 26 Silylated profiles (raised resist) which have been delineated using a short plasma etch.

tern that has been subjected to an oxygen plasma for a time sufficient to decorate the silylated areas but not completely etch the resist features. The oxygen etch has delineated the depth and lateral profile for the silylated regions [119]. It is interesting to note that along the edges of the silylated regions, some roughness is visible. The line edge roughness can be minimized by increasing the depth of silicon incorporation at the feature edges or by removing the thinner outer portions of the silicon hard mask during the dry development etch. The latter solution leads to changes in critical dimension with over-etch and is not a good solution from the point of view of process control. Although there is speculation that the molecular weight distribution of the resist could also influence the edge roughness, there have been no studies published to support this assertion.

8.2 The Prime Process

A variation of the DESIRE process for positive-tone images, called positive resist image by dry etching (PRIME), was developed by workers at LETI [84,120,121]. The PRIME process uses the same resist as the DESIRE process and differs only in the addition of a second near-UV flood exposure step (Fig. 27). Like a classical image reversal scheme, the PRIME process involves an initial exposure with DUV or e-beam followed by flood exposure at near-UV wavelengths to produce a positive-tone image. During the initial exposure, reaction of the photoactive compound results in cross-linking of the resist. For DUV exposure, only the top 300 Å of the resist is cross-linked, whereas the en-

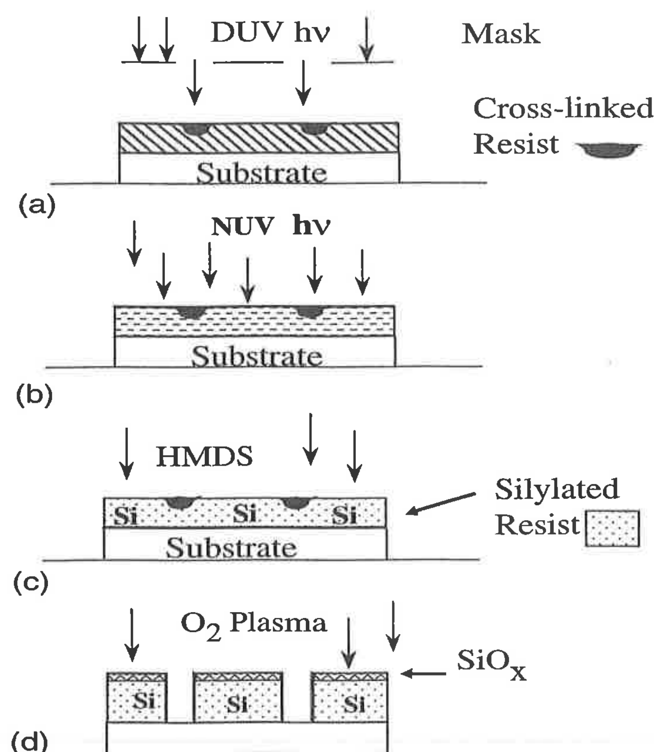

Figure 27 Schematic representation of the PRIME process. (a) DUV exposure; (b) NUV flood exposure; (c) presilylation bake and crosslinking; (d) silicon incorporation; and (e) oxygen plasma development.

tire resist thickness is cross-linked upon e-beam exposure. Degradation of the photoactive compound during the subsequent near-UV flood exposure increases the diffusion rate of the silylation agent in the previously unexposed areas. Silylation and dry development are performed in a manner similar to that in the DESIRE process, the end result being a positive-tone image. A major difficulty with the PRIME process is the high energies required for both the cross-linking step (400 mJ/cm^2 at 248 nm and 300 mC/cm^2 for e-beam at 50 keV) and the flood exposure (1–2 J/cm^2). Although some work with more sensitive resist formulations has been reported [122], this still remains a serious concern.

8.3 The SAHR Process

The silylated acid hardened resist (SAHR) process (Fig. 28) is a positive-tone single-layer process that relies on photoinitiated, acid-catalyzed cross-linking. In the SAHR process, DUV-induced acid generation in the imaging layer causes cross-linking in the exposed region during the postexposure bake step and renders these areas impermeable and unreactive to silylamines [123]. With gas-

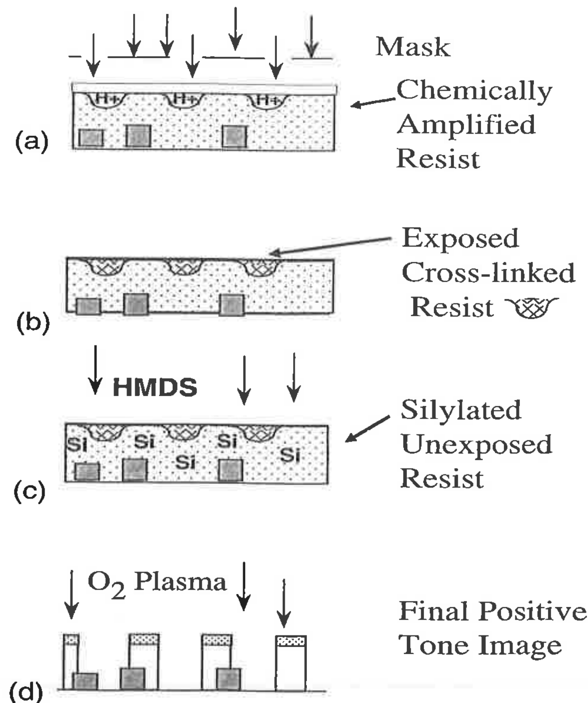

Figure 28 Silylated acid hardened resist process (SAHR). (a) Exposure and generation of photoacid; (b) post-exposure bake and crosslinking of exposed resist; (c) silicon incorporation into unexposed resist; and (d) dry etch transfer of image.

phase silylation, the unexposed resist incorporates 10–12% silicon by weight, which is adequate to protect the underlying resist during the final plasma development.

The chemically amplified resists used in the SAHR process require much lower exposure doses (5–30 mJ/cm^2 for DUV exposures) compared with the novolac resists for the DESIRE process. The original SAHR process suffers from severe limitations with respect to its practical implementation. The first is the variation of silicon penetration depth with feature size in which the larger features exhibit a much deeper silylation depth. This size-dependent variation of the silylated profiles make it difficult to control line width and maintain pattern sizing linearity. The differential silicon incorporation cannot be explained simply by decreased optical contrast, as this effect is observed at feature sizes much larger than the resolution limit of the exposure tool. A plausible explanation is that the interfacial tension per unit volume becomes much larger as the patterned dimensions shrink, causing this sizing dependence [124]. An additional problem with the SAHR process is the resist flow during silylation. Incorporation of silyl groups into the resist film causes resist swelling and

interferes with the hydrogen bonding, thus lowering the T_g of the resist film. As a consequence, during the silylation process the silylated resist overflows into the exposed (cross-linked) regions. This parasitic silicon incorporation degrades the silylation process contrast and requires extra processing steps to minimize the effect. Exposure of the resist to a bifunctional silane such as bis(dimethylamino)dimethylsilane prior to treatment with the silylating agent significantly diminishes the amount of silicon in the exposed areas by creating a thin cross-linked skin on the resist surface [124]. Alternatively, an aqueous development step prior to the silylation step eliminates both the flow problem and the size dependence of the silicon penetration depth. Surface depressions in the unexposed areas are created by this development step and are refilled by the swollen silylated material. However, this predevelopment step removes ~4000 Å of resist and requires thicker initial resist coatings.

Today, modified SAHR processes are being used with e-beam as well as shorter wavelength (193 and 13.5 nm) exposure tools [101,114,125–127]. For these shorter wavelength exposures the cross-linking is facile due to the high photon energy. A number of patterning techniques have exploited this fact to create differential diffusion rates of a silicon-containing reagent to achieve surface imaging at 193 nm [125,128] or 13–40 nm (extreme UV) [129]. For many of the 193-nm surface imaging techniques being explored, photochemical cross-linking, unaided by chemical amplification, is used [128].

8.4 Other Surface Imaging Techniques

Investigations targeted at developing surface imaging processes for high-resolution applications are yielding some interesting results. For example, work using plasma deposition of organosilicon shows promise for a single-layer and bilayer process [130–132]. An all dry patterning process involving the polymerization of methylsilane has demonstrated encouraging results with this thin conformal imaging layer [132]. In addition, non-silicon-containing single-layer and bilayer processes are being investigated. Near-surface imaging using metal plating to define an etch-resistant mask has also been demonstrated [133–135]. In this process, a substrate surface is treated with an organosilane and exposed to DUV 248 nm) radiation. This exposure modifies the wettability of the substrate surface and reactivity of the surface film. Subsequent treatment with a Pb/Sn catalyst followed by electroless copper and nickel metallization yields films several hundred angstroms thick in unexposed regions. This positive image can then be used as a plasma etch mask. The ultrathin films resulting from this process can lead to significant improvement in focal depth and resolution.

9 USE OF ALTERNATIVE PATTERN TECHNOLOGY IN MANUFACTURING

Surface imaging has traditionally been used to extend the capabilities of the current generation of optical lithography tools while allowing time for the newer tools to mature. Surface imaging or near-surface imaging techniques using bilayer approaches have found limited usage outside the research environment. There are, however, a few exceptions. [73,136,137] The DESIRE process was transferred to a pilot line at Texas Instruments and used in the early production and qualification of a 16-MB DRAM device [136]. The challenging topography and high reflectivity of the metal level necessitated the use of surface imaging resists. The DESIRE process was eventually replaced by a process using conventionally developed resist; however, use of an antireflective coating (ARC) and enhanced planarization techniques were necessary to achieve performance comparable to that of the DESIRE process. It is of interest to note that the measured defect levels and yield for the DESIRE process were comparable to those of the optimized ARC/conventional resist process [138]. As mentioned earlier, the CARL process has been used successfully at Seimens for manufacturing for a few [73].

Antireflective coatings, both top and bottom layer films, are necessary for many current IC applications and are employed in numerous manufacturing lines. The manufacturing issues for nonconventional resist techniques such as surface imaging or bilayer resist imaging have been discussed by several authors [78,138,139]. However, the ultimate selection of a photoresist process, whether conventional single-layer resist processing or one of the alternative processes we have discussed, will depend on the achievable patterning resolution and process latitude, robustness toward subsequent etching steps, line width control, ease of integration into current fabrication environments, yield, and ultimately cost.

9.1 Advantages and Disadvantages of Multilayer and Surface Imaging Techniques

Multilayer resist techniques and surface imaging processes are more complicated than conventional, single-layer, aqueous-developed resist techniques but have unique advantages. The improved depth of focus and resolution, insensitivity to topography, and ability to work with multiple stepper generations and wavelengths may, in certain applications, make them worth the added complications. The all dry process allows very high aspect ratio resist patterning. Among the alternative methods for providing enhanced patterning capabilities such as bilayer and trilayer processes [54,55,67], the single-layer surface imaging resist techniques are somewhat simpler from a processing standpoint.

IPR2016-01378 Page 0094

The advantages outlined above must be weighed against the additional complexity of these alternative process. Nontraditional equipment is required for many of these techniques. For silylation-based processes, a silylation tool and a plasma etcher are required. Although the use of organic antireflective coatings has introduced etch processes into many formerly conventional patterning techniques, the silylation step has no equivalent in the conventionally developed resist process. The higher exposure dose requirement for some alternative techniques translates into lower throughput and higher costs. As with any plasma process, there are concerns about damage and defects caused by the dry development plasma processing [140]. As device dimensions become smaller, additional concerns about the dry development etch arise. For instance, edge roughness dimensions become a larger fraction of the line width and must be minimized. Damage mechanisms that may not have been detected with larger design sizes may become more important with the smaller device designs. Working close to or below the intended resolution of the stepper, as is often the case for many of the multilayer and surface imaging techniques, often increases the proximity effects. To minimize the proximity effects, the dry development must be carefully optimized. Still of major concern is that no manufacturing equipment set is available for many of these alternative processes.

9.2 Prognosis for Multilayer and Surface Imaging Technologies

Multilayer and surface imaging techniques will probably play an important role in future lithography development. These processes are easily applied to numerous exposure tools including 193 nm, e-beam, and EUV exposure systems. This is especially important for the development of new exposure tools where the resists are problematic [128,141]. Fortunately, many aspects of the process are the same across different wavelengths, so the experience gained with a tool set of one generation is readily adapted to the next-generation exposure tool.

More variations are being added to the repertoire of available surface imaging or thin-film patterning processes. Both positive and negative tone silylated surface imaging resists are now available [89,90,101]. Novel silylating agents are also being explored [102,101]. Improvements in the multilayer resist processes, particularly for application to 193 nm and EUV exposure, are ongoing. Optical enhancement techniques such as modified illumination and phase shifting of reticles are complementary to near-surface and surface imaging resist techniques and can further extend the process capabilities. Surface imaging resist processing has become more widely known in the semiconductor industry. The equipment necessary for processing is becoming commercially available [142], and some of the nontraditional steps are becoming more familiar to

the lithographer because organic antireflective layers also require dry etching. In addition, the cost of implementing surface imaging or multilayer resist processes can compare favorably with that of conventional processing if the cost of additional processes to compensate for the deficiencies of single-layer resist (e.g., antireflective coatings, etch hard masks) is considered.

REFERENCES

1. Stillwagon, L. E., and Taylor, G. N., *Polymers in Microlithography: Materials and Processes*, ACS Symp. Ser. 412, American Chemical Society, Washington, DC, 1989, pp. 252–265.
2. Stillwagon, L. E., and Larsen, R. G., *J. Appl. Phys*, *63*, 5251 (1988).
3. Steigerwald, J. J., Murarka, S. P., and Gutmann, R. J., *Chemical Mechanical Planarization of Microelectronic Materials*, Wiley, New York, 1997.
4. Bruce, J. A., Lin, B. J., Sundling, D. L., and Lee, T. N., *IEEE Trans. Elect. Dev.*, *ED-34*, 2428 (1987).
5. Lin, B. J., Bassous, E., Chao, W., and Petrillo, K. E., *J. Vac. Sci. Technol. B*, *19*, 1313 (1981).
6. Lin, B. J., *Electrochem. Soc.*, *127*, 202 (1980).
7. Liu, E. D., O'Toole, M. M., and Chang, M. S., *IEEE Trans. Elect. Dev.*, *ED-28*, 1405 (1981).
8. Ting, C. H., and Liauw, K. L., *J. Vac. Sci. Technol. B*, *1*, 1225 (1983).
9. de Grandpre, M. P., Vidusek, D. A., and Leganza, M. W., *Proc. SPIE*, *539*, 103 (1985).
10. Todokoro, Y., *IEEE Trans. Elect. Dev.*, *ED-27*, 1443 (1980).
11. Lamarre, P. A., *IEEE Trans. Elect. Dev.*, *ED-39*, 1844 (1992).
12. Liu, E. D., *Solid State Technol.*, *26*, 66 (1982).
13. Ting, C. H., *Proc. Kodak Interface*, *83*, 40 (1983).
14. Havas, J. R., *Electrochem. Soc. Ext. Abst.*, *2*, 743 (1976).
15. Brewer, T., Carlson, R., and Arnold, J., *J. Appl. Photo. Eng.*, *7*, 184 (1981).
16. Coyne, R. D., and Brewer, T, *Proc. Kodak Interface*, *83*, 40 (1983).
17. Mimura, Y., and Aoyama, S., *Microelect. Eng.*, *21*, 47 (1993).
18. Ishii, W., Hashimoto, K., Itoh, N., Yamazaki, H., Yokuta, A., and Nakene, H., *Proc. SPIE*, 295 (1986).
19. Nölscher, C., Mader, L., and Scheegans, M., *Proc. SPIE*, *1086*, 242 (1989).
20. Such as Brewer Science ARC-XLN.
21. Reiser, A., *Photoreactive Polymers*, 323, Wiley, N.Y. (1989).
22. Yang, T. S., Koot, T., Taylor, J., Josephson, W., Spak, M., Dammel, R., *SPIE*, *2724*, 724 (1996).
23. Pavelchek E., Meudor, J., Guerrero, D., *SPIE*, *2724*, 692 (1996).
24. van den Berg, H., and van Staden, J., *J. Appl. Phys.*, *50*, 1212 (1979).
25. Martin, B., and Gourley, D., *Microelect. Eng.*, *21*, 61 (1993).
26. Ogawa, T., Nakano, H., Gocho, T., and Tsumori, T., *Proc. SPIE*,
27. Tani, Y., Mato, H., Okuda, Y., Todokoro, Y., Tatsuta, T., Sanai, M., and Tsuji, O., *Jpn. J. Appl. Phys.*, *322*, 5909 (1993).

28. Draper, B. L., Mahoney, A. R., and Bailey, G. A., *J. Appl. Phys.*, *62*, 4450 (1987).
29. Tompkins, H., Sellars, J., and Tracy, C., *J. Appl. Phys.*, *73*, 3932 (1993).
30. Smith, B., Alam, Z., and Butt, S., *Abstracts of the Second International Symposium on 193nm Lithography*, Colorado Springs, 1997.
31. Dean, K. R., Carpio, R. A., Rich, G. F., Proc. *SPIE*, *2438*, 514 (1995).
32. Smith, B. W., Butt, S., Alam, Z., Kurinec, S., and Lane, R., *J. Vac. Sci. Technol. B.*, *14*, 3719 (1996).
33. Hummel, R. E., *Electronic Properties of Materials*, Springer-Verlag, New York, 1993, pp. 186–230.
34. Palik, E. C., *Handbook of Optical Constants of Solids I*, (1985).
35. Smith, B. W., Butt, S., Alam, Z., *J. Vac. Sci. Technol. B, 14(6)*, 3714 (1996).
36. Cirelli, R. A., Weber, G. R., Kornblit, A., Baker, R. M., Klemens, F. P., and DeMarco, J., *J. Vac. Sci. Technol. B*, *14*, 4229 (1996).
37. Bencher, C., Ngai, C., Roma, B., Lian, S., and Vuong, T., *Solid State Technol.*, *20*, 109 (1997).
38. Brunner, T. A., *Proc. SPIE*, *1466*, 297 (1991).
39. Tanaka, T., Hasegawa, N., Shiraishi, H., and Okazaki, S., *J. Electrochem. Soc.*, *137*, 3900 (1990).
40. Bobroff, N., and Rosenbluth, A., *J. Vac. Sci. Technol. B*, *6*
41. Brunner, T. A., *Proc. SPIE*, *1466*, 297 (1991).
42. Shiraishi, H., and Okazaki, S., *Proc. SPE Reg. Tech. Conf. Photopolym.*, Ellenville, NY, 1991, p. 195.
43. Lyons, C. F., Leidy, R. K., and Smith, G. B., *Proc. SPIE*, *1674*, 523 (1992).
44. Bernard, D., and Arbach, H., *J. Opt. Soc. Am.*, *8*, 123 (1991).
45. Havas, J. R., U.S. Patent 4,025,191 (1977).
46. Wiebe, A. F., U.S. Patent 3,511,652 (1970).
47. Griffing, B. F., and West, P. R., *Polym. Eng. Sci.*, *23*, 947 (1983).
48. Hofer, D. C., Miller, R. D., and Willson, C. G., *Proc. Microcircuit Eng.*, *A5*, 1 (1984).
49. Halle, L. F., *J. Vac. Sci. Technol.*, *3*, 323 (1985).
50. Endo, M., Tani, Y., Sasago, M., Nomura, N., and Das, S., *J. Vac. Sci. Technol. B*, *7*, 1072 (1989).
51. Havas, J. R., U.S. Patent 3,873,361 (1973).
52. Lin, B. J., and Chang, T. H. P., *J. Vac. Sci. Technol.*, *1*, 1669 (1979).
53. Moran, J. M., and Maydan, D., *J. Vac. Sci. Technol.*, *16*, 1620 (1979).
54. Buiguez, F., Parrens, P., and Picard, B., *Proc SPIE*, *393*, 192 (1983).
55. Lin, B., in *Introduction to Microlithography* (L. Thompson, M. Bowden, and G. Wilson, eds.), American Chemical Society, Washington DC, 1983, pp. 287–349.
56. Bassous, E., Ephrath, L., Pepper, G., and Mikalsen, S., *J. Electrochem. Soc.*, *130*, 478 (1983).
57. Hatzakis, M., Paraszcak, J., and Shaw. J., *Proceedings of the Microelectronic Engineering Conference*, Lausanne, 1981, p. 386.
58. Paraszcak, J., Babich, E., McGouey, R., Heidenreich, J., Hatzakis, M., and Shaw, J., *Microelectron. Eng.*, *6*, 453 (1987).
59. For review see Hatzakis, M., Shaw, J., Babich, E., and Paraszczak, J., *J. Vac. Sci. Technol. B*, *6*, 2224 (1988).

60. Taylor, G. N., Stillwagon, L. E., and Venkatesan, T., *J. Electrochem. Soc.*, *131*, 1658 (1984).
61. Wolf, T. M., Taylor, G. N., Venkatesan, T., and Kraetsch, R. T., *J. Electrochem, Soc.*, *131*, 1664 (1984).
62. Taylor, G. N., and Wolf, T. M., *Polym. Eng. Sci.*, *20*, 1087 (1980).
63. Wilkins, C. W., Reichmanis, E., Wolf, T. M., and Smith, B. C., *J. Vac. Sci. Technol. B*, *3*, 306 (1985).
64. Saotome, Y., Gokan, H., Sargo, K., Suzuki, M., and Ohnishi, J., *J. Electrochem. Soc.*, *132*, 909 (1985).
65. Miller, R. D., Hofer, D., McKean, D. R., Willson, C. G., West, R., and Trefonas, P. T., in *Materials for Microlithography*, ACR Symp. Ser. 266 (L. F. Thompson, C G. Willson, and J. M. J. Frechet, Eds.), American Chemical Society, Washington, DC, 1984, pp. 293–310.
66. Reichmanis, E., MacDonald, S. A., and Iwayanagi, T., in *Polymers in Microlithography*, American Chemical Society, Washington, DC, 1989.
67. Miller, R. D., and Wallraff, G., *Adv. Mater. Opt. Electron.*, *4*, 95 (1994).
68. Wallraff, G. M., Miller, R. D., Clecak, N., and Baier, M., *Proc. SPIE*, *1466*, 211 (1991).
69. Schaedeli, U., Tinguely, E., Blakeney, A. J., Falcigno, P., and Kunz, R. R., *Proc. SPIE*, *2724*, 344 (1996).
70. Sezi, R., Sebald, M., Leuschner, R., Ahne, H., Birkle, S., and Borndorfer, H., *Proc. SPIE*, *1262*, 84 (1990).
71. Sebald, M., Berthold, J., Beyer, M., Leuschner, R., Noelscher, C., Scheler, U., Sezi, R., Ahne, H., and Birkle, S., *Proc. SPIE*, *1466*, 227 (1991).
72. Sebald, M., Leuschner, R., Sezi, R., Ahne, H., and Birkle, S., *Proc. SPIE*, *1262*, 528 (1990).
73. Leuschner, R., Ahne, H., Marquardt, U., Nickel, U., Schmidt, E., Sebald, E., and Sezi, R., *Microelectron. Eng.*, *20*, 305 (1993).
74. McColgin, W. C., Jech, J., Daly, R. C., and Brust, T. B., *Proc. Symp. VLSI Technol.*, 1987, p. 9.
75. Wheller, D. R., Hutton, S., Stein, S., Baiocchi, F., Cheng, M., and Taylor, G. N., *J. Vac. Sci. Technol. B*, *11*, 2789 (1993).
76. Taylor, G., Hutton, R., Stein, S., Boyce, C., Wood, O., LaFontaine, B., MacDowell, A., Wheeler, D., Kubiak, G., Ray-Chaudhure, A., Berger, K., and Tichenor, D., *Proc. SPIE*, *2437*, 308 (1995).
77. Horn, M. W., Maxwell, B. E., Knuz, R. R., Hibbs, M. S., Eriksen, L. M., Palmateer, S. C., and Forte, A. R., *Proc. SPIE*, *2438*, 760 (1995).
78. McDonnell Bushnell, L. P., Gregor, L. V., and Lyons, C. F., *Solid State Technol.*, June, 133 (1986).
79. Miller, K. P., and Sachdev, H. S., *J. Vac. Sci. Technol. B*, *10*, 2560 (1992).
80. MacDonald, S. A., Schlosser, H., Ito, H., Clecak, J., and Willson, C. G., *Chem. Mater.*, *3*, 435 (1991)
81. Ito, H., MacDonald, S. A., Miller, R. D., and Willson, C. G., U.S. Patent 4,552,833 (1985).
82. Coopmans, F., and Roland, B., *Proc. SPIE*, *631*, 34 (1986).
83. Roland, B., and Vrancken, A., Eur. Patent Appl. 85870142.8 (1985).

84. Pierrat, C., Tedesco, S., Vinet, Lerme, M., and Dal'Zotto, B., *J. Vac. Sci. Technol. B*, *7*, 1782 (1989).
85. Mutsaers, C. M. J., Vollenbroek, F. A., Nijssen, W. P. M., and Visser, R. J., *Microelectron. Eng.*, *11*, 497 (1990).
86. Pavelchek, E. K., Bohland, J. F., Thackery, J. W., Orsula, G. W., Jones, S. K., Dudley, B. W., Bobbio, S. M., and Freeman, P. W., *J. Vac. Sci. Technol. B*, *8*, 1497–1501 (1990).
87. Shaw, J. M., Hatzakis, M., Babich, E. D., Paraszczak, J. R., Witman, D. F., and Stewart, K. J., *J. Vac. Sci. Technol. B*, *7*, 1709, (1989).
88. La Tulipe, D. C., Pomerene, A. T. S., Simons, J. P., Seeger, D. E., *Microelectron. Eng.*, *17*, 265(1992).
89. LaTulipe, D. C., Simons, J. P., and Seeger, D. E., *Proc. SPIE*, *2195*, 372 (1994).
90. Coopmans, F., and Roland, B., *Proc. SPIE*, *631* 34 (1986).
91. Roland, B., Lombaerts, R., Jacus, C., and Coopmans, F., *Proc. SPIE*, *771*, 69 (1987).
92. Visser, R. J., Schellenkens, J. D. W., Reuhman-Huiskens, M. E., and Ijzendoorn, L. J., *Proc. SPIE*, *771*, 110 (1987).
93. Baik, K. H., van den Hove, L., Goethals, A. M., Op de Beeck, M., and Roland, R., *J. Vac. Sci. Technol. B*, *8*, 1481 (1990).
94. Op de Beeck, M., and Van den Hove, L., *J. Vac. Sci. Technol. B*, *10*, 701 (1992).
95. Hanratty, M. A., and Tipton, M. C., *Proc. SPIE*, *1674*, 894 (1992).
96. Goethals, A. M., Lombaerts, R., Roland, B., and van den Hove, L., *Microelectron. Eng.*, *13*, 37 (1991).
97. Roland, B., Lombaerts, R., Vandendriessche, J., and Godts, F., *Proc. SPIE*, *1262*, 151 (1990).
98. Roland, B., Vandendriessche, J., Lombaerts, R., Denturck, B., and Jakus, C., *Proc. SPIE*, *920*, 120 (1988).
99. Goethals, A. M., Nichols, D. N., Op de Beeck, M., De Geyter, P., Baik, K. H., van den Hove, L., Roland, B., and Lombaerts, R., *Proc. SPIE*, *1262*, 206 (1990).
100. Goethals, A. M., Baik, K. H., Ronse, K., van den Hove, L., and Roland, B., *Microelectron. Eng.*, *21* 239 (1993).
101. Wheeler, D., Hutton, R., Boyce, C., Stein, S., Cirelli, R., and Taylor, G., *Proc. SPIE*, *2438*, 762 (1995).
102. Baik, K. H., van den Hove, L., and Roland, B., *J. Vac. Sci. Technol. B*, *9*, 3399 (1991).
103. Rouhman-Huisken, M. E., Mutsaers, C. M. J., Vollenbroek, F. A., and Moonen, J. A., *Microelectron. Eng.*, *9*, 551 (1989).
104. Doa, T. T., Spence, C. A., and Hess, D. W., *Proc. SPIE*, *1466*, 257 (1991).
105. Baik, K. H., Ronse, K., van den Hove, L., and Roland, B., *Proc. SPIE*, *1672*, 362 (1992).
106. Lombaerts, R., Roland, B., Goethals, A. M., and van den Hove, L., *Proc. SPIE*, *1262*, 43 (1990).
107. Dijkstra, H. J., *J. Vac. Sci. Technol B*, *10*, 2222 (1992).
108. LaPorte, P., van den Hove, L., and Melaku, Y., *Microelectron. Eng.*, *13*, 469 (1991).

IPR2016-01378 Page 0099

109. Garza, C. M., Misium, G., Doering, R. R., Roland, B., and Lombaerts, R., *Proc. SPIE*, *1896*, 229 (1989).
110. Watanabe, F., and Ohnishi, Y., *J. Vac. Sci. Technol. B*, *4*, 422 (1986).
111. Hartney, M. A., Hess, D. W., and Soane, D. S., *J. Vac. Sci. Technol. B*, *7*, 1 (1989).
112. Paniez, P. J., Joubert, O. P., Pons, M. J., Oberlin, J. C., Vachette, T. G., Weill, A. P., Pelletier, J. H., and Fiori, C., *Microelectron. Eng.*, *13*, 57 (1991).
113. Jurgensen, C. W., Hutton, R. S., and Taylor, G. N., *J. Vac. Sci. Technol. B*, *10*, 2542 (1992).
114. Palmateer, S. C., Kunz, R. R., Horn, M. W., Forte, A. R., and Rothschild, M., *Proc. SPIE*, *2438*, 455(1995)
115. Pons, M., Pelletier, J., and Joubert, O., *J. Appl. Phys.*, *75*, 4709 (1994).
116. Hutton, R. S., Boyce, C. S., and Taylor, G. N., *J. Vac. Sci. Technol. B*, *13*, 2366 (1995).
117. Roland, B., Lombaerts, R., and Coopmans, F., *Dry Process Symposium*, *98*, (1988).
118. Hutton, R. S., Kostelak, R. L., Nalamasu, O., Kornbit, A., McNevin, G., and Taylor, G., *J. Vac. Sci. Technol. B*, *8*, 1502 (1990).
119. Misium, G. R., Douglas, M. A., Garza, C. M., and Dobson, C. B., *Proc. SPIE*, *1262*, 74 (1990).
120. Pierrat, C., Tedesco, S., Vinet, F., Lerme, M., and Dal'Zotto, B., *Proc. J. Vac. Sci.*, *7*, 1782 (1989).
121. Pierrat, C., Tedesco, S., Vinet, F., Mourier, T. Lerme, M. Dal'Zotto, B., and Guibert, J. C., *Microelectron. Eng.*, *11*, 507 (1990).
122. Vinet, F., Chevallier, M., Pierrat, C., Guibert, J. C., Rosilio, C., and Mouanda, B., *Proc. SPIE*, *1466*, 558 (1991).
123. Thackeray, J. W., Bohland, J. F., Pavelchek, E. K., Orsula, G. W., McCullough, A. W., Jones, S. K., and Bobbio, S. M., *Proc. SPIE*, *1185*, 2 (1990).
124. Calabrese, G. S., Bohland, J. F., Pavelchek, E. K., Sinta, R., Dudley, B. W., Jones, S. K., and Freeman, P. W., *Microelectron. Eng.*, *21*, 231 (1993).
125. Hartney, M., Kunz, R., Ehrlich, D., and Shaver, D., *Proc. SPIE*, *1262*, 119 (1990).
126. Irmscher, M., Hoefflinger, B., Springer, R., Stauffer, C., and Peterson, W., *Proc. SPIE*, *2724*, 564 (1996).
127. Ohfuji, T., and Aizaki, N., *Digest of Technical Papers—Symposium on VLSI Technology*, 1994, p. 93.
128. Hartney, M. A., Kunz, R. R., Ehrlich, D. J., and Shaver, D. C., *J. Vac. Sci. Technol. B*, *8*, 1476 (1990)
129. Oizumi, Y., Yamashita, Y., and Ohtani, M., *Microelectron. Eng.*, *30*, 291 (1996).
130. Horn, M. W., Pang, S. W., and Rothschild, M., *J. Vac. Sci. Technol. B*, *8*, 1493 (1991).
131. Weidman, T. W., and Joshi, A. M., *Appl. Phys. Lett.*, *62*, 372 (1993).
132. Kostelak, R. L., Weidman, T. W., Vaidya, S., Joubert, O., Palmateer, S. C., and Hibbs, M., *J. Vac. Sci. Technol. B*, *13*, 2994 (1995).
133. Schilling, M. L., Katz, H. E., Houlihan, F. M., Stein, S. M., Hutton, R. S., and Taylor, G. N., *J. Electrochem. Soc.*, *143*, 691 (1996).
134. Calabrese, G. S., Abali, L. N., Bohland, J. F., Pavelchek, E. K., Sricharoenchaikit, P., Vizvary, G., Bobbio, S. M., and Smith, P., *Proc. SPIE*, *1466*, 528 (1991).

135. Calvert, J., Chen, M., Dulcey, C., George, J., Peckerar, M., Schnur, O., and Schoen, P., *J. Vac. Sci. Technol. B*, *9*, 3447 (1991).
136. Garza, C. M., Catlett, D. L., and Jackson, R. A., *Proc. SPIE*, *1466*, 616 (1991).
137. Tipton, M. C., and Hanratty, M. A., *Microelectron. Eng.*, *17*, 47 (1992).
138. Garza, C. M., Solowiej, E. J., and Boehm, M. A., *Proc. SPIE*, *1672*, 403 (1992).
139 Seeger, D. E., La Tulipe, D. C., Kunz, R. R., Garza, C. M., and Hanratty, M. A., *IBM J. Res. Dev.*, *41*, 105 (1997).
140. Fonash, S. J., Viswanathan, C. R., and Chan, V. D., *Solid State Technol.*, *37*(7), 5 (1994).
141. Allen, R. D., Wallraff, G. M., Hofer, D. C., Knuz, R. R., Palmateer, S. C., and Horn, M. W., *Microlithography World,* Summer, 21 (1995).
142. Park, B. J., Baik, K. H., Kim, H. K., Kim, J. W., Bok, C. K., Vertommen, J., and Rosenlund, R., *Proc. SPIE*, in press.